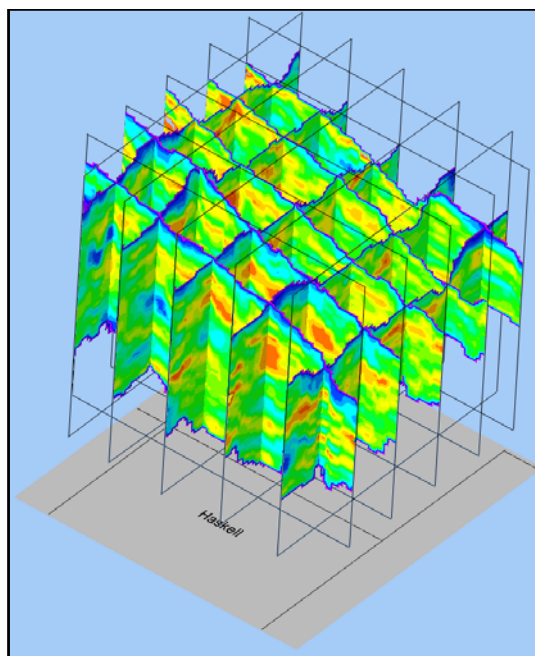
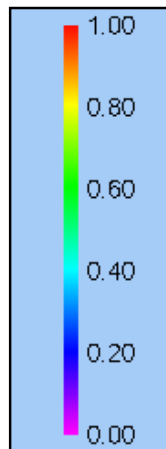

Kansas Geological Survey

DISTRIBUTION OF THE PERMEABLE FRACTION AND PRACTICAL SATURATED THICKNESS IN THE OGALLALA PORTION OF THE HIGH PLAINS AQUIFER IN THE SOUTHWEST KANSAS GROUNDWATER MANAGEMENT DISTRICT 3

by

P. Allen Macfarlane and Nicholas Schneider

Permeable
Fraction



Kansas Geological Survey Open-file Report 2007-28
December 2007

GEOHYDROLOGY

KU KANSAS
GEOLOGICAL
SURVEY
The University of Kansas

The University of Kansas, Lawrence, KS 66047 (785) 864-3965; www.kgs.ku.edu

KANSAS GEOLOGICAL SURVEY
OPEN-FILE REPORTS

>>>>>>>>>NOT FOR RESALE<<<<<<<<<<<

Disclaimer

The Kansas Geological Survey made a conscientious effort to ensure the accuracy of this report. However, the Kansas Geological Survey does not guarantee this document to be completely free from errors or inaccuracies and disclaims any responsibility or liability for interpretations based on data used in the production of this document or decisions based thereon. This report is intended to make results of research available at the earliest possible date, but is not intended to constitute final or formal publication.

Table of Contents

Executive Summary	1
Introduction.....	3
Previous Work	4
The Study Area	4
Extent	4
Stratigraphy and Lithic Composition of Cenozoic Sediments.....	4
Cenozoic Geologic History.....	4
Methodology	5
Data Sources	5
Log Selection	6
Georeferencing Well/Testhole Locations	6
Estimation of land surface elevation for each data point.....	6
Field Checking of Drillers' Log Quality.....	6
Estimation of Total Thickness and Fraction of Permeable Sediments	8
Mapping Permeable Thickness and Fraction in 2- and 3-D	9
Distribution of Permeable Zones in the Cenozoic Deposits	12
Statistical Characteristics of Total Permeable Fraction Values in GMD 3	12
Regional Distribution of the Total Thickness and Fraction of Permeable Deposits.....	12
Haskell Co. Index Monitoring Well.....	16
The Northeast Haskell Area.....	22
The Central GMD 3 Subregion.....	27
The Strip Subregion	30
Changes in PST from Pre-development to 2006.....	46
Discussion	52
REFERENCES CITED.....	58
APPENDIX A: 2-D MODEL ERROR DISTRIBUTIONS.....	61

List of Figures

Figure 1.	Profile showing the vertical distribution of the permeable fraction in the Cenozoic deposits based on the descriptions provided in the accompanying driller’s log and using the interpretation of driller’s log entries in Table 2.....	11
Figure 2.	Subareas of investigation for 2-D and 3-D mapping	12
Figure 3.	Cumulative distribution of the total permeable fraction in Cenozoic deposits, southwest Kansas.....	13
Figure 4.	The mean and variability of the permeable fraction in relation to Cenozoic sediment thickness (by depth interval) in southwest Kansas.....	13
Figure 5.	Thickness of permeable sediment in Cenozoic deposits in GMD 3	14
Figure 6.	Permeable sediment fraction of Cenozoic deposits in GMD 3.....	15
Figure 7.	Location of the northeast Haskell County index monitoring well plotted on a map of the elevation of the bedrock surface and shown as a red dot.....	17
Figure 8.	Comparison of the gamma-ray and simplified driller’s and sample logs of the open borehole for the northeast Haskell County index well in SW SE NW Sec. 36, T. 27 S., R. 31 W	21
Figure 9.	Thickness of Cenozoic deposits in the northeast Haskell study area derived using the default kriging algorithm to compute model grid values in RockWorks® 2004	23
Figure 10.	Thickness of permeable deposits within the Cenozoic sequence in the northeast Haskell study area derived using the default Kriging algorithm to compute model grid values in RockWorks® 2004	23
Figure 11.	Permeable fraction of the Cenozoic sequence in the northeast Haskell study area derived using the default kriging algorithm to compute model grid values in RockWorks® 2004.....	24
Figure 12.	NW-SE panel of the fence diagram for the northeast Haskell area centered on the northeast Haskell County index monitoring well in NW Sec. 36, T. 31 S., R. 26 W.....	25
Figure 13.	NE-SW panel of the fence diagram for the small study area centered on the northeast Haskell County index monitoring well in NW Sec. 36, T. 31 S., R. 26 W	26

Figure 14.	Elevation of the bedrock surface in the central GMD 3 subregion with the dashed line showing approximate updip edge of the Greenhorn Limestone (Macfarlane et al., 1993).....	28
Figure 15.	Thickness of Cenozoic deposits in the central GMD 3 subregion derived using the default kriging algorithm to compute model grid values in RockWorks [®] 2004.....	28
Figure 16.	Thickness of permeable Cenozoic deposits in the central GMD 3 subregion derived using the default kriging algorithm to compute model grid values in RockWorks [®] 2004.....	29
Figure 17.	Permeable fraction of the Cenozoic sequence in the central GMD 3 subregion derived using the default kriging algorithm to compute model grid values in RockWorks [®] 2004.....	29
Figure 18A.	Distribution of the permeable fraction in Cenozoic deposits that underlie the central GMD 3 subregion as revealed by north-south and east-west fence diagrams.	31
Figure 18B.	Distribution of the permeable fraction in Cenozoic deposits that underlie the central GMD 3 subregion as revealed by north-south and east-west fence diagrams.	32
Figure 18C.	Distribution of the permeable fraction in Cenozoic deposits that underlie the central GMD 3 subregion as revealed by north-south and east-west fence diagrams	33
Figure 18D.	Distribution of the permeable fraction in Cenozoic deposits that underlie the central GMD 3 subregion as revealed by north-south and east-west fence diagrams	34
Figure 18E.	Distribution of the permeable fraction in Cenozoic deposits that underlie the central GMD 3 subregion as revealed by north-south and east-west fence diagrams	35
Figure 19.	Elevation of the bedrock surface beneath the Cenozoic sequence in the strip subregion derived using the default kriging algorithm to compute model grid values in RockWorks [®] 2004.....	38
Figure 20.	Thickness of Cenozoic deposits in feet within the strip subregion derived using the default kriging algorithm to compute model grid values in RockWorks [®] 2004.....	39

Figure 21.	Thickness of permeable Cenozoic deposits in feet within the strip subregion derived using the default kriging algorithm to compute model grid values in RockWorks® 2004.....	40
Figure 22.	The distribution of the permeable sediment fraction in Cenozoic deposits in the strip subregion derived using the default kriging algorithm to compute model grid values in RockWorks® 2004	41
Figure 23.	Fence diagram of the strip subregion in GMD 3 showing the distribution of the permeable fraction in Cenozoic deposits	42
Figure 23. (cont'd)	Fence diagram of the strip subregion in GMD 3 showing the distribution of the permeable fraction in Cenozoic deposits	43
Figure 23. (cont'd)	Fence diagram of the strip subregion in GMD 3 showing the distribution of the permeable fraction in Cenozoic deposits	44
Figure 24.	Fine-grained sediment near the top of the Cenozoic section near Crooked Creek in NW NW Sec. 21, T. 33 S., R. 28 W	45
Figure 25.	The hydrograph and the profile of permeable fraction for an irrigation well in NE NE SE Section 28, T. 27 S., R. 34 W	46
Figure 26.	Pre-development PST in GMD 3.....	48
Figure 27.	Predevelopment PST/ST fraction expressed as a percent.....	49
Figure 28.	2006 PST in GMD 3	50
Figure 29.	The 2006 PST/ST fraction expressed as a percent.....	51
Figure 30.	Erosional surfaces delineating sand and gravel, cut-and-fill sequences in the Cenozoic succession exposed in a gravel pit near the Cimarron River in NW NE Section 35, t. 33 S., R. 32 W.....	53
Figure 31.	Cut-and-fill channel sequence exposed in a gravel pit in the Ogallala Formation in NE NE Section 33, T. 33 S., R. 28 W	54
Figure 32.	Comparison of the strip subregion models generated using the closest point algorithm with smoothing (A) and without smoothing with the high-fidelity option to better honor the input data (B).....	57

Figure A1.	Distribution of residuals plotted from modeling of the Cenozoic deposit thickness in the northeast Haskell area in map (a) and histogram (b) forms and derived using the default kriging algorithm to compute model grid values in RockWorks [®] 2004.....	62
Figure A2.	Distribution of residuals plotted from modeling of aggregate water-yielding sediment thickness in the northeast Haskell area in map (a) and histogram (b) forms and derived using the default kriging algorithm to compute model grid values in RockWorks [®] 2004	63
Figure A3.	Distribution of residuals plotted from modeling of the water-yielding fraction in the northeast Haskell area in map (a) and histogram (b) forms derived using the default kriging algorithm to compute model grid values in RockWorks [®] 2004.....	64
Figure A4.	Distribution of residuals from mapping the Cenozoic thickness in the central GMD 3 subregion using the closest point algorithm	65
Figure A5.	Distribution of residuals from mapping the aggregate thickness of water-yielding deposits in the Cenozoic in the central GMD 3 subregion using the closest point algorithm.....	66
Figure A6.	Distribution of residuals from mapping the fraction of water-yielding deposits in the Cenozoic in the central GMD 3 subregion using the closest point algorithm.....	67
Figure A7.	Map (a) and histogram (b) of the residuals from modeling the thickness of Cenozoic deposits in the strip subregion	68
Figure A8.	Map (a) and histogram (b) of the residuals from modeling the aggregate thickness of water-yielding sediment in Cenozoic deposits mapped across the strip subregion.....	69
Figure A9.	Map (a) and histogram (b) of the residuals from modeling the aggregate fraction of water-yielding sediment in Cenozoic deposits mapped across the strip subregion	70

List of Tables

Table 1.	Stratigraphy classifications of Cenozoic deposits above the bedrock surface in southwest Kansas	5
Table 2.	Rules used to translate driller’s log descriptions of drill cuttings into estimates of the permeable fraction of the total sediment thickness.....	8
Table 3.	The KGS sample log of the cuttings produced from drilling the borehole at the northeast Haskell Co. index well site.....	18
Table 4.	The log of the cuttings produced by the driller at the northeast Haskell Co. index well site.	20
Table 5.	Statistical characteristics of the Cenozoic thickness and the total thickness and fraction of permeable deposits distributions within the local study area based on 109 water well logs	22
Table 6.	Characteristics of the Cenozoic deposit thickness and total thickness and fraction of permeable deposits distributions within the central GMD 3 subregion based on 1,668 water well logs	27
Table 7.	Characteristics of the Cenozoic thickness and total thickness and fraction of permeable sediments distributions within the strip subregion based on 3,031 water well logs	36

DISTRIBUTION OF THE PERMEABLE FRACTION AND PRACTICAL SATURATED THICKNESS IN THE OGALLALA PORTION OF THE HIGH PLAINS AQUIFER IN THE SOUTHWEST KANSAS GROUNDWATER MANAGEMENT DISTRICT 3

By

P. Allen Macfarlane and Nicholas Schneider

Executive Summary

Ground-water availability from the High Plains aquifer in Southwest Kansas Ground-water Management District 3 (GMD 3) is declining. Water-use density, defined as the annual amount of water pumped from the aquifer per unit of land area, is high over much of GMD 3 and greatly exceeds annual recharge. Coupled with the fact that the Ogallala is a classic example of a regionally unconfined heterogeneous aquifer, these factors support subdividing the aquifer into smaller subunits for tailored management of the remaining water resource. These factors argue for a tailored approach to manage the remaining supplies in the aquifer. A key element in determining the best method to subdivide the High Plains aquifer into smaller units for management purposes is the geospatial distribution of permeable, water-yielding zones. One approach to characterizing the distribution of permeable zones within the High Plains aquifer is to mine the information contained in the thousands of drillers' logs of test holes and production wells drilled for water supply in GMD 3. The sheer abundance of these logs makes them an attractive source of information even though many geologists and hydrogeologists downplay their value.

Managers and planners use saturated thickness (ST) as a measure of ground-water availability in unconfined aquifers. However, in using ST for this purpose, it is assumed that all water-saturated sediments contribute water to pumping wells equally. The practical saturated thickness (PST) concept considers only the net thickness of saturated sediments that significantly contribute to well yield. Thus, PST provides a more accurate picture of water availability and may also provide insight into future water-level trends at the scale of an individual well.

We conducted a project in GMD 3 to demonstrate the utility of the PST concept. The project objectives were to (1) delineate the 3- D distribution of permeable zones within the saturated and unsaturated Ogallala portion of the High Plains aquifer in GMD 3 derived from drillers' logs and (2) map the PST in order to assess the change in water availability from predevelopment through the year 2006.

Methodology

In the order of their abundance, the data sources used in this project included (1) WWC-5 records of water wells completed since 1975 and maintained at the Kansas Geological Survey (KGS), (2) test-hole logs from water-well contractors, and (3) test-hole logs from the KGS county bulletins. A driller's log was selected preliminarily for inclusion in the project database if it appeared from the narrative description that the borehole penetrated the bedrock surface. There are 7,195 drillers' logs currently in the project database. Point-based well and test-hole locations were converted into a Geographic Information System (GIS) data layer based on geographic

coordinates (public land survey or latitude-longitude) for each well location. The USGS National Elevation Dataset (NED) 30 m x 30 m grid was used to estimate a surface elevation for each well location.

Descriptions of the drill cuttings recorded on a driller's log are highly individualized and reflect the driller's experience and his observational and writing skills. For this project, permeable sediment fraction determination required formulation of rules to translate log-entry phrasing into the relative proportion of the permeable sediments within each interval noted on the driller's log. These rules were based on drillers' terminology, the phrasing of their descriptions, the authors' experience with interpretation of drill cuttings in the field, and interviews with drilling contractors. Permeable sediment thickness for each described interval was determined from interval permeable sediment fraction and its thickness.

Maps of permeable sediment thickness and fraction for the entire GMD were prepared from coverages developed in ARC-GIS software. To better interpret the ARC-GIS produced maps, two subregions and one local area of GMD3 were selected for detailed subsurface examination of the Cenozoic sequence using RockWorks 2004® software to produce fence diagrams derived from 3-D models. The two subregions of the aquifer included a (1) 1,296-mi² area referred to as the central GMD 3 subregion, and a (2) 4,248-mi² area referred to as the strip subregion. A 144-mi² local study area centered on the recently drilled observation well and included in both subregions was also investigated to better understand local heterogeneity and its influence on larger-scale patterns of permeability revealed in the subregional models.

Results

Across GMD 3 the permeable fraction varies from near 0 to 100% with mean and median values slightly higher than 50% and in the central part, the sequence is thicker and a higher percentage of it is permeable than elsewhere. The fence diagrams indicate that over most of both subregional areas 40% to 80% of the late Cenozoic sequence is in the permeable range. Intermediate permeable fraction values suggest that regionally the lower saturated part of the aquifer consists locally of thin, highly permeable zones interlayered with non-productive zones. Intervals of sediment greater than 80% permeable are considered highly permeable, whereas intervals less than 40% permeable are considered barriers to ground-water flow or confining layers in the saturated part of the sequence. In the subsurface, thick, subregionally extensive intervals of highly permeable sediment are present at various levels in this part of the GMD 3. The existence of these zones is a clear indication that recognizable, preferred pathways for lateral and vertical water transmission exist within the sequence. Likewise, sinuous and sheet-like zones of less permeable sediment can be traced laterally over appreciable distances in the subsurface covering large swaths of GMD 3 and could be considered subregional, leaky confining layers. The fence diagrams also reveal that the deepest parts of the sequence do not necessarily consist of highly permeable deposits.

The range and distribution of predevelopment PST thickness and PST/ST fraction values are similar to that of total permeable thickness and fraction and suggest that water availability was much less than previously assumed based on ST. Changes in the PST/ST fraction from predevelopment to 2006 were pronounced and not uniform and reflect variability in water-use density across GMD 3 and locally the permeability fraction distribution. Water-use density is

highest in the central part of GMD 3 and these areas have seen the greatest decline in PST thickness from predevelopment to 2006. Significant decreases in the PST/ST fraction have not occurred across GMD 3. However, the PST/ST fraction has increased in some local areas and decreased in others. The arrangement of water-producing and non-producing zones implies that high annual decline rates are likely to continue and possibly accelerate depending on the local connectivity of these zones.

Introduction

Ground-water availability in the Ogallala portion of the High Plains aquifer is diminishing in the Southwest Kansas Groundwater Management District 3 (GMD 3) as it is in the other western Kansas districts. GMD 3 covers most of the highly productive Ogallala in the southwest part of the state. Water-use density, defined as the amount of water pumped from the aquifer per unit of land area, is high but variable and the water table decline rate is high. Regional investigations of the aquifer indicate that the thickness, composition, and properties of the aquifer are highly variable (Gutentag et al., 1981; Stullken et al., 1985; and Macfarlane and Wilson, 2006). These factors argue for a subdividing the aquifer in GMD 3 into smaller subunits based on the need for tailored management of the remaining water resource.

A key element in determining how the Ogallala in GMD 3 could be subdivided into smaller units is understanding its heterogeneity structure. More specifically, what is lacking at the moment is the subsurface distribution of permeable zones and lower permeability, confining units, all of which bear on the hydrologic properties of the sediment sequence. One approach to developing a better understanding of the permeable pathways through the aquifer is to mine the information contained in the thousands of logs that have been generated from the drilling of test holes and production wells for water supply. The sheer abundance of the logs makes this an attractive source of information even though many geologists and hydrogeologists downplay their value.

Saturated thickness (ST) is the total thickness of an unconfined aquifer from its base to the water table and has been traditionally used by hydrogeologists to assess ground-water availability. However, application of the ST concept to heterogeneous aquifers, such as the Ogallala, provides a distorted view of the total amount that can be readily pumped from an aquifer because not all the lithologies that make up its framework (e.g., fine-grained sediment) contribute water equally to pumping wells. Water-saturated, fine-grained sediments slowly release water to the more permeable sediments within an unconfined aquifer over longer time scales and hence act as a minor source of water to pumping wells at rates that depend on leakance. A more conservative assessment of water availability takes into account only the net thickness of the most productive zones within the aquifer. In this paper, the practical saturated thickness (PST) is the total thickness of water-saturated, permeable sediment and serves this purpose.

The purpose of this paper is to (1) present research results on the distribution of permeable zones within the saturated and unsaturated Ogallala portion of the High Plains aquifer in GMD 3 derived from drillers' logs and (2) use these results to assess the impact of pumping on water availability in the District from predevelopment to 2006 using the PST parameter.

Previous Work

The heavy reliance in this research on drillers' logs is not new. Bredehoeft and Farvolden (1964) used drillers' logs of boreholes drilled for water to better understand the distribution permeable sediments in the fill of several intermontane basins in northern Nevada. Russell et al. (1998) described methods that could be used to standardize subsurface log descriptions in order to make possible comparisons within and between datasets derived from different sources, including water-well drilling. Berg et al. (2002) used subsurface data from borings for water wells, geologic investigations, and engineering data and surface mapping and outcrop descriptions with RockWorks 2002® and ArcView 3.2 to develop a geologic model of the sediments underlying a 25-mile segment of the Illinois River valley in north-central Illinois. Macfarlane et al. (2005) reported on a pilot study to map the distribution of permeable deposits in the Ogallala in an 8-township area centered on the "four corners" area where Finney, Haskell, Kearny, and Grant counties meet in GMD 3.

The Study Area

Extent

The study area includes parts or all of Hamilton, Kearny, Finney, Stanton, Grant, Haskell, Gray, Ford, Morton, Stevens, Seward, and Meade counties within GMD 3. Situated within the Arkansas and Cimarron river basins, the study area encompasses portions of the High Plains and the Arkansas River Lowlands physiographic provinces (Schoewe, 1949).

Stratigraphy and Lithic Composition of Cenozoic Sediments

Cenozoic sediments form the Ogallala aquifer framework and consist of a heterogeneous assemblage of unconsolidated-to-cemented Miocene-Pliocene (Neogene) and Quaternary alluvial deposits of gravel, sand, silt, and clay, lacustrine freshwater limestone and marl, and volcanic ash overlain by undifferentiated eolian and fluvial sediments (Table 1; Smith, 1940; Gutentag, 1981; Izett and Honey, 1995). Some lenses of coarser sediment are cemented by calcium carbonate to form discontinuous layers of calcrete, which are abundantly distributed throughout the Ogallala. Caliche nodules are abundant in some lenses of fine-grained sediment. Cenozoic deposits underlie most of the surface in GMD 3 except for localized areas in Morton, Stanton, Hamilton and Ford counties where Permian- and Mesozoic-age bedrock units crop out at the surface.

Cenozoic Geologic History

Throughout the Cenozoic Era, the region has been strongly influenced by (1) periods of uplift and erosion of the Rocky Mountains and the adjacent piedmont to the west, (2) climatically induced cycles of erosion, deposition, and stability, and (3) dissolution of shallow evaporites in the Permian bedrock and associated subsidence of the bedrock surface resulting in a fixation of the drainage and the formation of incised valley systems and lake basins (Macfarlane and Wilson, 2006). The resulting bedrock surface slopes to the east at approximately 12 feet/mile with local relief as much as 150 feet/mile.

Methodology

Data Sources

In order of abundance, the data sources for this project were the WWC-5 records database of water wells completed since 1975 and maintained at the Kansas Geological Survey (KGS); test-hole logs from the files of Henkle Drilling and Supply Co., Garden City; and test-hole logs from the KGS county bulletins. Gamma-ray logs of boreholes drilled for oil and gas were for the most part only marginally useful because they were obtained from logging runs made in steel-cased holes. In rare cases where the logs had been generated from runs in uncased holes to the surface, the gamma-ray curves were difficult to correlate with nearby drillers' logs because of local heterogeneity and variability in the arkosic sediment (produced from the weathering of granitic rocks, primarily quartz and orthoclase feldspar) composition of the coarse fraction.

Table 1. Stratigraphic classifications of Cenozoic deposits above the bedrock surface in southwest Kansas.

System	Series	Grant & Stanton Counties (Fader et al., 1964)	Meade County (after Hibbard, 1953, 1958; Hibbard and Taylor, 1960)	Irish Flats NE Quadrangle Meade County (Izett and Honey, 1995)	
Quaternary	Holocene	Upper Pleistocene	Sanborn Group	Alhwinium/ Upland Deposits	
				Basin-fill Deposits	
	Pleistocene	Lower Pleistocene	Meade Group	Crooked Creek Formation	Upper unnamed Member
					Lava Creek B ash bed
Tertiary	Pliocene	Ogallala Formation	Ballard Formation	Cerro Toledo B ash bed	
				Huckleberry Ridge ash bed	
	U. Miocene				Stump Arroyo Member
					Rexroad Formation
				Ogallala Formation	

Log Selection

The project used drillers' logs from a database that initially was developed for the 2004 enhancement of the bedrock-surface mapping project reported in Macfarlane and Wilson (2006) and funded by the Kansas GIS Policy Board and GMD3. Additional well logs submitted to the KGS Data Library since the end of data gathering for that project were included if the log indicated that the borehole had penetrated the bedrock surface beneath the Cenozoic. Note that the log of the recently drilled Garretson index well in northeast Haskell County was also added to the database. There are 7,195 drillers' logs currently in the project database.

Georeferencing Well/Testhole Locations

The locations of wells and test holes are recorded on the logs using public land survey (PLS) notation with the accuracy of the location dependent on the finest subdivision of a section (approximately 1 mile²) specified in the notation, typically, down to the quarter, quarter section or better. The locations reported on the WWC-5 forms are routinely hand-checked before they are entered into the KGS WWC-5 well record database by comparing the recorded information on the form with (1) directions to the well from the nearest city; (2) topographic maps; (3) water-right information supplied by the Kansas Department of Agriculture, Division of Water Resources; and (3) other sources of information, including rural phone directories. None of the WWC-5 records were field-checked for location unless they are included in the KGS annual water-level survey network.

Point-based well and test-hole locations were converted into a Geographic Information System (GIS) data layer based on geographic coordinates for each well location. The KGS LEO conversion program was used to convert the PLS description (i.e. SWNE Sec 4, T. 3 S. R. 40 W.) into geographic coordinates that represented the center of that legal description (i.e., 101.81140 W Longitude, 39.82367 N. Latitude). Point-associated data of the PLS description, geographic coordinates, county FIPS code, well depth (if known), identified depth to bedrock, data source (i.e., WWC-5), drilling company (if known), and other identification information were recorded with the GIS point-based data layer.

Estimation of land surface elevation for each data point

The USGS National Elevation Dataset (NED) was used to estimate a surface elevation for each well location. The NED is based on the highest resolution, highest quality, digital elevation models for the conterminous United States. In the area of this project, the NED is composed of approximately 30 meter x 30 meter grid cells that have a land surface elevation value interpolated exclusively from the contour lines of equal elevation on 1:24,000 scale maps. Using GIS overlaying techniques, land surface elevations from the NED were assigned to the well locations and converted from meters into feet. For more information on the NED data set, please refer to <http://ned.usgs.gov/>.

Field Checking of Drillers' Log Quality

Drillers are not formally trained as well-site geologists. Thus, a driller's ability (1) to determine the depth to significant stratigraphic horizons (such as the bedrock surface) and changes in lithology and (2) accurately describe and write down what he observes in the drill cuttings are issues that need to be addressed when using this source of information to characterize subsurface geology.

In fiscal year 2007 one of the priorities of the KGS Ogallala-High Plains aquifer support program was to establish one index monitoring well in each of the western Kansas GMDs for high-frequency, water-level monitoring. A well was installed within the study area in SW SE NW Sec. 36, T. 27 S., R. 31 W., northeast Haskell County. Drilling and well installation provided an opportunity for KGS personnel to be on site to (1) collect samples of the cuttings and produce a sample log from their examination, (2) obtain a gamma-ray log of the Cenozoic sequence penetrated by the borehole, and (3) compare these logs with the driller's log for this hole and the drillers' logs of nearby wells that had been completed by other water-well contractors.

The sample and driller's logs: A sample log was prepared by KGS personnel based on a visual examination of the cuttings in the field and refined from more detailed inspection at KGS. Lithologies represented and their abundance in the cuttings was noted along with color of fine-grained sediments and other characteristics of the samples. Changes in rig behavior during drilling were made in the field and correlated to changes in lithology. Independently, the driller kept his own log as the hole was being drilled. KGS personnel noted that the driller took care to track what was being drilled by periodically pausing the drilling to circulate the borehole and flush the most recently drilled cuttings back up to the surface for examination. On completion of the drilling, the borehole was logged geophysically by the water-well contractor to produce resistivity, SP, and gamma-ray logs of the borehole.

Gamma-ray logging: All earth materials emit natural gamma radiation, which can be attributed to the decay of trace amounts of radioactive elements contained within them (Doveton, 1986). The radioactive elements of interest here are uranium, thorium, and the radioactive isotope potassium-40. The intensity of radiation and energy emitted depend on the total and relative amounts of these isotopes contained in the rocks. In general clay-bearing, fine-grained rocks and those bearing minerals with naturally radioactive elements (such as orthoclase in this case in the sands and gravels) tend to emit higher levels of radiation than those that are relatively free of these lithologies or minerals (such as quartz).

A gamma-ray log is produced by lowering to the bottom of the borehole a detector (a Geiger counter) mounted in a logging tool that is attached by a cable to the end of a winch (Doveton, 1986). The winch slowly draws the tool back to surface. As the tool moves up the borehole it measures and records the gamma-ray intensity emitted by the adjacent rocks/sediment. These readings are recorded as counts per second and transmitted electronically back to the surface through the cable and recorded as a graph of radiation intensity vs. depth below the surface or some other datum. The graph is referred to as the gamma-ray log. On the log clayey zones and those containing an abundance of orthoclase can be distinguished from quartzose sands because the gamma-ray curve moves to the right on the log indicating higher intensities of emitted gamma radiation. Other lithologies not containing radioactive minerals will show low intensities of natural radioactivity and the curve will remain on the left side of the log.

The gamma-ray log is used to more precisely pinpoint lithologic changes in the subsurface than a log that describes samples of the drill cuttings. This is because the logging tool makes discrete point measurements on the rocks in place with reference to a datum rather than the cuttings, which, in this case, have been retrieved over a drilling interval of 10 feet. Lithologic changes are

often tied to surfaces that bound geologic units. Thus, by comparing the log of the borehole with the descriptions of cuttings, it is possible to “fine-tune” estimates of the depth to these boundaries. In addition, the shape of the gamma-ray curve may elucidate additional detail about the nature of the rock that are not obvious from a description of the drill cuttings samples alone.

Estimation of Total Thickness and Fraction of Permeable Sediments

Descriptions of the drill cuttings from in the WWC-5 forms are highly individualized and reflect the driller’s observational skills in describing the extremely diverse assemblage of cuttings that return to the surface during drilling.

To quantify the proportion of permeable sediments from drillers’ logs required a consistent means (1) to translate the descriptions into lithologic descriptions, (2) to quantify the relative proportions of each lithology where more than one type of sediment is mentioned and (3) to assign an estimate of the proportion of each lithology that is capable of yielding water to wells. In this project simple, logical rules were formulated to translate the log entries into relative proportions of different lithologies that would likely contribute significant amounts of water to wells or be non-contributing (Table 2). These rules were based on drillers’ terminology, the phrasing of their descriptions, the authors’ experience with interpretation of drill cuttings in the field, and interviews with drilling contractors. The interpreted percentages that follow from the phrasing of log entries assume that the order in which each lithology is listed follows from its relative abundance. Seni (1980) adopted a similar approach using driller’s logs for regional lithofacies mapping in the Ogallala in Texas.

Table 2. Rules used to translate driller’s log descriptions of drill cuttings into estimates of the permeable fraction of the total sediment thickness.

Lithology/Phrasing of the Description	Percentage of the Interval That is Permeable/Quantitative Interpretation of Lithology
Clayey sand	70% Contributing
Sandy clay	30% Contributing
Sand or sand and gravel	100% Contributing
Brown rock, silt, clay, shale, caliche, or cemented sandstone	Non-contributing
A with a lens, streak or thin strips of B	80% A and 20% B
A with B	90% A and 10% B
A and B or A, B (as a list)	60% A and 40% B
A, B, C (as a list)	50% A, 30% B, and 20% C
A, B, C, D, ... (as a list)	40% A, 25% B, 20% C, and 15% D

Assignment of the percentage of each lithology that is permeable in table 2 is arbitrary but based on what most hydrogeologists would consider to be productive aquifer and non-aquifer earth material. Irrigation, public supply, and industrial wells require aquifers with a relatively high hydraulic conductivity in order to produce water at the required sustained rates. The Ogallala portion of the High Plains aquifer in southwest Kansas is composed primarily of mixtures of permeable sand and sand & gravel at one end of the spectrum and low-permeability caliche,

sandstone depending on its degree of cementation, silt and clay, and brown rock (interpreted to be siltstone or claystone) at the other end. Clayey silt and clay typically have values of hydraulic conductivity less than 0.01 feet/day, whereas sand and sand & gravel have hydraulic conductivity values 2 to 4 orders of magnitude higher depending on sediment grain size, sorting and silt content (Schwartz and Zhang, 2003). Intuitively, these lithologic end members can be perceived in terms of their permeability. Thus, sand and sand & gravel are considered to be 100% permeable and brown rock, silt, clay, shale, caliche, and cemented sandstone are considered to be non-contributing (0% permeable), but capable of storing significant amounts of water (Table 2). In between these extremes are mixtures of permeable and non-contributing lithologies that must be estimated. After a brief survey of the sand-silt-clay sediment classifications in the literature (Shepard, 1954; Huang, 1962; and Folk, 1968) the dominant end member (sand or silt-clay) was arbitrarily set to constitute 70% the total of the bulk sediment and non-dominant end member 30%. Following this rule, sandy clay or silt is 30% and clayey or silty sand, 70% permeable.

Using the values in table 2 the total thickness of permeable sediment for each interval in the driller’s log is calculated from the proportion of permeable sediments (sand and sand & gravel) in the interval and the interval thickness. The following is an example of how this approach is applied to estimate the total permeable fraction thickness for a particular interval on a driller’s log with multiple lithologies in the interval description.

Depth Below Surface	Driller’s Description
300 feet to 325 feet	Sand, sandy clay, clay, and caliche

Total thickness of the interval is 25 feet. Translation of this entry into a permeable sediment thickness value is covered by the rule listed at the bottom of table 2. From the table, sand corresponds to item A, sandy clay, to B; clay, to C; and caliche, to D.

$$\text{Permeable Sediment Thickness} = 25[(0.4)(1.0) + (0.25)(0.3) + (0.2)(0) + (0.15)(0)] \quad \text{Eqn. 1}$$

$$\text{Permeable Sediment Thickness} = 11.875 \text{ feet} \cong 12 \text{ feet} \quad \text{Eqn. 2}$$

In Eqn. 1, sand accounts for 40% of the interval, sandy clay, 25%; clay, 20%; and caliche, 15%. The 1.0 multiplier in the first term indicates that the entire sand thickness contributes to permeable fraction. The sandy clay is assumed to consist of 30% sand, all of which contributes to the total permeable thickness (multiplier of 0.3). No contribution to the permeable sediment thickness is made by either the clay or caliche lithologies (multiplier of 0). The permeable sediment thickness of this interval is approximately 12 feet or slightly less than 50% of the total interval thickness. The total permeable fraction and by extension the total permeable thickness is the sum of the interval fractions and thicknesses between the surface and the base of the aquifer as show in Figure 1.

Mapping Permeable Thickness and Fraction in 2- and 3-D

Maps of permeable thickness and fraction for the entire GMD were prepared using ARC-GIS software. To better interpret the ARC-GIS produced maps, two subregions and one local area of GMD3 were selected for detailed examination using RockWorks 2004® software to produce

maps, 3-D models, and fence diagrams derived from 3-D models (Figure 2). The two subregions of the aquifer included (1) a square 36-township (1,296-mi²) area in southern Finney, western Gray, eastern Grant, southeastern Kearny, and most of Haskell County in the central part of GMD 3, referred to as the central GMD 3 subregion, and (2) a rectangular strip, 17 townships by 7 townships (4,248-mi²) in size, that extended on the west from near the Kansas-Colorado border eastward through southern Gray and Meade counties, referred to as the strip subregion. A small, 4-township (144-mi²) local study area centered on the Section 36, T. 27 S., R. 31 W. within the central GMD 3 was also investigated.

The central GMD 3 subregion was selected because it encompassed a priority area of concern for GMD 3. The strip subregion was selected to look for trends in permeable zone distribution along the assumed direction of transport of sediment eroded from the Rocky Mountains to the west. The small area was selected in support of a Kansas Water Office-funded Ogallala-High Plains Aquifer study being conducted by the KGS to install an index-monitoring well in GMD 3 at a site in northeastern Haskell County.

Data were input from Excel spreadsheets and imported into the Borehole Manager and the Geological Utilities worksheets of RockWorks 2004® to create the 2- and 3-D visualizations. To produce visualizations RockWorks 2004® first establishes a 2-D grid of cells or a 3-D volume of voxels based on the spatial data distribution and a user-selected easting, northing, and vertical spacing between grid nodes. In this project the grid spacing for the easting and northing directions was set at 750 feet and 10 feet in the vertical direction. The software can populate the cell centers of 2-D grids or of the rectangular solids of 3-D grids by selecting any one of a number of available algorithms to calculate values of the parameter to be mapped. The kriging algorithm was selected to create 2-D maps of the thickness of the Cenozoic section, the bedrock elevation, and land-surface elevation model grids and contour maps because these parameters are reasonably continuous across each subregion.

Three-D models of permeable sediment fraction were generated using the closest-point algorithm to populate the model volume of voxels. This algorithm was selected because no other data related to correlation lengths, anisotropy, or weighting are required for its use. An additional step was taken to smooth the voxel parameter values to highlight permeability trends in the fence diagram panels. An additional 3-D model of permeable fraction was created using the closest point algorithm without smoothing and with the high fidelity option to investigate the effects of smoothing on the representation of the permeable fraction distribution in the strip subregion.

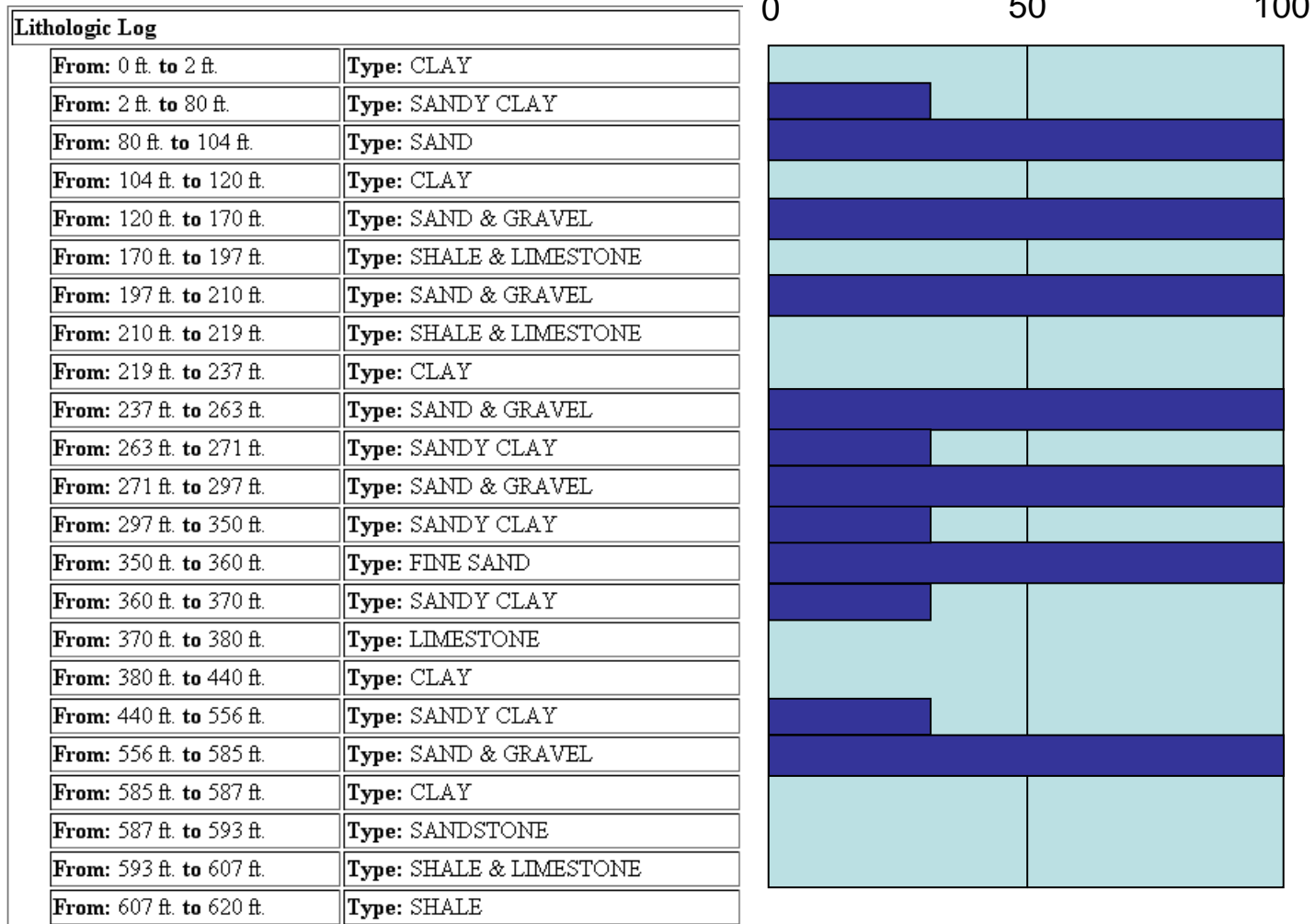


Figure 1. Profile showing the vertical distribution of the permeable fraction in the Cenozoic deposits based on the descriptions provided in the accompanying driller's log and using the interpretation of driller's log entries in Table 2. The total footage of permeable deposits is 231.5 feet and the permeable fraction is 38%.

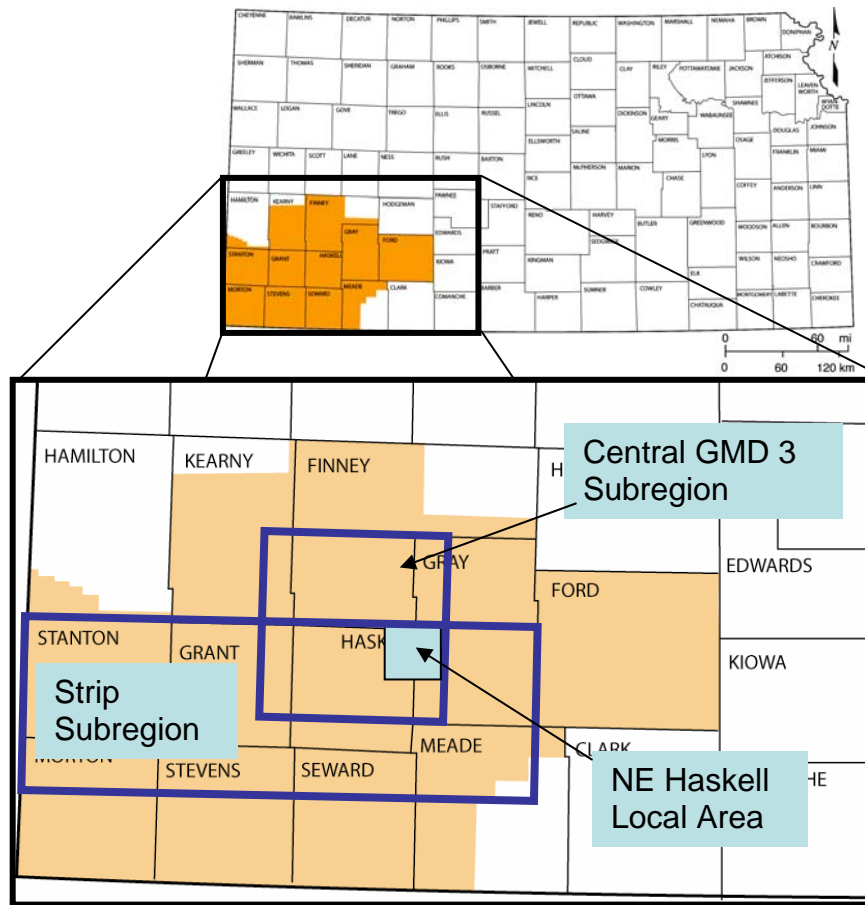


Figure 2. Subareas of investigation for 2-D and 3-D mapping.

Distribution of Permeable Zones in the Cenozoic Deposits

Statistical Characteristics of Total Permeable Fraction Values in GMD 3

For GMD 3 as a whole, the permeable fraction data set is normally distributed and the mean and median permeable fractions are 52% and 52.9%, respectively (Figure 3). The total permeable fraction appears to be related to the total thickness of Cenozoic deposits in GMD 3 (Figure 4). The mean total permeable fraction ramps up from 43% up to values 55%-57% in the 501-600 feet thick class. The steepest increase in mean fraction occurs between the less than 100 feet class and the 101-200 feet thick class. Likewise the variability as measured by the standard deviation decreases from 24% to the 12% to 16% range between the less than 100 feet thickness class and the 301-400 feet thickness class.

Regional Distribution of the Total Thickness and Fraction of Permeable Deposits

Total thickness of permeable deposits is greatest in a broad band that extends through the central part of GMD 3 that includes southern Finney, most of Haskell, Seward, the southern two-thirds of Stevens, and the northwest half of Meade counties (Figure 5). A linear trend where total thickness is greater extends from northwest Stanton into northern Stevens counties. This

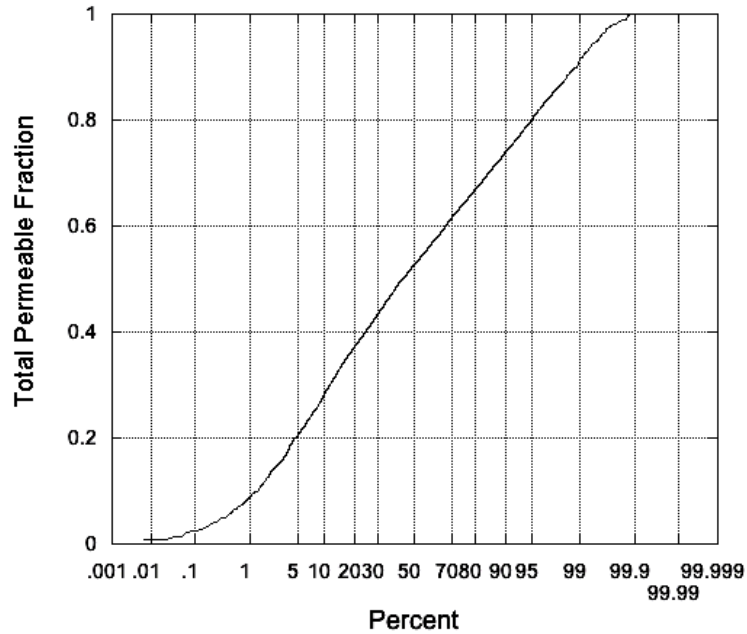


Figure 3. Cumulative distribution of the total permeable fraction in Cenozoic deposits, southwest Kansas.

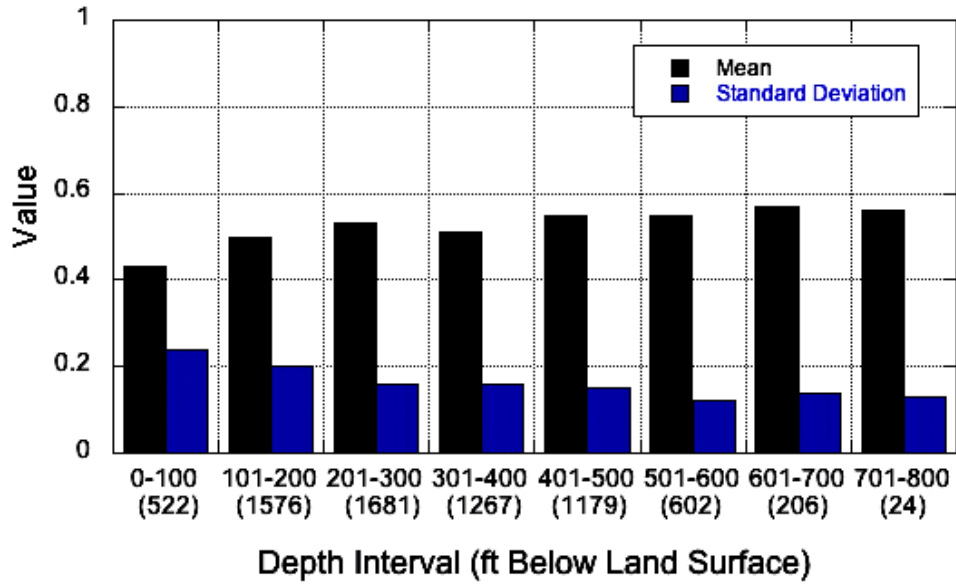


Figure 4. The mean and variability of the permeable fraction in relation to Cenozoic sediment thickness (by depth interval) in southwest Kansas. The standard deviation is taken as a measure of overall variability. The numbers in parentheses represent the number of data points that fall into each depth interval class.

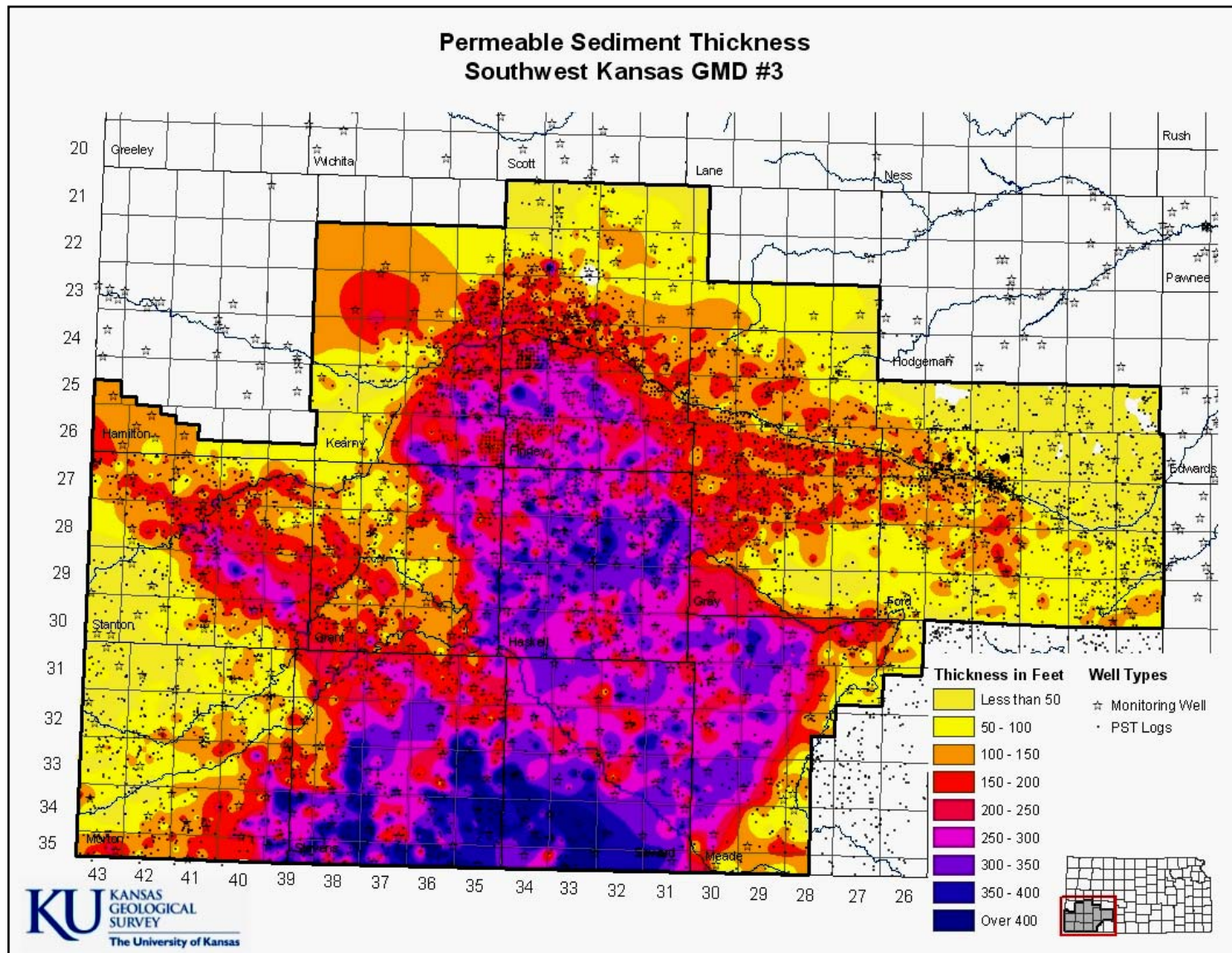


Figure 5. Thickness of permeable sediment in Cenozoic deposits in GMD 3.

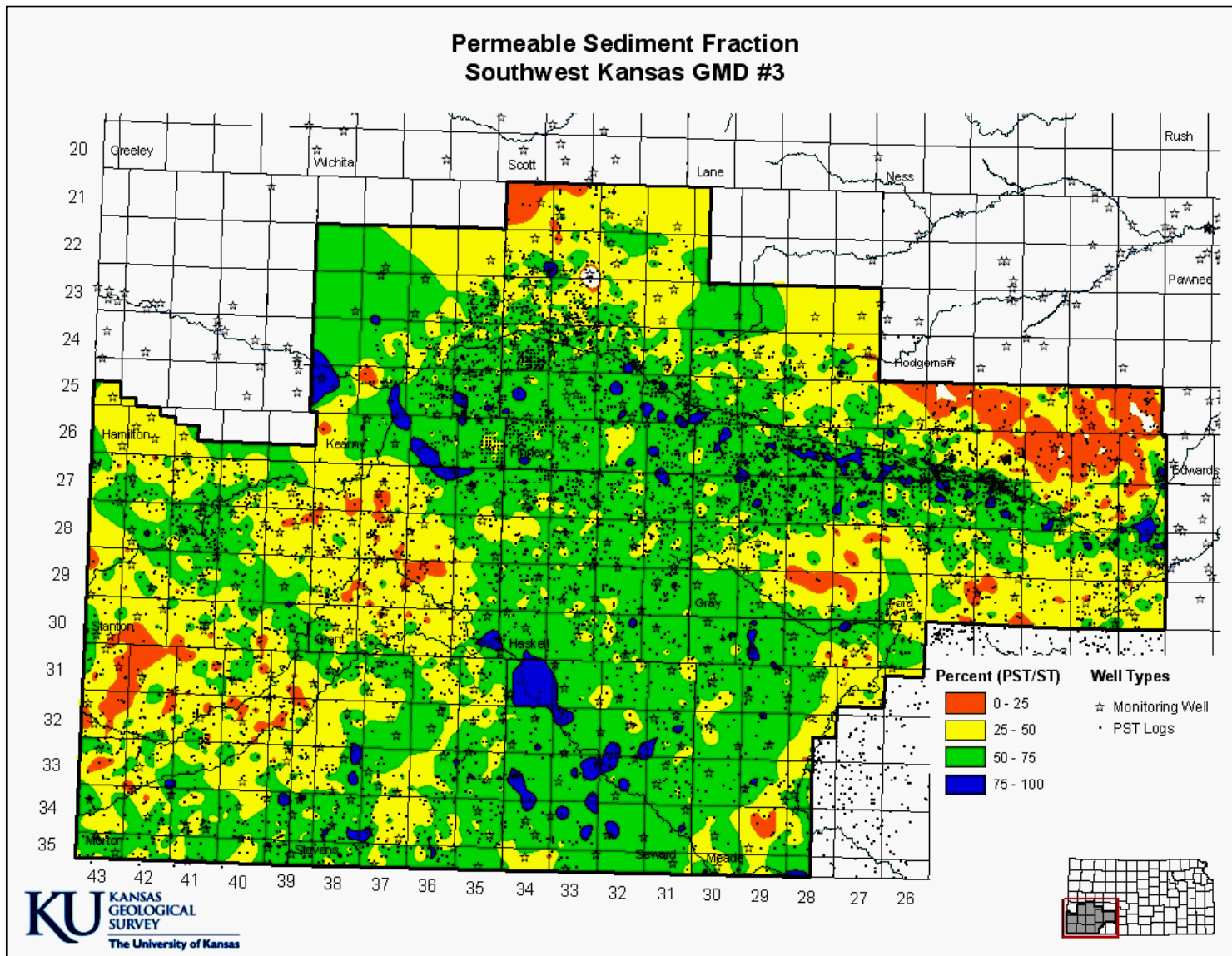


Figure 6. Permeable sediment fraction of Cenozoic deposits in GMD 3.

localized linear trend of greater total thickness in Stanton County is located in a paleovalley that Macfarlane and Wilson (2006) believed might have been occupied by the ancestral Arkansas River. Where total thickness exceeds 250 feet, the permeable fraction is generally 50% to 75% (Figure 6). In southwestern Stanton, most of the northwest half of Morton, and southeastern Gray and northern Ford counties, total thickness is less than 50 feet and the fraction of total Cenozoic thickness is less than 50%. Beneath the western two-thirds of Stanton County, total thickness is low and makes up less than 50% of the Cenozoic sequence. Aggregate thickness is generally 100-200 feet along reach of the Arkansas River from Lakin to Dodge City and the permeable fraction is generally 50% to 75%, but locally may exceed 75%.

Haskell Co. Index Monitoring Well

The northeast Haskell County index monitoring well is located in SW SE NW Sec. 36, T. 27 S., R. 31 W. along the trend of string of bedrock lows interpreted to be a paleochannel of an incised pre-Miocene-Pliocene drainage. The site is also located at the foot of the buried Greenhorn Limestone escarpment (Figure 7; Macfarlane et al., 1993; Macfarlane et al 1998; Macfarlane and Wilson, 2006). The lithologies encountered during drilling are typical of the Cenozoic deposits in southwest Kansas (Tables 3 and 4, Figure 8). From bottom to top the sequence consists of: (1) a thin interval of fine to coarse sand and pea gravel, (2) a thick section of medium brown to dark yellowish orange clay and silty clay, (3) thick sequence of fine to coarse sands and gravels with recovered clasts up to 4 centimeters in size, and (4) finer grained silt, silty clay, and sand at the top. Caliche is abundant in fine-grained deposits and pea-size fragments of calcite-cemented fine sand, some of it recycled, were recovered from the coarser-grained sections. Gravel clasts consist of quartz from a variety of sources, granitic intrusive igneous rocks, basalt, and metamorphic rocks. Clasts of reworked bedrock were found in the sand and gravel interval at the base of the Cenozoic sequence. Sand grains are dominantly quartz with minor amounts of orthoclase and microcline feldspar and traces of mica, and magnetite weathered out from the basalt. The thick sequence of medium brown clay noted in Table 5 shows evidence of soil development with manganese oxide coatings on what might have been ped surfaces. Caliche occurs as nodules and in at least one case as hard, cryptocrystalline masses. The bedrock beneath the index well site is gray upper Dakota Formation siltstone.

The driller's and sample logs compare favorably to each other and to the gamma-ray log (Figure 8). The driller's and the sample logs agree on the major lithologic units and the depths to changes in lithology within the Cenozoic sequence. Using the rules in Table 2, the total thicknesses of permeable sediment above the bedrock are 238.7 feet and 268 feet from the descriptions in the driller's and the sample logs, respectively. Total permeable sediment thickness derived from the driller's log is about 11% less the value derived from the sample log.

The gamma-ray log of the borehole displays both low frequency, low amplitude and high frequency, high amplitude fluctuations caused by vertical lithology changes, the high rate of sampling of radiation intensity, and the inherent stochastic behavior of radioactive decay (Doveton, 1986). In spite of its noisy character, the log displays changes that correlate with lithologic changes indicated on the sample and driller's logs. The uppermost fine-grained sediments are reflected in the higher counts/second recorded on the gamma-ray log. Note that the lower counts/second values at about 30 feet below surface correlate with thin lenses of sand interbedded with the finer-grained sediments. Within the thick sand and gravel intervals of the

borehole, the decrease in radiation intensity is less than expected or non-existent because of the radiogenic potassium in the grains of orthoclase and granitic rocks that make up a significant fraction of the sediment.

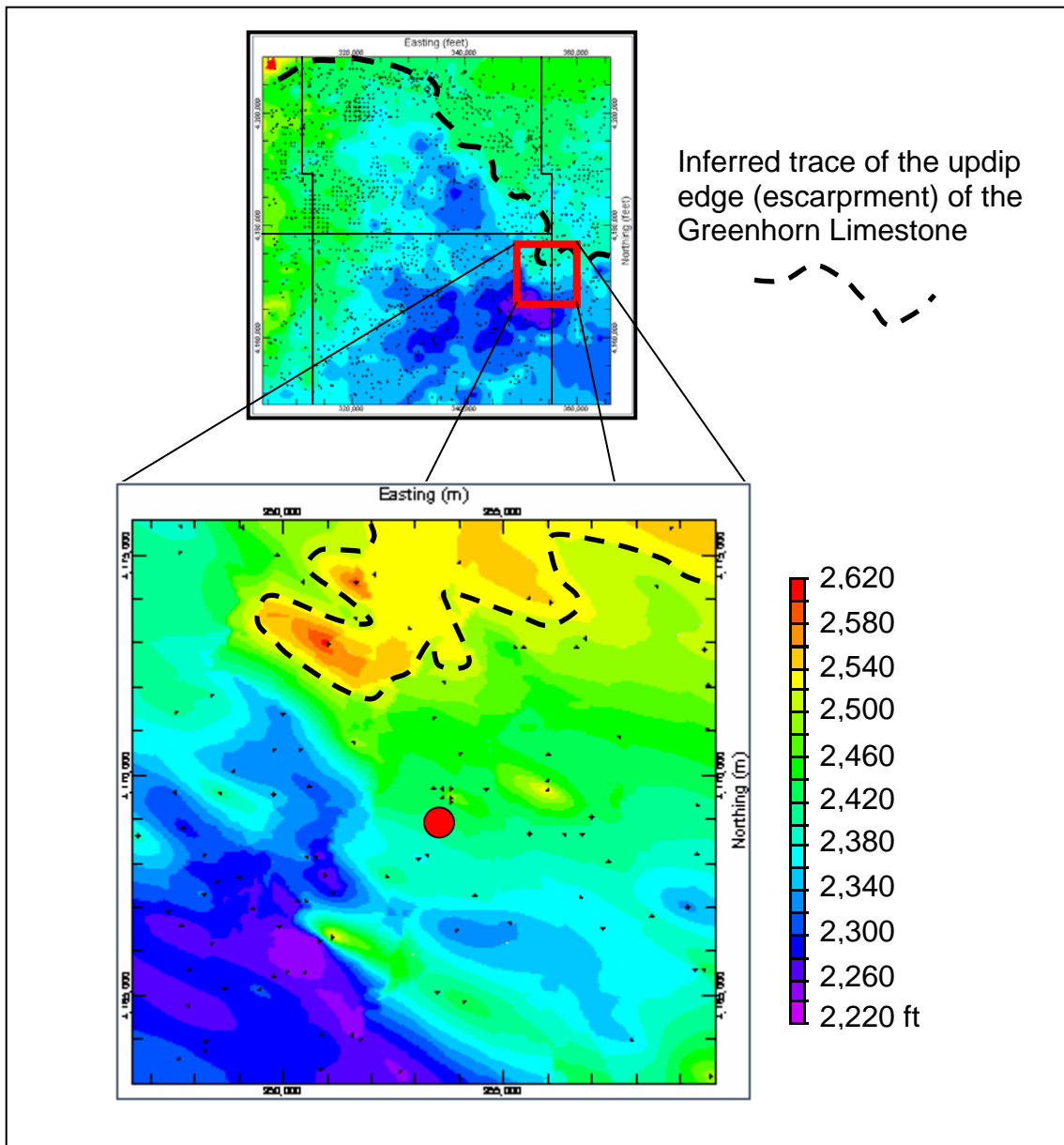


Figure. 7. Location of the northeast Haskell County index monitoring well plotted on a map of the elevation of the bedrock surface and shown as a red dot. The elevation of the bedrock surface map was derived using the default kriging algorithm to compute values for the model grid in RockWorks® 2004.

Table 3. The KGS sample log of the cuttings produced from drilling the borehole at the northeast Haskell Co. index well site. The letters and numbers in parentheses following the colors are the standardized colors from a rock color chart of Goddard et al. (1975). The depth to bedrock at this site is 432 feet below surface based on the sample log and the gamma-ray log of the borehole. The driller's log indicates a depth to bedrock of 433 feet.

Depth Interval (feet)	Sample Description/ Rig Behavior
0 – 10	Light brown (5YR 6/4) silty sand to sandy silt with grayish pink (5R 8/2) to very light gray (N8) caliche nodules. Sand is very fine, subrounded to rounded, and dominantly quartzose with minor orthoclase and dark rock fragments.
10 – 20	-do-
20 – 28	-do- plus medium to coarse rounded quartz and minor feldspar sand grains
28 - 35	Sand is very fine to coarse grained and dominantly quartzose with minor orthoclase, perthite, and dark rock fragments at 28 feet.
35 – 50	Light brown (5YR 6/4) sandy silt; minor amounts of caliche.
50 – 65	Light brown (5YR 6/4) sandy silt and fine sand some cemented; caliche more abundant at 56 and 63 feet.
65 – 70	Cemented fine sand described by the driller as “firm” at 68 feet
70 – 80	Fine to medium quartzose sand; some grains stained with manganese oxides.
81 – 95	-do- cemented fine to medium sand more abundant. Some black grains are magnetite.
95 – 107	Very fine to coarse grained sand and cemented sand; sand grains manganese and iron oxide stained. Rig chattery 95 to 105 feet
107 – 115	Dark yellowish orange (10YR 6/6) silty clay
115 – 120	White (N9) to very light gray (N8) to pale yellowish orange (10YR 8/6) silty clay with manganese oxide staining. Fine to coarse quartzose sand and pea gravel with grains of orthoclase; light gray (N7) speckled very-fine cemented sand. Rig chattery.
120 – 130	Gray-tan (5Y 7/2) silt and very fine to coarse sand and pea gravel. Quartz grains subangular to subrounded. Basalt fragments angular and containing magnetite. Caliche nodules subrounded and grayish olive green (5GY 3/2), light gray (N7) and moderate brown (5YR 3/4). Pea gravel consists of chert, quartz and orthoclase clasts. Rig chattery.
130 – 140	Fine to coarse sand and gravel with clasts up to 2.5 cm. Sand is subrounded to well rounded and gravel is subangular to subrounded. Sand is quartzose with minor orthoclase and perthite. Gravel clasts are felsic to basaltic igneous rocks with the basaltic clasts primarily angular. Dark yellowish orange (10YR 6/6) cemented medium to coarse sand grains with manganese oxide staining.
140 – 150	-do- some clasts of plagioclase
150 – 160	-do- with moderate yellowish brown (10YR 5/4) silty clay
160 – 170	-do-
170 – 180	-do- finer grained sand and smaller gravel grain sizes
180 – 190	-do-

Table 3. Continued.

190 – 200	Fine to coarse sand and pea gravel with rounded cemented sand clasts.
200 – 210	Fine to coarse sand and gravel up to more than 2.5 cm.
210 – 220	-do- rig very chattery.
220 – 230	Fine to coarse sand and gravel with clasts up to 5 cm. Clasts subrounded to rounded and consisting of quartz, felsic rocks, and basalt
230 – 240	-do- gravel pea size to 2.5 cm. Rig very chattery
240 – 250	-do- gravel clasts 1 to 3.7 cm, subangular to subrounded; grayish black (N2), greenish gray (5G 6/1) and pale olive (10Y 6/2) clay with iron oxide staining. Rig chattery. At 250 feet added a bag of calcium phosphate (?) to the drilling fluid to help lift the cuttings from the bottom of the hole.
250 – 260	Fine to coarse sand and gravel pea size up to 1.2 cm and cemented sand. Rig chattery.
260 – 270	-do- with caliche nodules. Rig chattery.
270 – 280	-do- up to pea gravel size and cemented sand; rig not as chattery
280 – 290	Moderate brown (5YR 4/4) sandy silty clay and cemented sand; gravel up to 2.5 cm.
290 – 300	Moderate brown (5YR 4/4) to pale olive (10Y 6/2) clay with manganese oxide coatings and small millimeter to pea size caliche nodules. Rig quiet with easy penetration
300 – 310	-do- with dark yellow orange (10YR 6/6) clay.
310 – 320	-do- with grayish yellow green (5GY 7/2) clay and cemented sand.
320 – 330	-do- cemented fine sand
330 – 340	-do- caliche more abundant.
340 – 350	Fine to medium sand, caliche, and cemented fine to medium sand
350 – 360	Dark yellowish orange (10YR 6/6) silt and caliche
360 – 370	Moderate yellowish brown (10YR 5/4) sandy clay; caliche much less abundant
370 – 380	-do- with cemented fine sand.
380 – 390	Grayish yellow green (5GY 7/2) clay and coarse sand and gravel up to 1 cm.
390 – 400	Coarse sand and pea gravel with cemented sand and caliche nodules.
400 – 410	-do- with very pale orange (10YR 8/2) opaque microcrystalline angular fragments of calcite
410 – 420	Fine to coarse quartz sand with minor caliche, cemented sand, feldspar, and pea gravel consisting of igneous rock fragments including basalt. Rig chatter at 415 feet.
420 – 430	Coarse sand and pea gravel with some cemented sand and caliche. Rig chattery.
430 – 432	Coarse sand and gravel up to 2.2 cm; Cemented sand, basalt, and felsic rock clasts some iron oxide stained. Some caliche.
432 – 455	Dark yellowish orange (10YR 6/6) clay passing into medium light gray (N6) shale bedrock (probably Dakota Formation). Rig quiet with slow penetration.

Table 4. The log of the cuttings produced by the driller at the northeast Haskell Co. index well site. Log taken from the submitted WWC-5 record by Clarke Well & Equipment Co.

Depth Interval (feet)	Driller's Description
0-2	Topsoil
2-28	Clay, tan, silty some caliche
28-34	Sand fine to coarse
34-45	Clay, tan, white, silty
45-56	Clay, red, brown, with caliche
56-63	Sand, fine to very fine
63-68	Clay, tan, white, with streaks of caliche and cemented sand, thin
68-80	Sand very fine, silty
80-95	Cemented sand, soft, with clay, brown, and caliche streaks
95-107	Sand, fine to coarse
107-115	Clay, tan, white, sandy, with some caliche
115-130	Sand, gravel, fine to medium
130-145	Sand, gravel, fine to coarse, with clay streaks, thin, yellow
145-245	Sand, gravel, fine to coarse
245-250	Sand, gravel, fine to coarse, with clay, gray
250-280	Sand, gravel, fine to coarse, with clay streaks, thin, yellow
280-296	Sand, gravel, fine to medium, with clay streaks, thin, yellow
296-370	Clay, tan, brown, yell, with some cemented sand, shale pieces, and caliche
370-413	Clay, tan, brown, sandy, with caliche streaks
413-433	Sand, gravel, fine to medium
433-445	Weathered shale, yellow, black
445-460	Clay, red, gray, white

Close examination of the gamma-ray log through the thick sand and gravel interval in figure 4 reveals a vertical stacking of 20-40 feet thick intervals each defined by increasing gamma-ray intensity from bottom to top from 110 feet to 285 feet below surface. The upward increase in gamma-ray intensity within each interval suggests a progressive upward change in sediment composition. Typically, this gradual upward increase within each interval would be interpreted as a fining upward of the sediment with the coarser grained quartzose sand grading upward to fine-grained deposits of silt and clay. However, in this case it could also possibly signify a progressive upward decrease in the amount of orthoclase within each interval. Because these sediments were deposited in an alluvial environment, the cyclic changes in gamma-ray intensity observed in the gamma-ray log may reflect periodic changes in the flow regime of the ancient fluvial system or shifting channels. These intervals were not detected in the cuttings recovered from drilling.

The Northeast Haskell Area

The area selected for detailed study is 64 mi² in size centered on Section 36, T. 31 S., R. 26 W., the approximate location of the index monitoring well and covers portions of northeast Haskell and adjacent western Gray counties (Figure 2). Investigation of this smaller area provided an opportunity to evaluate local variability in the distribution of permeable zones in the Cenozoic sequence and the influence of that variability on regional trends in the permeable fraction. A total of 109 logs of water wells in this local area were suitable for analysis.

Statistical Characteristics of the Thickness and Permeable Fraction Parameters: Cenozoic sequence thickness ranges from 200 feet to 657 feet (Table 5). Total permeable sediment thickness and fraction range from 81.5 feet to 449 feet and 0.28 to 0.93, respectively. The mean and median values of each parameter's distribution differ slightly and both are slightly higher than the values for the entire GMD. Standard error values are low, but higher than for the subregional study area parameters (Tables 6 and 7). The apparent increase in standard error is likely due to the small number of well logs used in the analysis.

Table 5. Statistical characteristics of the Cenozoic thickness and the total thickness and fraction of permeable deposits distributions within the local study area based on 109 water well logs. The local study area is located within the central GMD 3 subregion.

	Mean (ft)	Median (ft)	Standard Error (ft)	Range (ft)
Cenozoic Thickness	457	435	12.2	200 - 657
Total Thickness of Permeable Deposits	258	245	8.0	81.5 - 449
Permeable Fraction	0.57	0.55	0.01	0.28 - 0.93

Areal Distributions: Maps of the elevation of the bedrock surface, Cenozoic thickness, total permeable deposit thickness, and fraction are presented in figures 7, 9, 10, and 11, respectively. The residuals from modeling these parameters are presented in Appendix A. Cenozoic deposits are thickest in the southwest part of the local area and thinnest in the northeast and extreme southeast part where the underlying bedrock is shallower (Figures 7, 9). Total thickness of permeable deposits generally follows this pattern, but is not as pronounced (Figure 10). Regions of higher and lower than average permeable deposit thickness are patchy and occur only in the southwest part of the local study area. Over most of the local area the permeable fraction is between 50% and 70% (Figure 11). However, in numerous local areas the permeable fraction is less than 50%. Isolated areas where the permeable fraction is greater than 75% occur near the northwest and northeast corners of the small study area.

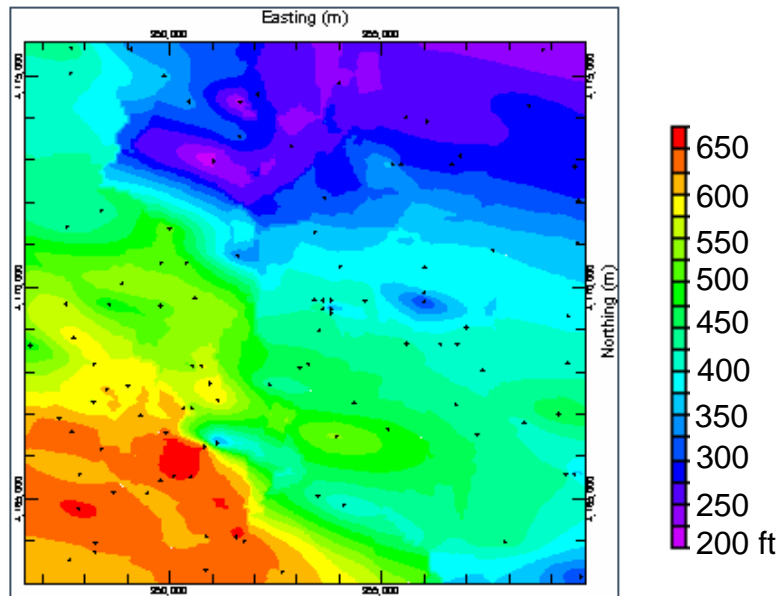


Figure 9. Thickness of Cenozoic deposits in the northeast Haskell study area derived using the default kriging algorithm to compute model grid values in RockWorks® 2004.

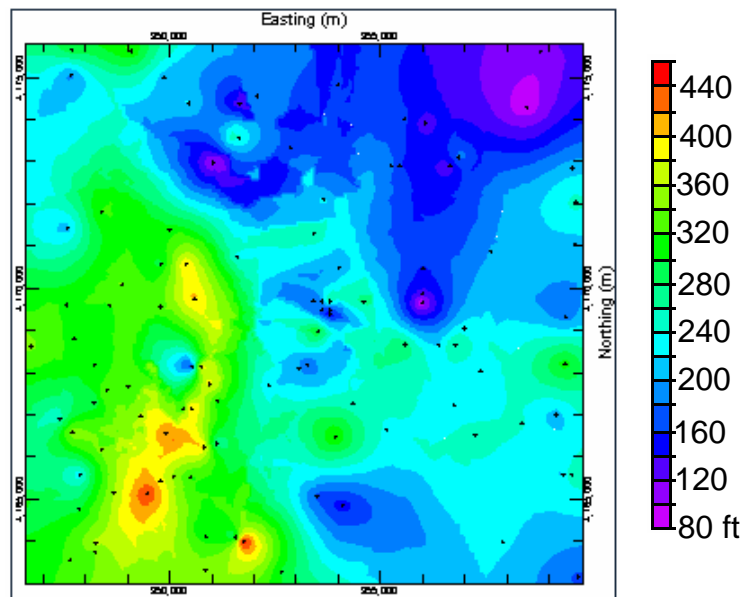


Figure 10. Thickness of permeable deposits within the Cenozoic sequence in the northeast Haskell study area derived using the default kriging algorithm to compute model grid values in RockWorks® 2004.

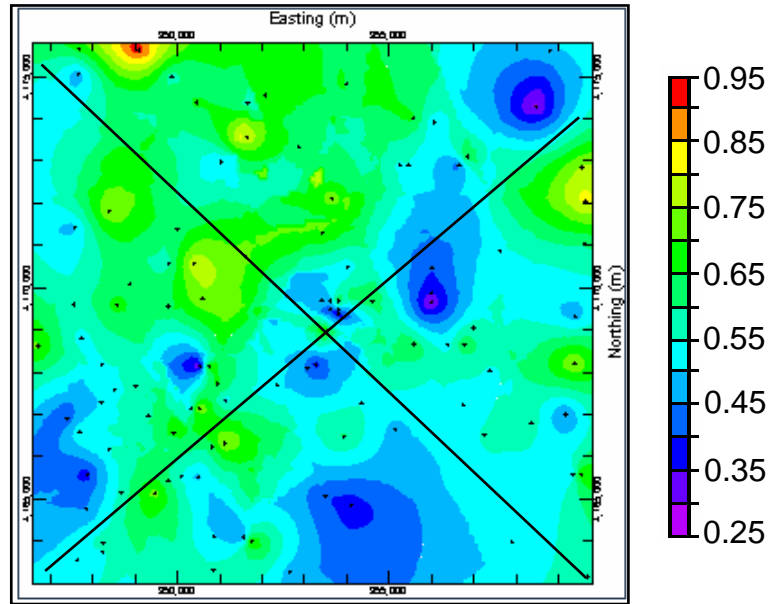


Figure 11. Permeable fraction of the Cenozoic sequence in the northeast Haskell study area derived using the default kriging algorithm to compute model grid values in RockWorks® 2004. The lines on the map indicate traces of fence diagram panels shown in figures 12 and 13.

3-D Distribution of the Permeable Fraction: The complexity of the Cenozoic sequence with respect to its permeable characteristics is pronounced in the NW-SE and NE-SW panels of the fence diagram in figures 11, 12, and 13. The top and bottom of each fence panel represents the land and bedrock surfaces, respectively. The permeable fraction is scaled from 0 to 1, where 0 is interpreted to represent non-contributing clays, silts, and cemented sands and gravels and 1 to represent permeable sand and sand & gravel (Table 2). Fractional values in between the extremes indicate variable proportions of permeable and non-contributing sediments.

The irregular, patchy mosaic of the intervals in different colors in the diagrams illustrates the high local variability in permeable fraction and by implication, lithology. Intervals in shades of yellow and red indicate zones that are primarily sand or sand and gravel, but intervals in shades of blue are primarily clay and silt with or without caliche. Intervals of cemented sand or sand and gravel were not encountered in the samples from the monitoring well or were not noted in the drillers' logs descriptions of nearby boreholes for water wells. The thick sand and gravel-silty clay sequence encountered in the northeast Haskell index monitoring well borehole is poorly represented in both fence diagram panels because of the method of interpolation used in the closest point algorithm. For the most part, permeable sediments are not present in the lower part of the sequence, including areas where prominent paleovalleys have been incised into the underlying bedrock. In most cases these depressions are filled with deposits that are less than 60% water yielding, which suggests interlayering of thin permeable and non-contributing zones

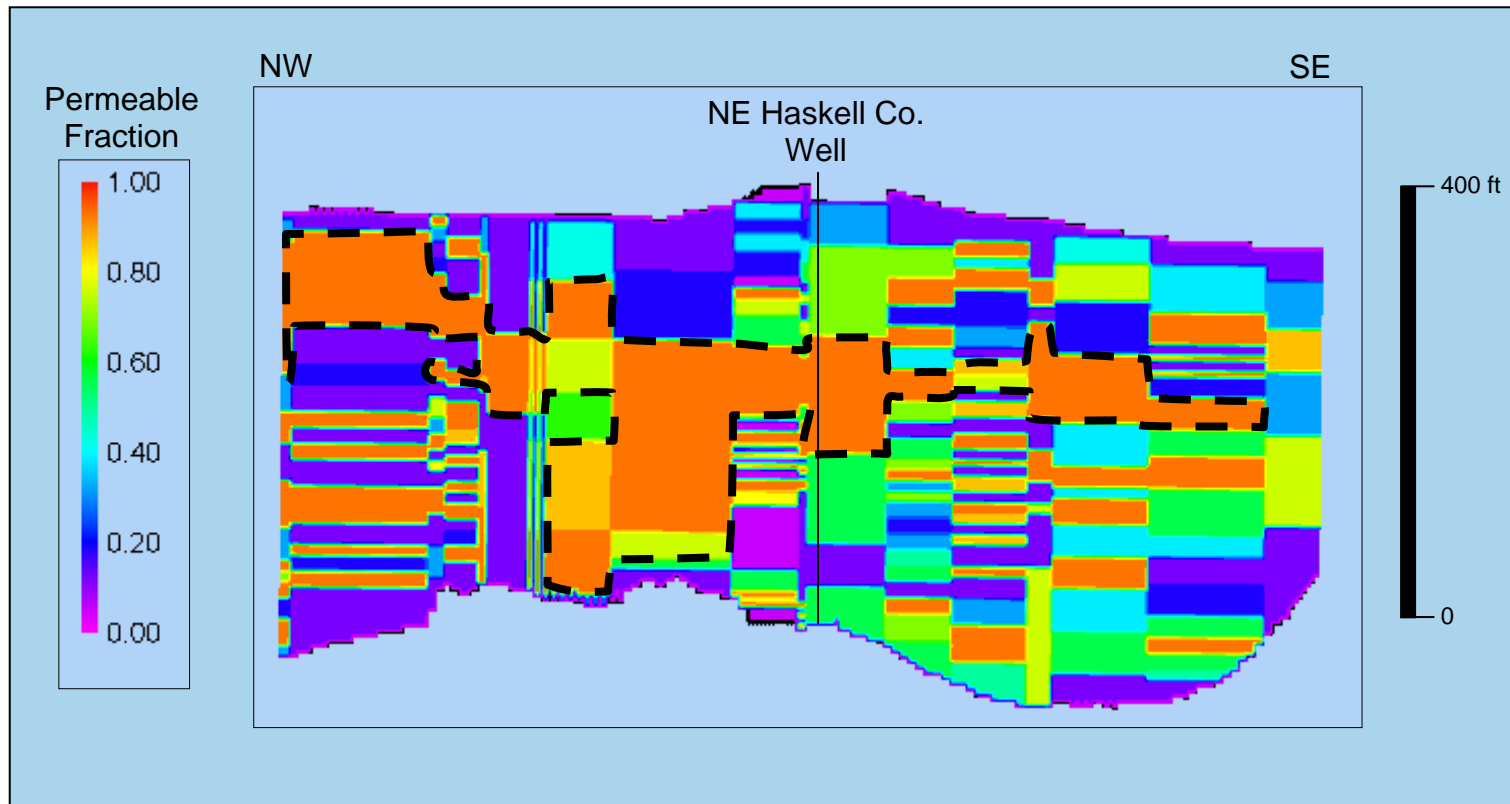


Figure 12. NW-SE panel of the fence diagram for the northeast Haskell area centered on the northeast Haskell County index monitoring well in NW Sec. 36, T. 31 S., R. 26 W. The dashed line in the panel outlines the subregionally extensive upper permeable zone in the figure.

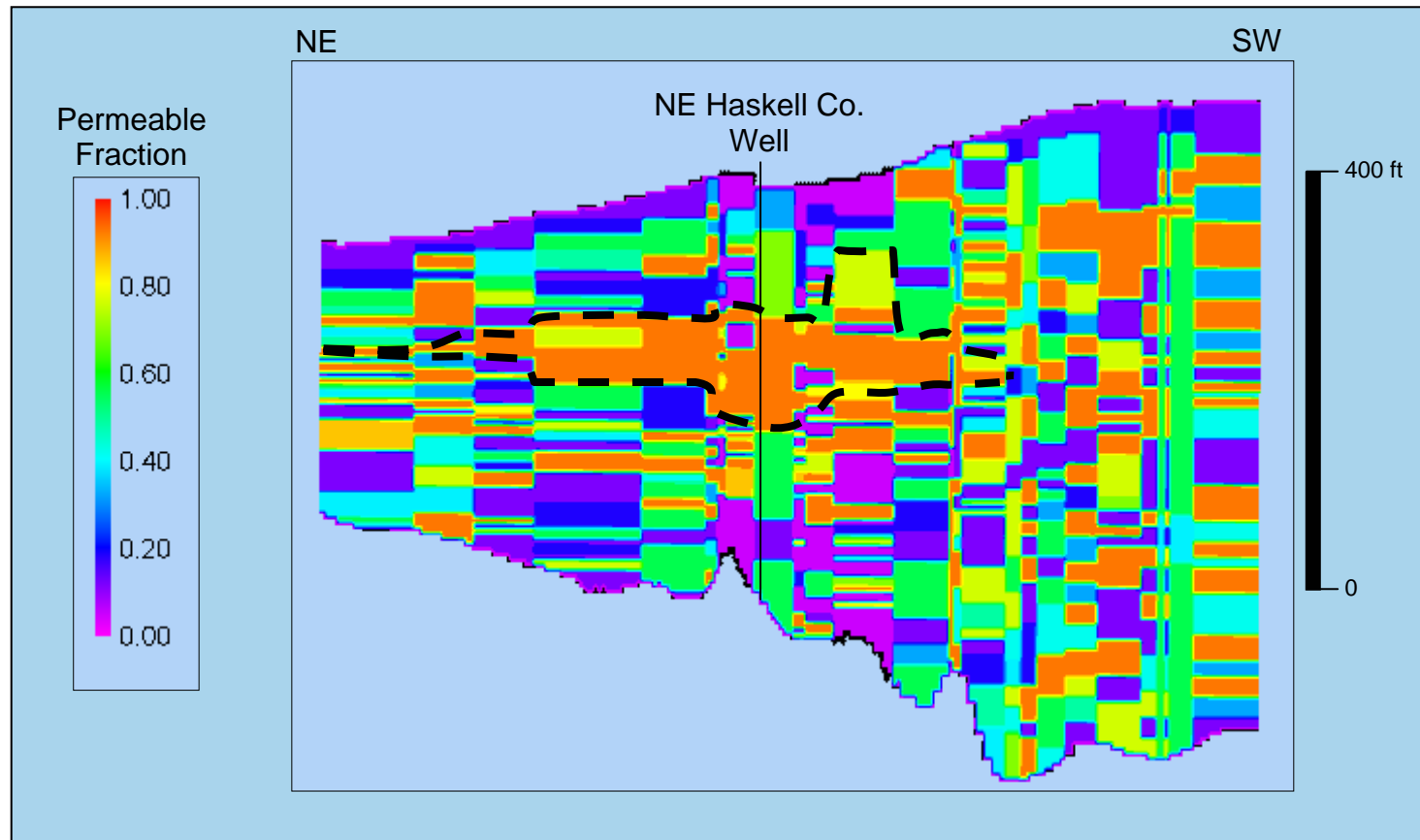


Figure 13. NE-SW panel of the fence diagram for the small study area centered on the northeast Haskell County index monitoring well in NW Sec. 36, T. 31 S., R. 26 W. The dashed line in the panel outlines the subregionally extensive upper permeable zone in the figure.

The Central GMD 3 Subregion

The central GMD 3 subregion straddles Finney-Haskell county line and includes western Gray and eastern Kearny and Grant counties. A total of 1,668 logs of water wells in this subregion were suitable for this analysis.

Statistical Character of the Thickness and Permeable Fraction Parameters: Total Cenozoic thickness and the thickness and fraction of permeable deposits in the central GMD 3 subregion reflect the distributions of these parameters for the entire District (Table 6). Total Cenozoic thickness ranges from 132 feet to 657 feet. The total thickness and fraction of permeable deposits ranges from 61 feet to 474 feet and 0.15 to 1, respectively. Mean and median values of each parameter's distribution are essentially the same but higher than the mean and median values for the entire GMD. Standard error values are low for all parameters.

Table 6. Characteristics of the Cenozoic deposit thickness and total thickness and fraction of permeable deposits distributions within the central GMD 3 subregion based on 1,668 water well logs.

	Mean (ft)	Median (ft)	Standard Error (ft)	Range (ft)
Cenozoic Thickness	405	410	2.8	132 - 657
Total Thickness of Permeable Deposits	235	236	1.9	61 - 474
Permeable Fraction	0.59	0.58	0.003	0.15 – 1.0

Areal Distributions: Maps of elevation of the bedrock surface, Cenozoic deposit thickness, permeable deposits thickness, and the fraction of the deposits considered permeable are presented in figures 14, 15, 16, and 17, respectively. The residuals from application of the RockWorks 2004 ® contouring of the model grid values of these parameters are presented in the Appendix A.

Cenozoic deposits are thickest in the south-central part of the subregion where the Greenhorn Limestone has been eroded and in the deepest section of a paleochannel incised into the underlying Dakota Formation bedrock (Figure 15). Deposits are thinnest in the northeast part of the subregion where the underlying bedrock includes the Greenhorn Limestone and other younger Cretaceous units and the bedrock surface is higher in elevation. The total thickness of permeable deposits also follows this pattern, but is not as pronounced (Figure 16). Regions of higher and lower than average total thickness are patchy. Over most of the subregion the permeable fraction brackets the subregion average, between 50% and 70% (Figure 17). However, the fraction is much lower in the southwest of the subregion where the bedrock elevation is higher (Figure 14). Isolated areas where the fraction is greater than 75% are present in the northern half of the subregional study area.

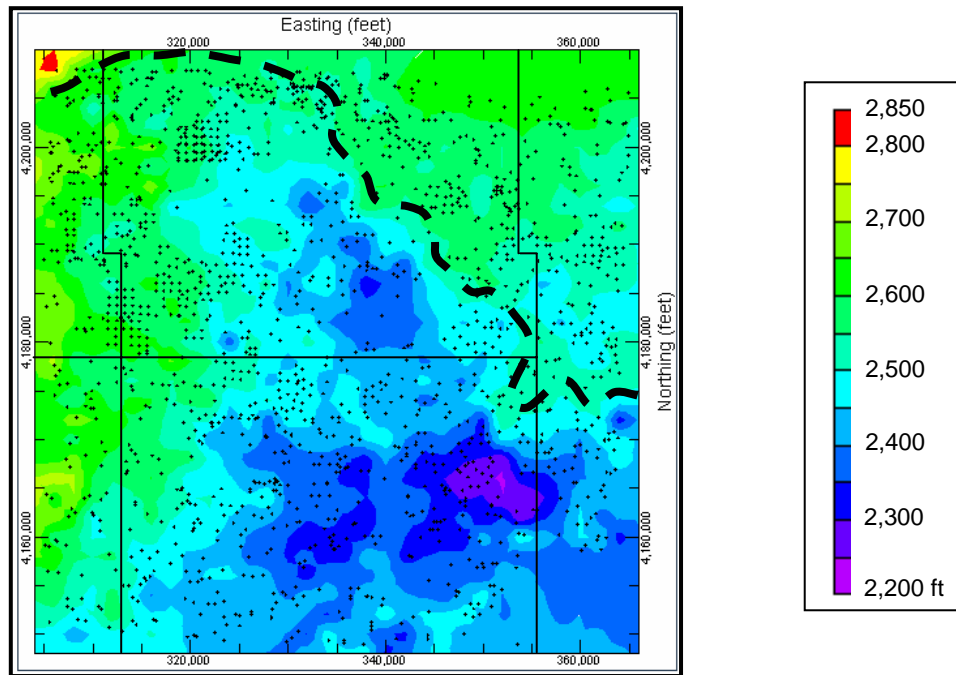


Figure 14. Elevation of the bedrock surface in the central GMD 3 subregion with the dashed line showing approximate updip edge of the Greenhorn Limestone (Macfarlane et al., 1993).

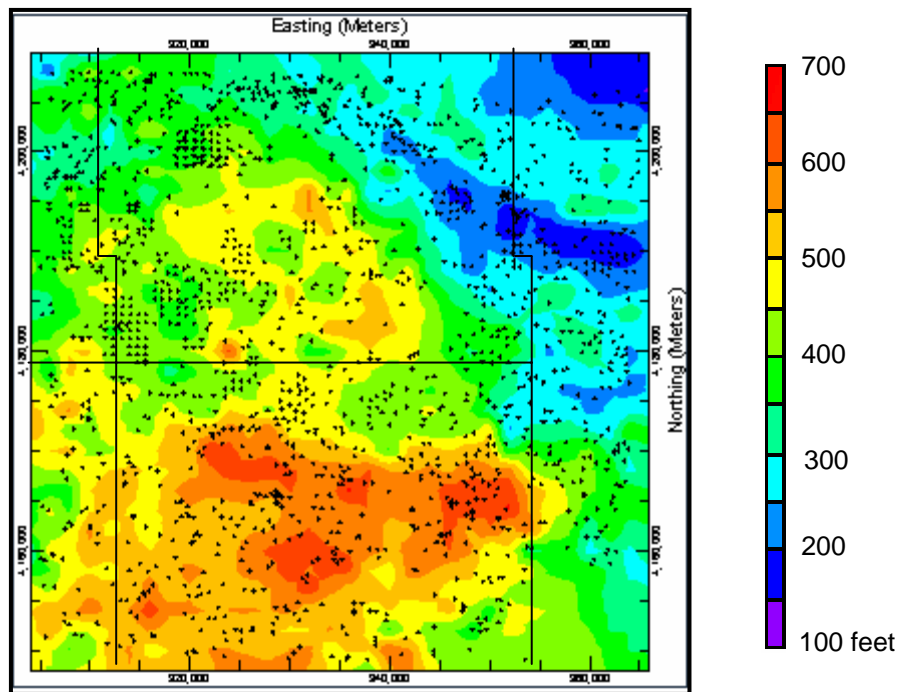


Figure 15. Thickness of Cenozoic deposits in the central GMD 3 subregion derived using the default kriging algorithm to compute model grid values in RockWorks® 2004.

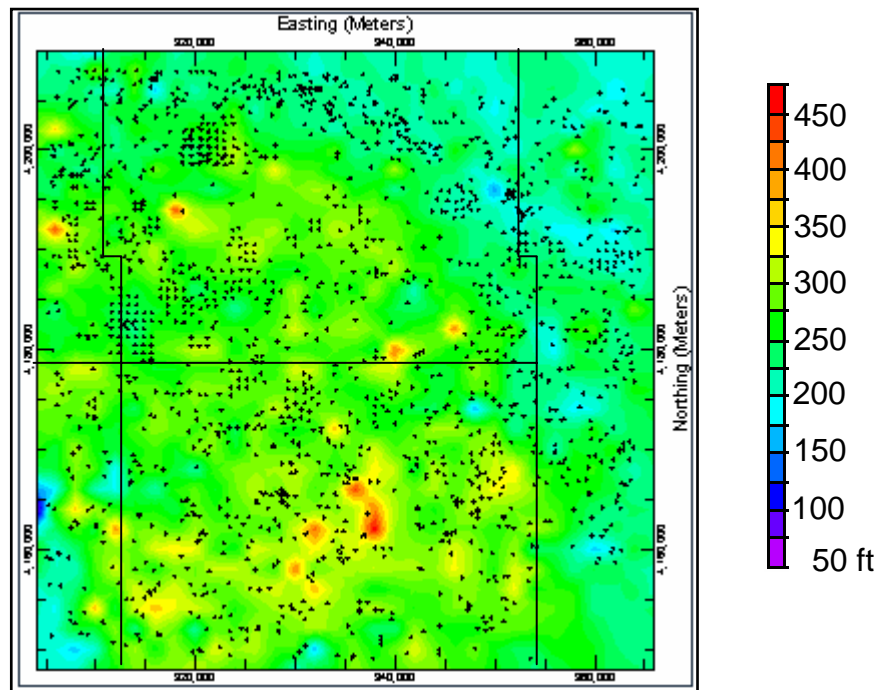


Figure 16. Thickness of permeable Cenozoic deposits in the central GMD 3 subregion derived using the default kriging algorithm to compute model grid values in RockWorks® 2004.

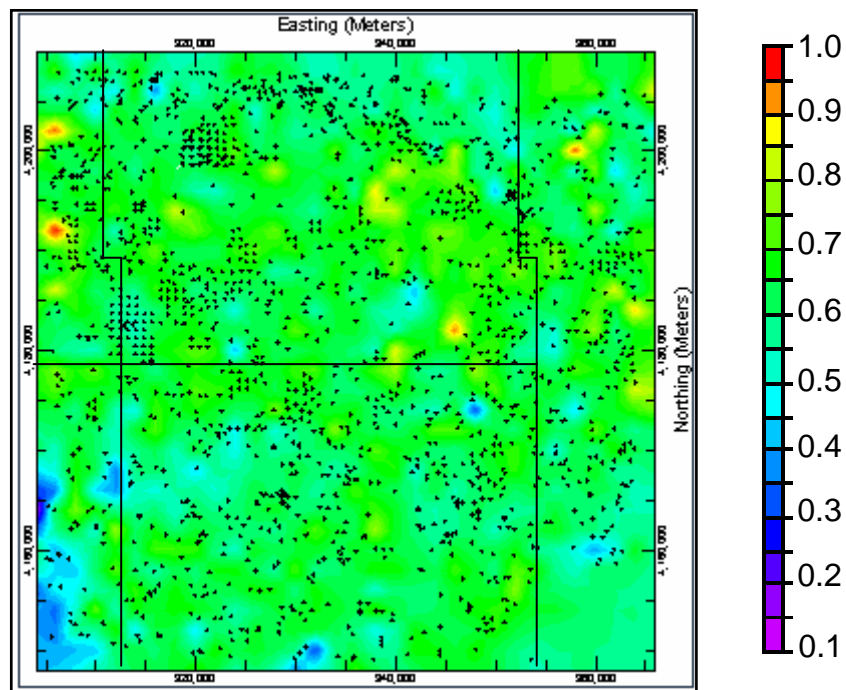


Figure 17. Permeable fraction of the Cenozoic sequence in the central GMD 3 subregion derived using the default kriging algorithm to compute model grid values in RockWorks® 2004.

3-D Distribution of the Permeable Fraction: North-south and east-west fence diagram panels viewed from the southwest in figures 18A-E portray vertical sections of the permeable fraction distribution in the central GMD 3 subregion. Successive paired north-south and east-west fences are displayed in each figure to provide perspective and illustrate the complex distribution of permeable zones within the subregion.

The main water yielding sediment zones (greater than 80% permeable sediment) and zones dominated by non-contributing sediment (less than 40% permeable) occur at several levels within the Cenozoic in the subregion. However, most of the sequence consists of 40% to 60% permeable sediment. A major permeable zone occurs in the mid to upper levels of the Cenozoic sequence that can be traced across most of the fence diagrams (Figure 18A-E). The zone extends into the northeast part of the subregion where it thins and becomes less distinct (compare Figures 18C-E to observe this progressive change). This zone appears to coincide with the thick upper sand and gravel interval from 110 feet to 285 feet encountered in the borehole for the index monitoring well that was drilled by KGS in northeast Haskell County. In the lower part of the Cenozoic section another permeable zone is best developed in the northwest part of the subregion, but elsewhere is not as prominent (Figures 18A, C-E). Zones of non-contributing deposits are tabular and occur near the surface, but at depth the zones are more sinuous in shape (Figures 18A-D). Sinuous lenses of non-contributing sediment are prominent and can be traced from panel to panel just below the middle of the Cenozoic across the southern part of the subregion (Figures 18A-E). The fence diagram panels also reveal that non-contributing sediments are as likely to fill paleovalleys incised into the bedrock as permeable sediments in this subregion.

The Strip Subregion

The strip subregion also includes the southern parts of the central GMD 3 subregion and the northeastern Haskell area. A total of 3,031 logs of boreholes drilled in this subregion were suitable for this analysis.

Overall Character of the Thickness and Permeable Fraction Parameters: As in the other study areas Cenozoic thickness, and the thickness and the fraction of permeable deposits parameters generally follow the regional distributions for the entire District (Table 7). Cenozoic deposit thickness ranges from 20 feet to 712 feet of these parameters. Permeable deposit thickness and its fractional amount ranges from 0 feet to 565 feet and 0 to 0.99, respectively. The mean and median values of each parameter's distribution are lower than in the central GMD 3 subregion. The mean and median permeable fraction values of the subregion are the same as the values for all of the Cenozoic in GMD 3. The standard error values of these parameters are low and equal to values for the central GMD 3 subregion.

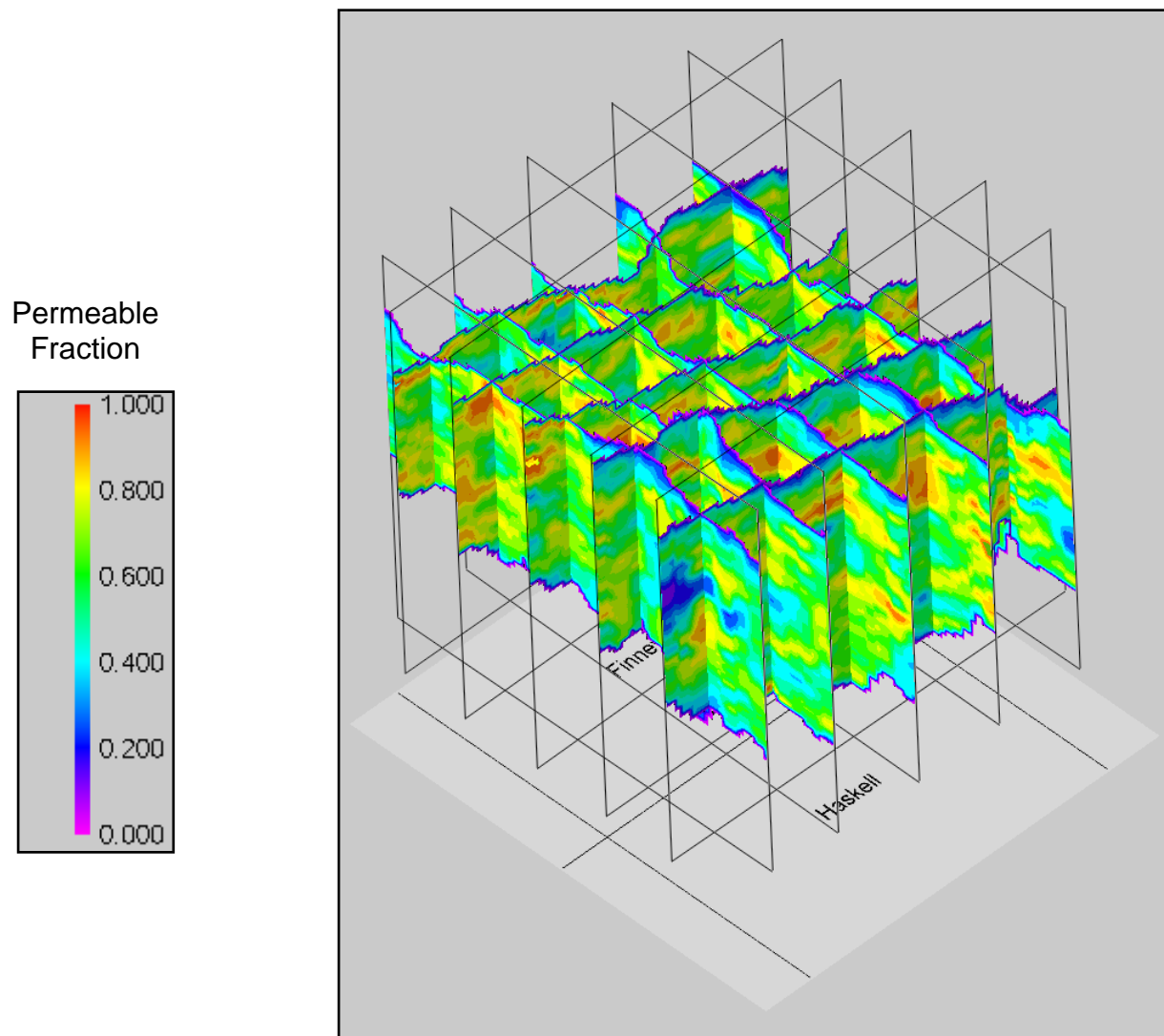


Figure 18A. Distribution of the permeable fraction in Cenozoic deposits that underlie the central GMD 3 subregion as revealed by north-south and east-west fence diagrams. The view is to the northeast from the southwest corner.

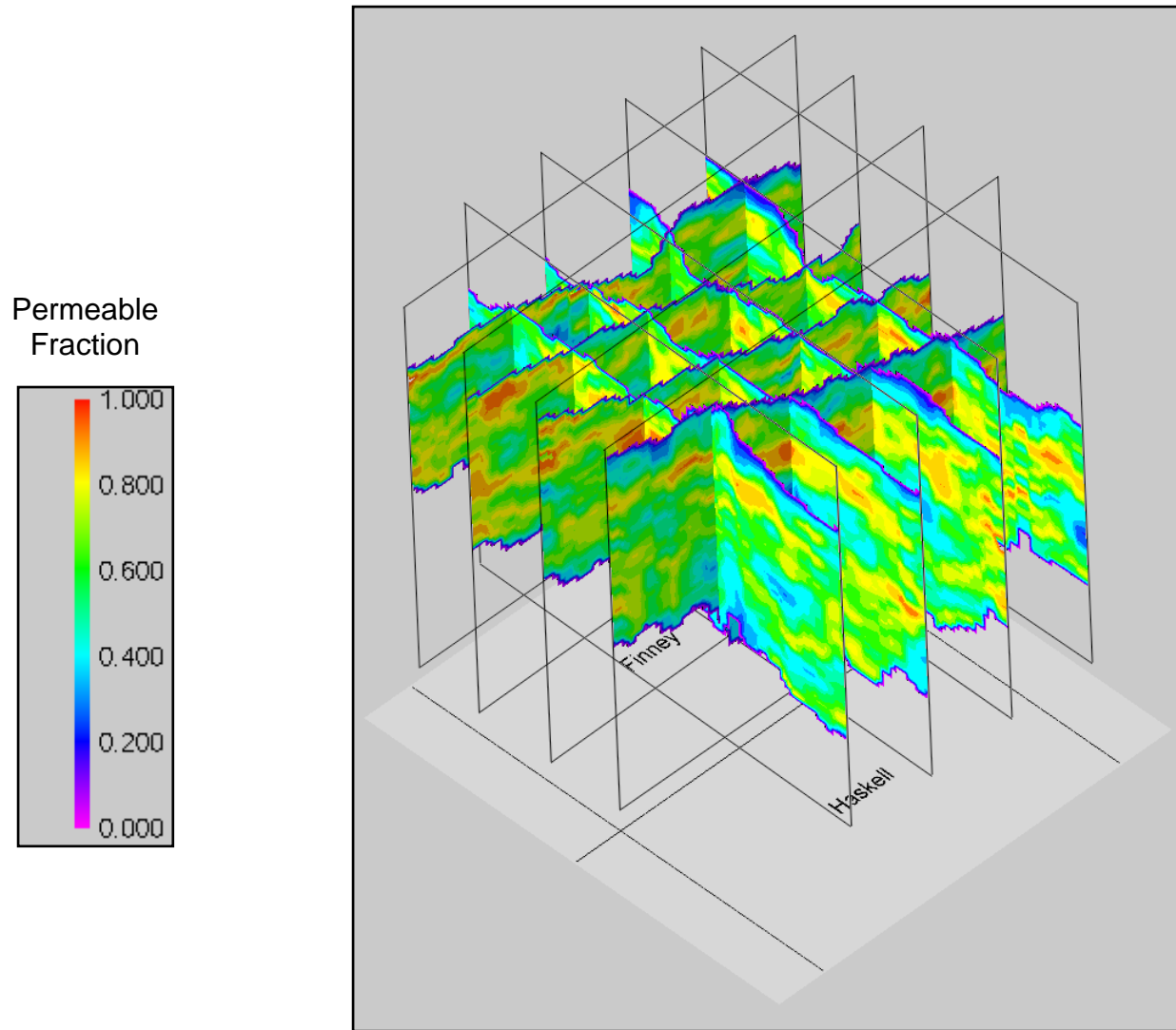


Figure 18B. Distribution of the permeable fraction in Cenozoic deposits that underlie the central GMD 3 subregion as revealed by north-south and east-west fence diagrams. The view is to the northeast from the southwest corner.

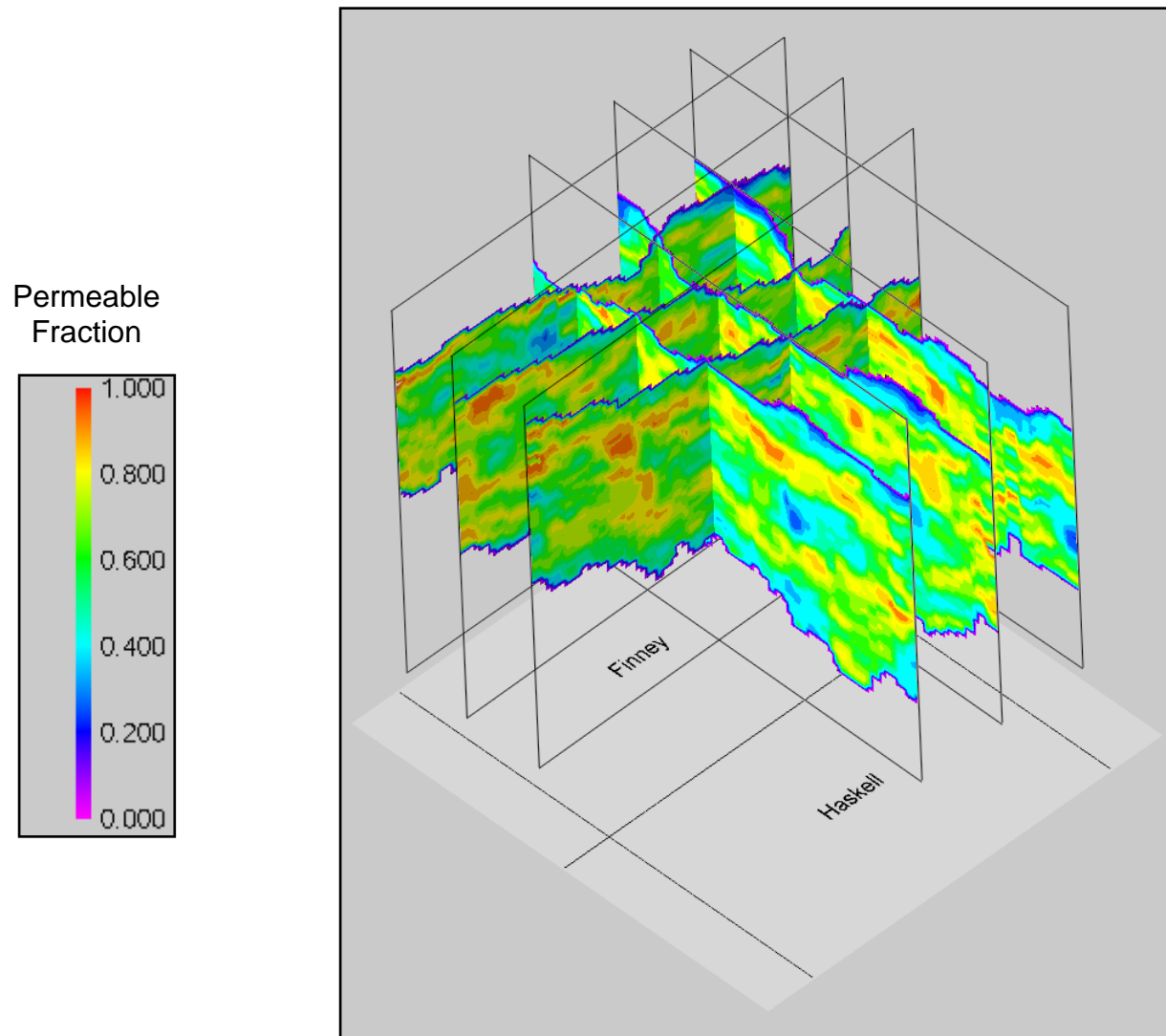


Figure 18C. Distribution of the permeable fraction in Cenozoic deposits that underlie the central GMD 3 subregion as revealed by north-south and east-west fence diagrams. The view is to the northeast from the southwest corner.

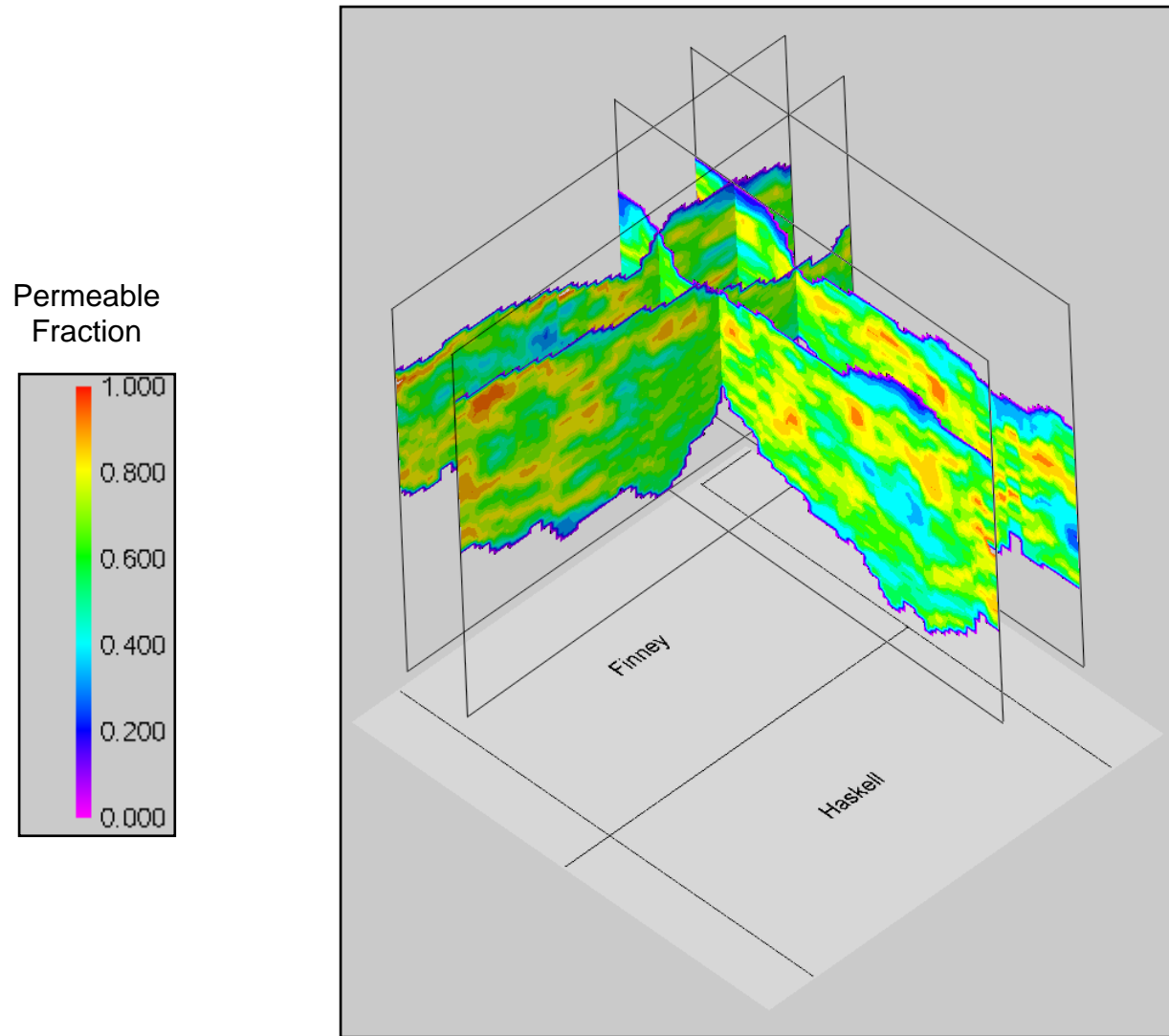


Figure 18D. Distribution of the permeable fraction in Cenozoic deposits that underlie the central GMD 3 subregion as revealed by north-south and east-west fence diagrams. The view is to the northeast from the southwest corner.

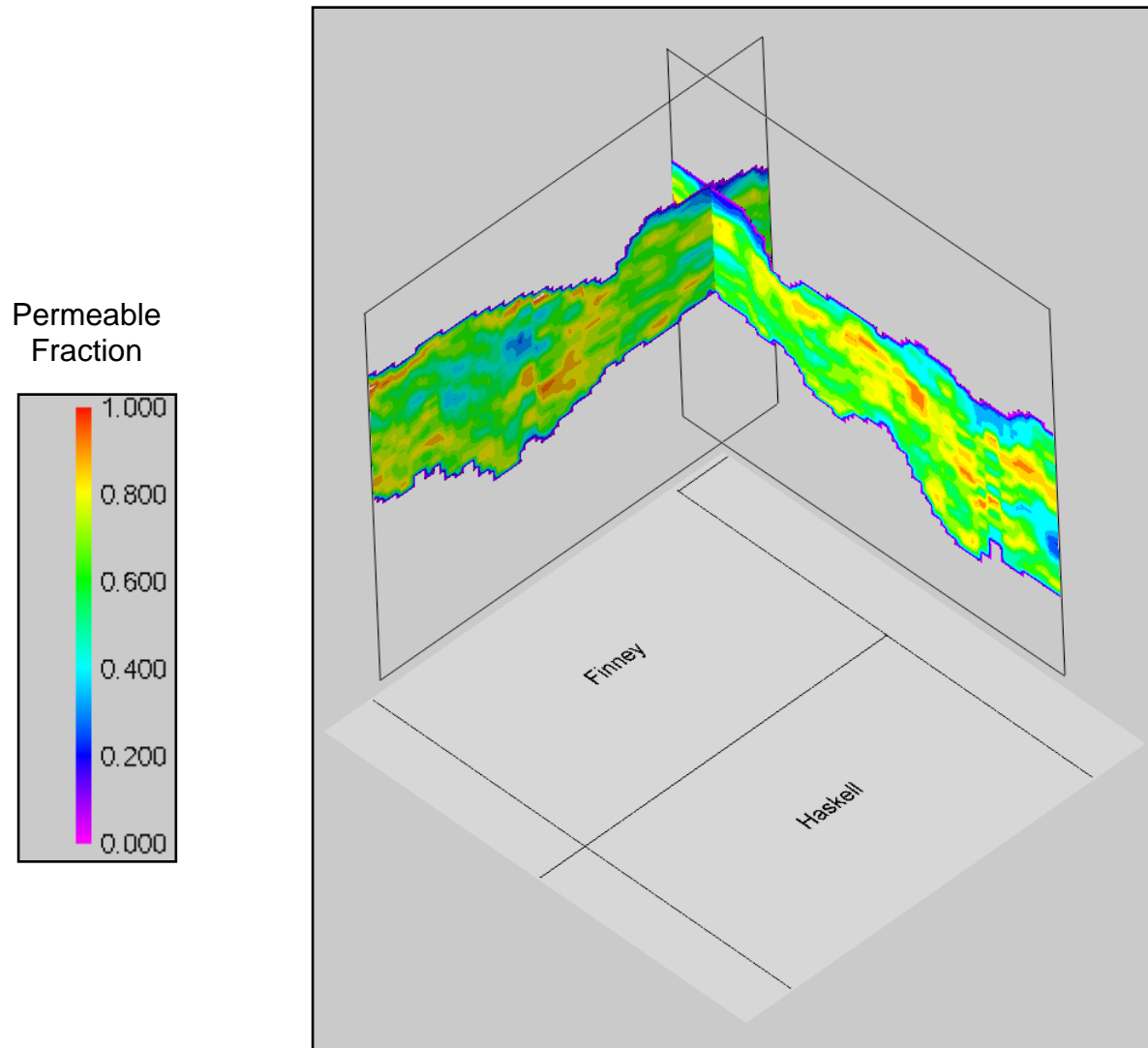


Figure 18E. Distribution of the permeable fraction in Cenozoic deposits that underlie the central GMD 3 subregion as revealed by north-south and east-west fence diagrams. The view is to the northeast from the southwest corner.

Table 7. Characteristics of the Cenozoic thickness and total thickness and fraction of permeable sediments distributions within the strip subregion based on 3,031 water well logs.

	Mean (ft)	Median (ft)	Standard Error (ft)	Range (ft)
Cenozoic Thickness	372	390	2.2	20 - 712
Total Thickness of Permeable Deposits	193	183	1.9	0 - 565
Permeable Deposit Fraction	0.50	0.52	<0.01	0- 0.99

Areal Distributions: Maps of the bedrock surface elevation, Cenozoic deposits thickness, and total thickness and fraction of permeable deposits are presented in figures 19, 20, 21, and 22, respectively.

The bedrock surface slopes eastward from near the eastern flank of the Sierra Grande Uplift to the Crooked Creek-Fowler evaporite-dissolution zone in Meade County (Figure 19; Macfarlane and Wilson, 2006). Permian units subcrop beneath the Cenozoic in the southeast part of the subregion and along the southern subregion border (Macfarlane et al 1998). Northward from the Permian subcrop, progressively younger Mesozoic units underlie the Cenozoic sequence. In the northeastern part of the area the resistant Upper Cretaceous Greenhorn Limestone underlies the Neogene and forms an escarpment near its southwestern extent in the subregion in southern Gray County.

Cenozoic deposits are thinner in the western, northeastern, and southeastern parts of the subregion and thicker in the northwestern and central part of the subregion where the bedrock surface elevation is higher. Cenozoic deposit thickness is lower beneath the Cimarron River valley, where the river has cut down through the upper part of the sequence (Figure 20). In the northwestern part of the subregion, a thick section of Cenozoic deposits fills a paleovalley that overlies the Bear Creek evaporite-dissolution zone (Macfarlane and Wilson, 2006). The total thickness of permeable deposits in the sequence generally follows the Cenozoic thickness pattern, but is not as pronounced (Figure 21). Isolated areas of higher and lower than average total thickness occur throughout the subregion. Many of these localized, anomalously high or low values correlate with high or low residuals from mapping using the kriging gridding algorithm and thus represent map error (Appendix A, Figure A8). Over most of the subregion the permeable fraction is between 45% and 70% (Figure 22). However, there are numerous patchy areas where the fraction is less than 50% primarily where Cenozoic thickness is less in the western and eastern parts of the subregion.

3-D Distribution of the Permeable Fraction: Views of the fence diagram panels in figure 23 show that most of the Cenozoic sequence in the strip subregion consists of at least 45 % to 70% permeable sediment. The patches of blue and green in the western and eastern parts of the fence

diagram indicate that much of the Cenozoic is dominated by less permeable sediment. In contrast, the reds, yellows, and greens in the central part and eastern parts of the subregion indicate that the Cenozoic is more permeable. This pattern is consistent with the mapped distribution of thickness and fraction of permeable deposits for the entire GMD (Figures 5 and 6).

Zones of greater than 70% permeable sediment can be traced across most of the subregion at various levels within the Cenozoic (Figure 23). The upper permeable zone that is continuous across Haskell and eastern Grant counties is the same as that described in the central GMD 3 subregion and the northeast Haskell area sections of this report. A lower zone extends continuously from central Seward into the central part of Meade County but becomes discontinuous and less permeable in Grant, Haskell, and Gray counties. Individual pods of greater than 75% permeable sediment tend to be elongated vertically suggesting stacking and amalgamation of individual lenses of permeable sediment in paleovalley systems. In figure 6 a band of more permeable sediment extends from northwestern Stanton County into northern and southwestern parts of Stevens County. Inspection of the fence diagram panels in the vicinity of the band indicates that the sediments are 45% to 70% permeable with isolated zones of more permeable sediment especially in the north-south panel that crosses southeastern Stanton County (Figure 24).

Zones of low permeable sediment fraction are displayed in shades of blue and are sinuous to tabular in shape and occur at all levels in the Cenozoic sequence. Low permeable fraction zones are more numerous in the sequence in the western half of the strip subregion. McMahon et al. (2003) reported finding several clay-silt zones in at several levels in boreholes penetrating the unsaturated zone in Morton and Finney counties. They noted encountering a brown silty clay that graded into a stiff, plastic, blue clay in the CAL-122 borehole near the Finney-Haskell County line and approximately 7 miles northwest of the northeast Haskell County index monitoring well site. This zone of low permeability sediment is portrayed in the northernmost east-west panel of the fence diagram (Figure 23). In the eastern part of the subregion, these zones are predominantly shallow and may represent loess and fine-grained floodplain deposits bearing volcanic ashes (Figure 23; Frye, 1942; Izett and Honey, 1995). Zones of less permeable sediment also occur deeper in the sequence. In southeastern Grant County a thick zone of less permeable sediment shown in blue is present in the middle upper part of the sequence (Figure 24). Logs of wells drilled in the vicinity indicate that a thick section of gray-tan to blue-gray clayey silt and fine sand bearing fragments of lignite and mollusk shells occurs in the middle of the Cenozoic section (Feder et al., 1964). The extent and thickness of this feature in the fence diagram coupled with the lithologies and preserved organic remains recovered from drilling suggest local deposition of fine grained sediment over an extended period in an environment that was at least occasionally wet.

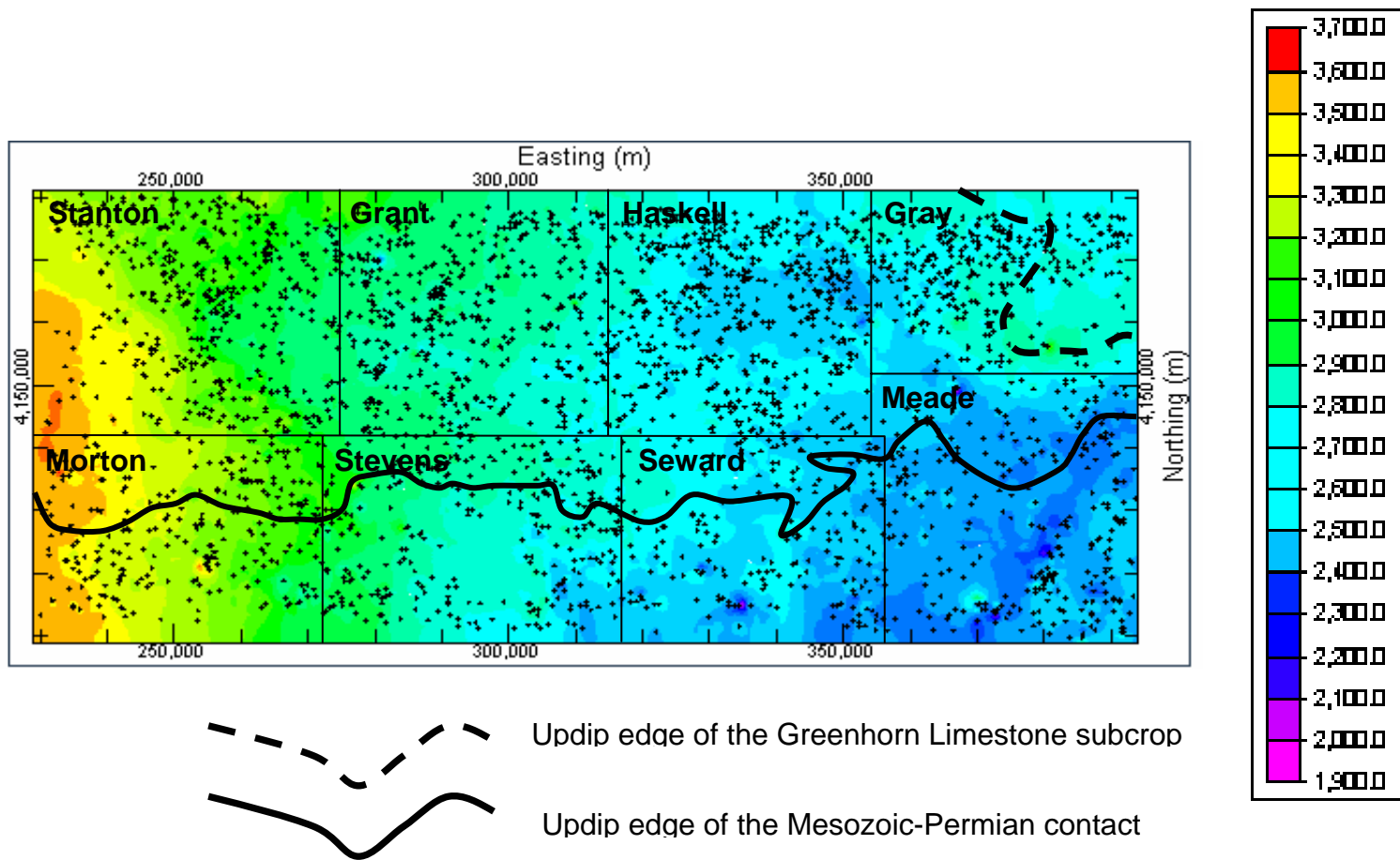


Figure 19. Elevation of the bedrock surface beneath the Cenozoic sequence in the strip subregion derived using the default kriging algorithm to compute model grid values in RockWorks® 2004.

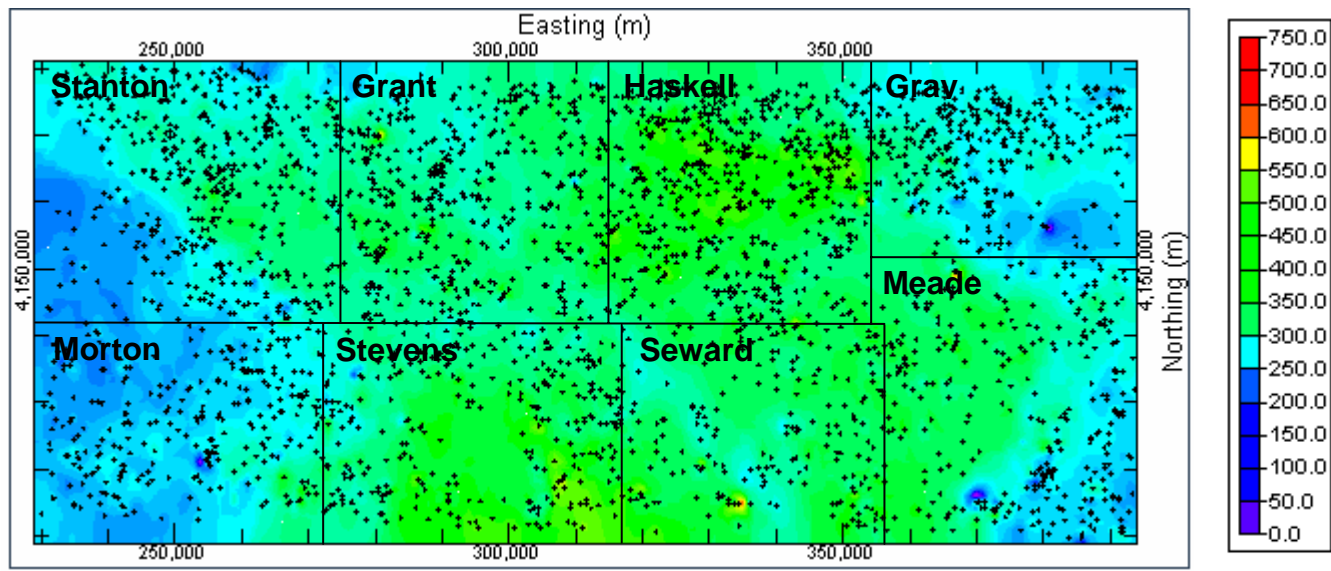


Figure 20. Thickness of Cenozoic deposits in feet within the strip subregion derived using the default kriging algorithm to compute model grid values in RockWorks® 2004.

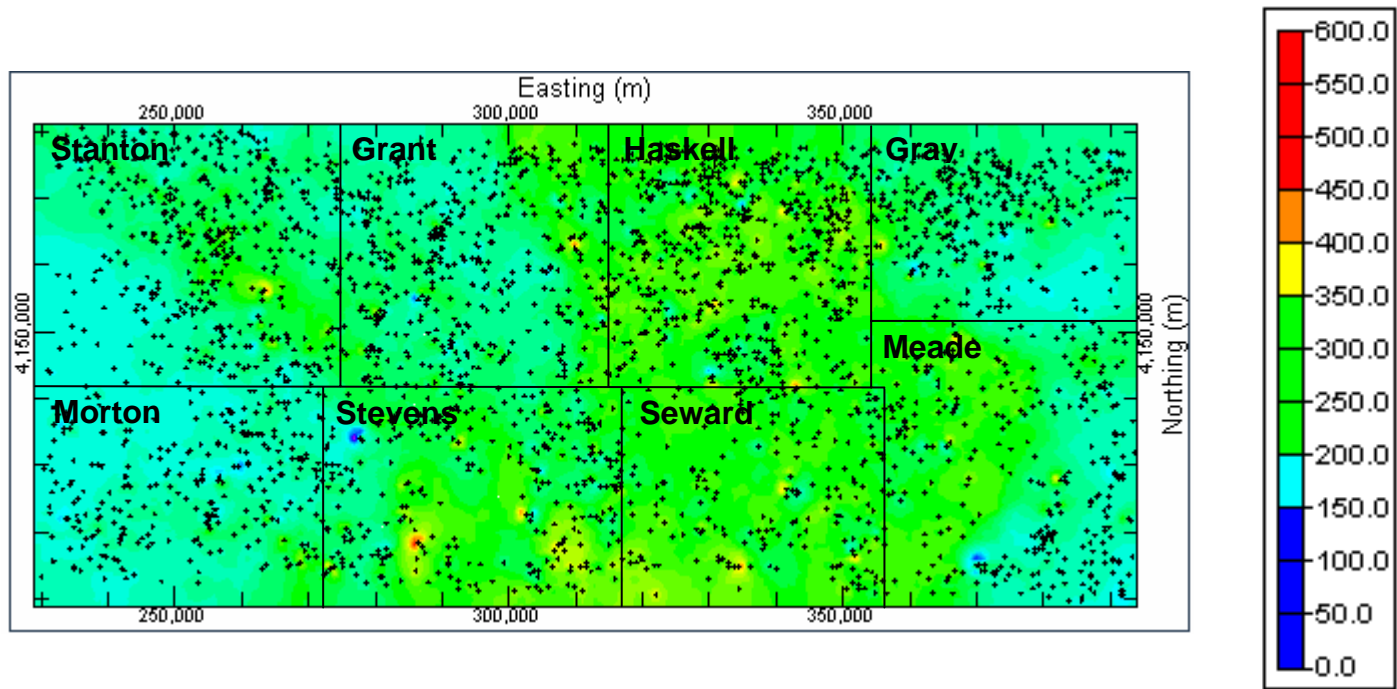


Figure 21. Thickness of permeable Cenozoic deposits in feet within the strip subregion derived using the default kriging algorithm to compute model grid values in RockWorks® 2004.

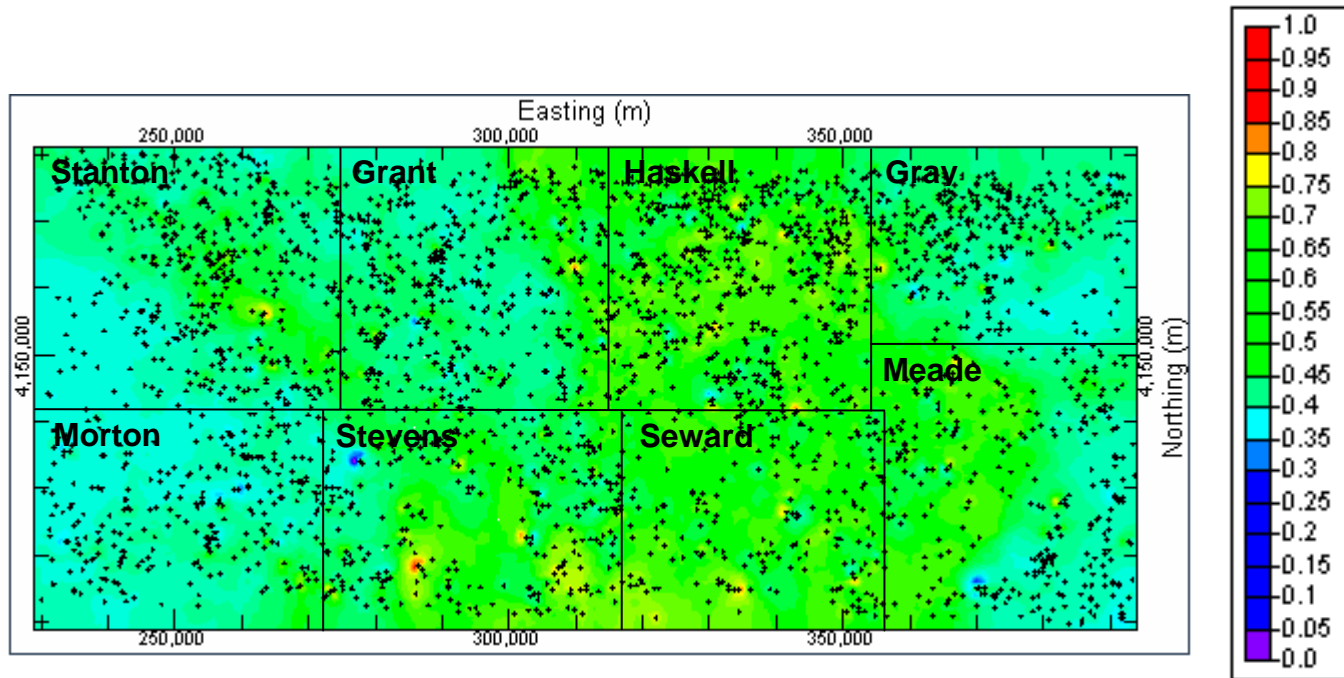


Figure 22. The distribution of the permeable sediment fraction in Cenozoic deposits in the strip subregion derived using the default kriging algorithm to compute model grid values in RockWorks® 2004.

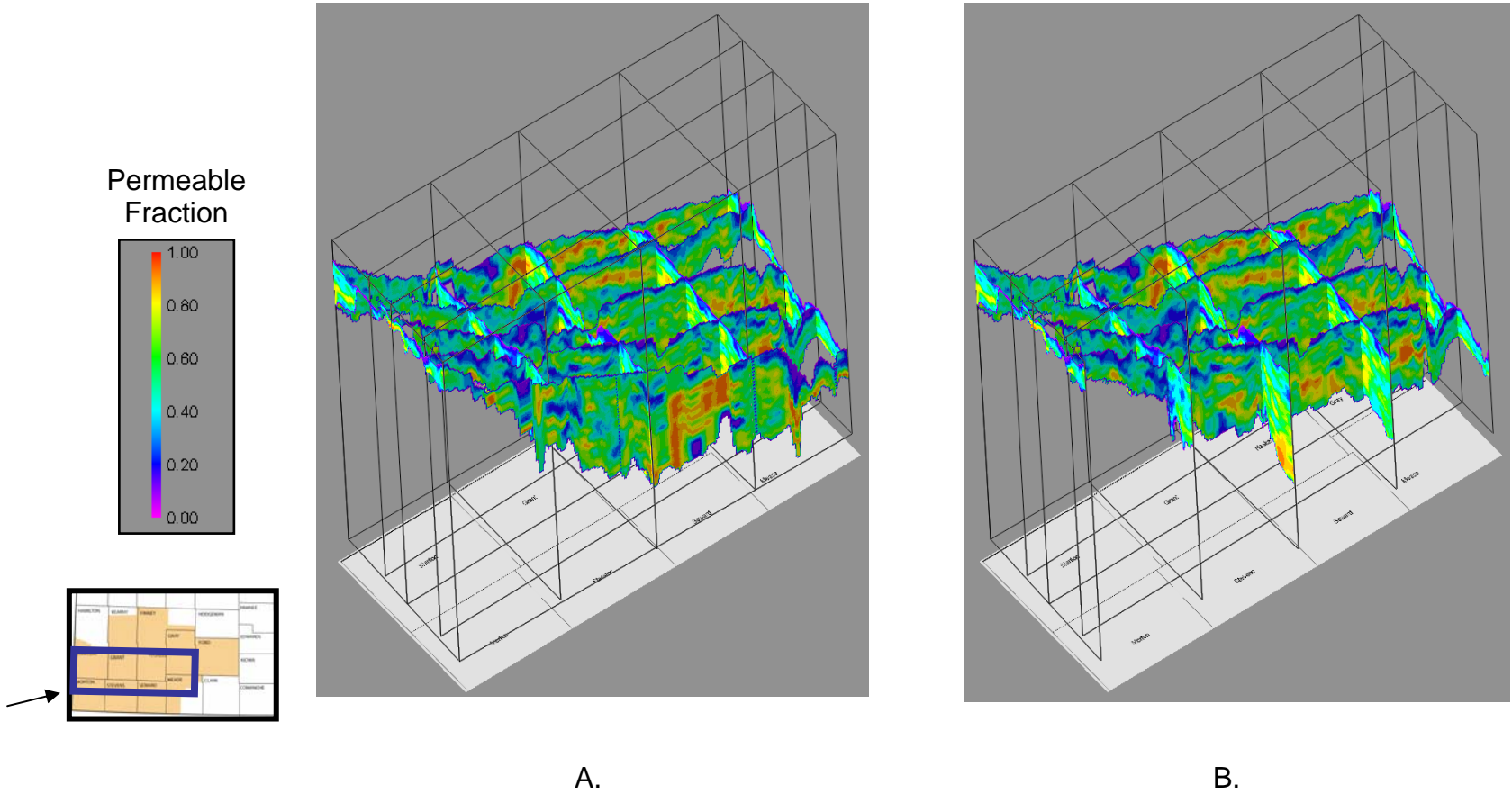
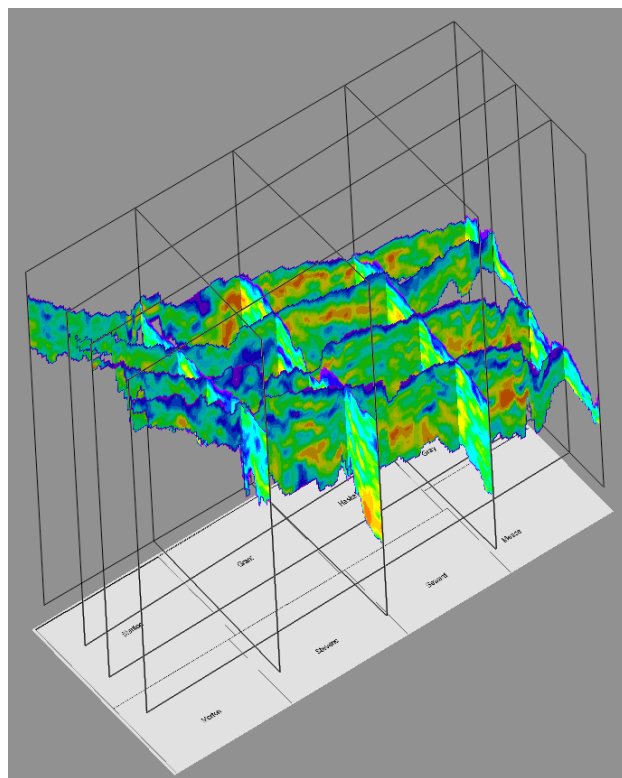
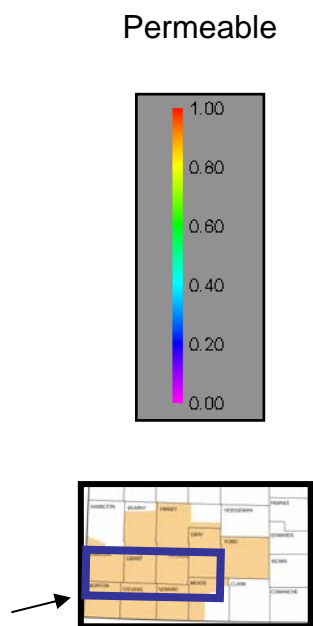
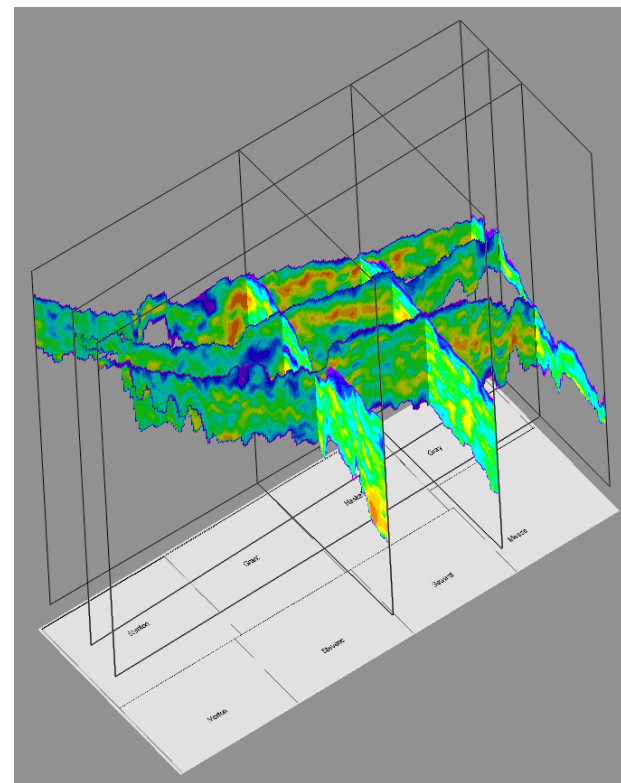


Figure 23. Fence diagram of the strip subregion in GMD 3 showing the distribution of the permeable fraction in Cenozoic deposits.

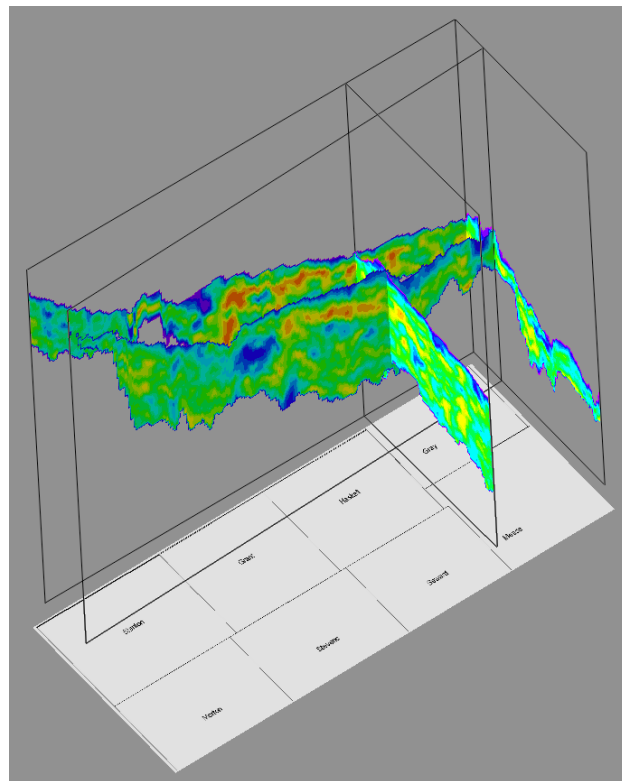
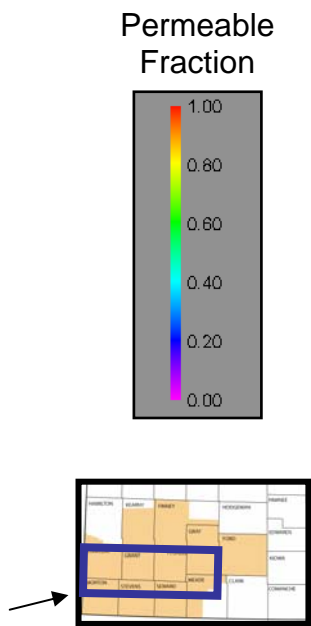


C.

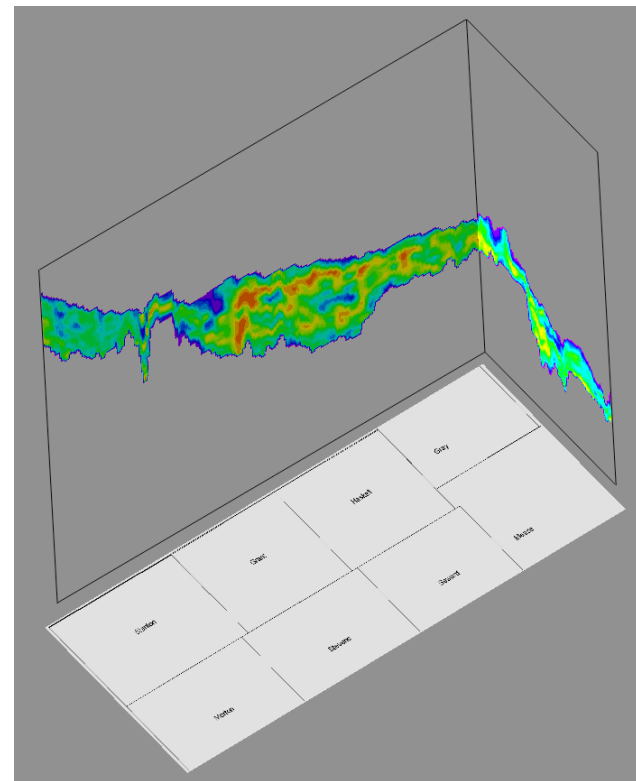


D.

Figure 23 (continued). Fence diagram of the strip subregion in GMD 3 showing the distribution of the permeable fraction in Cenozoic deposits.



E.



F.

Figure 23 (continued). Fence diagram of the strip subregion in GMD 3 showing the distribution of the permeable fraction in Cenozoic deposits.



Figure 24. Fine-grained sediment near the top of the Cenozoic section near Crooked Creek in NW NW Sec. 21, T. 33 S., R. 28 W.

Practical Saturated Thickness

PST is the total thickness of permeable sediments in the saturated aquifer that contribute significantly to well yield. Excluded are sediments that do not contribute significantly. These low-permeability lithologies generally have high porosities and may be capable of storing significant quantities of water that can be released very slowly to more permeable saturated sediments. However, the amount of water released from clay and silt layers appears to be small in comparison to the amount pumped from the aquifer. For example, the trend of the hydrograph of a well in NE NE SE Section 28, T. 27 S., R. 34 W. shows an overall fairly steady increase in the depth to water from the measurement point over time (Figure 25). However, the apparent increase accelerates as the water level in the well passes across less permeable intervals and there is an apparent leveling off of the increase in depth to water at the point where there is a change in the permeable fraction or lithology. The acceleration in the rate of change as the water table passes from sand to clay is interpreted to result from the lack of contribution of water to wells during the pumping season. The leveling off of the rate of change could be interpreted as leakage of water from less permeable sediment to the underlying water table. The other interpretation is that the apparent stair-step pattern of the hydrograph may result from the transition from locally confined to unconfined conditions as the water table passes across

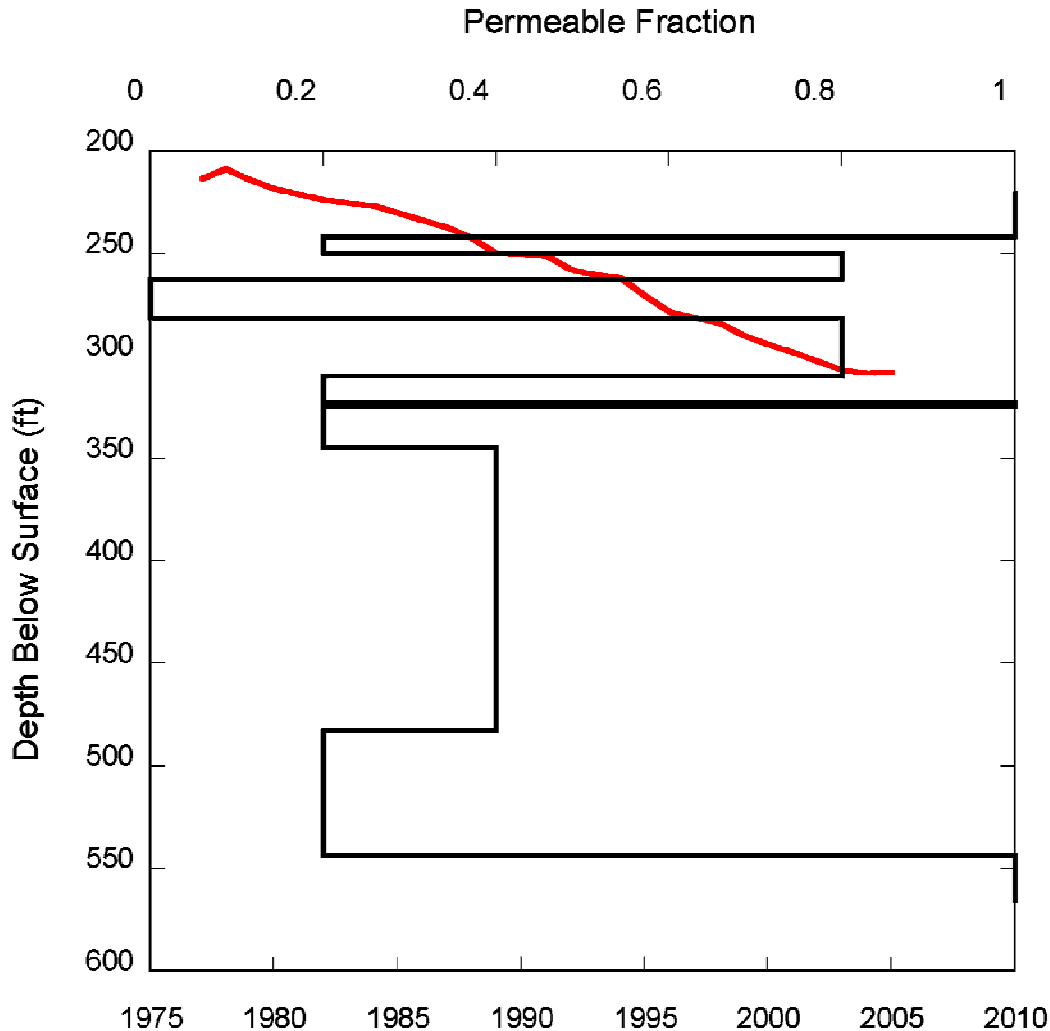


Figure 25. The hydrograph and the profile of permeable fraction for an irrigation well in NE NE SE Section 28, T. 27 S., R. 34 W.

boundaries separating lithologies of differing permeability with the pause representing the addition of leakage to the water table. The impact of leakage on the rate of increase in the depth to water over time though measurable is minor in comparison to effects of withdrawal by pumping wells.

Changes in PST from Pre-development to 2006

Under pre-development, PST exceeded 150 feet in most of the central part of GMD 3 and exceeded 450 feet in parts of southern Stevens and Seward counties (Figure 26). Elsewhere in the District PST was less than 150 feet. The PST/ST fraction distribution under pre-development is similar to the permeable fraction distribution in the Cenozoic with higher values in the central part and lower values in the western part of GMD 3 and near the Crooked Creek-Fowler evaporite dissolution zone in Meade and southern Ford counties where the Cenozoic thickness is thin (Figure 27). Pre-development PST/ST fraction and PST are higher in a band that extends

from northwest to southeast Stanton to north central and southwest Stevens counties. PST/ST fraction values are generally higher and PST is less than 150 feet along and south of the Arkansas River valley in eastern Finney, Gray, and Ford counties.

Between pre-development and the 2006 annual water-level measurement survey, irrigation has reduced the PST thickness most significantly in the central part of GMD 3 where water use density is highest with more localized changes in the PST fraction of ST (Figures 28-29). Under pre-development PST exceeded 150 feet in the parts of southeastern and northwest Stanton County, the northern half of Seward, most of Haskell, and southern Finney counties. In 2006 PST exceeds 150 feet in only a few isolated areas of these counties. The areas least impacted by ground-water withdrawals appear to be in Stevens, Seward, and the western half of Meade counties. Elsewhere, areas with less than 50 feet of PST have expanded in the western, northern and eastern parts of the District, particularly in Morton, Stanton, southern Hamilton, Kearny, northern Finney, Gray, and Ford counties. Changes in the PST/ST fraction from pre-development to 2006 are not consistent across the District with some local areas having experienced an increase while other areas experienced a decrease. This results because of the non-uniform vertical distribution of permeable lithologies within the aquifer. In areas where the PST/ST fraction decreased the saturated part of the aquifer in 2006 consists of relatively less permeable sediment, but in areas where the fraction increased the saturated aquifer now consists of relatively more permeable sediment.

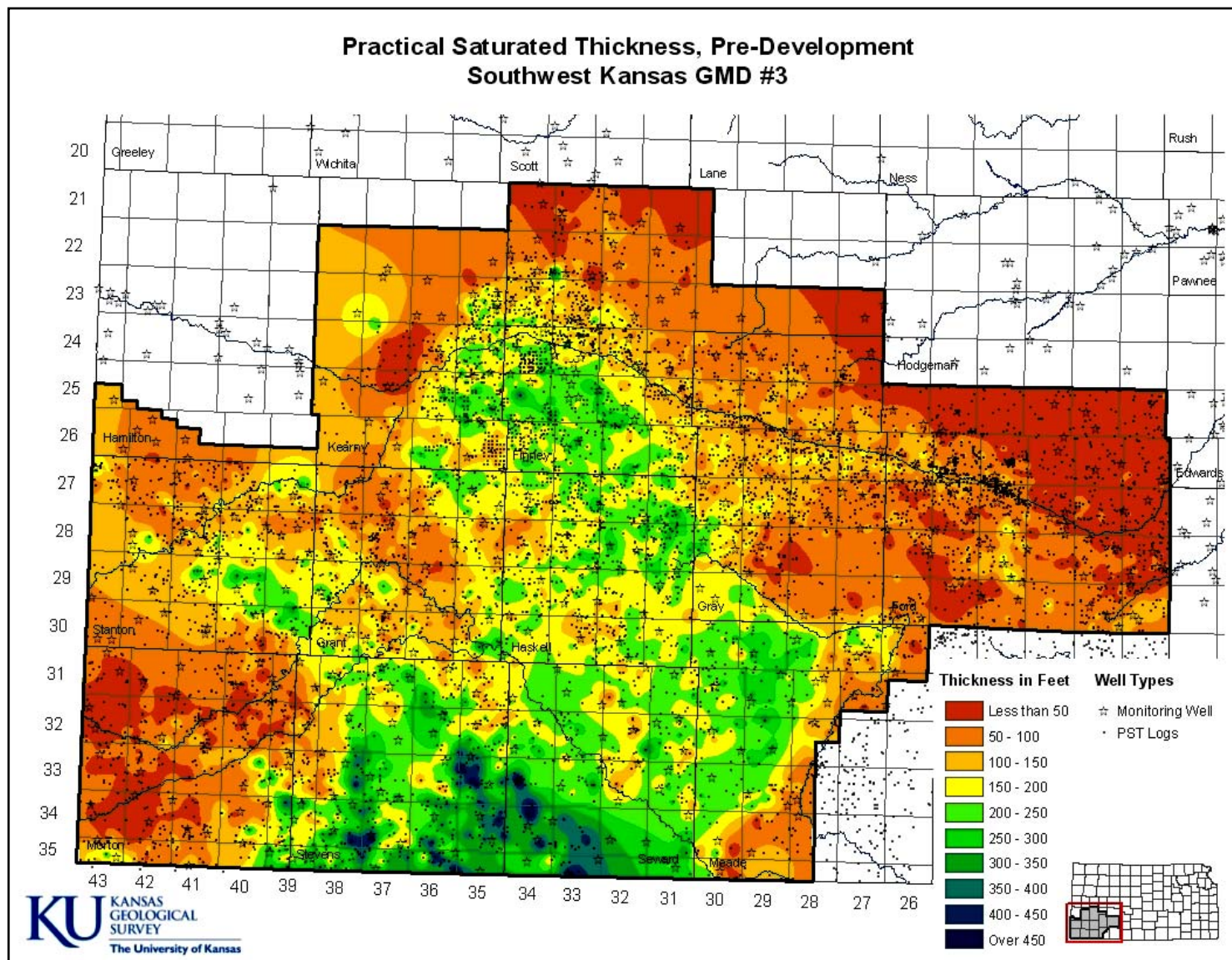


Figure 26. Pre-development PST in GMD 3.

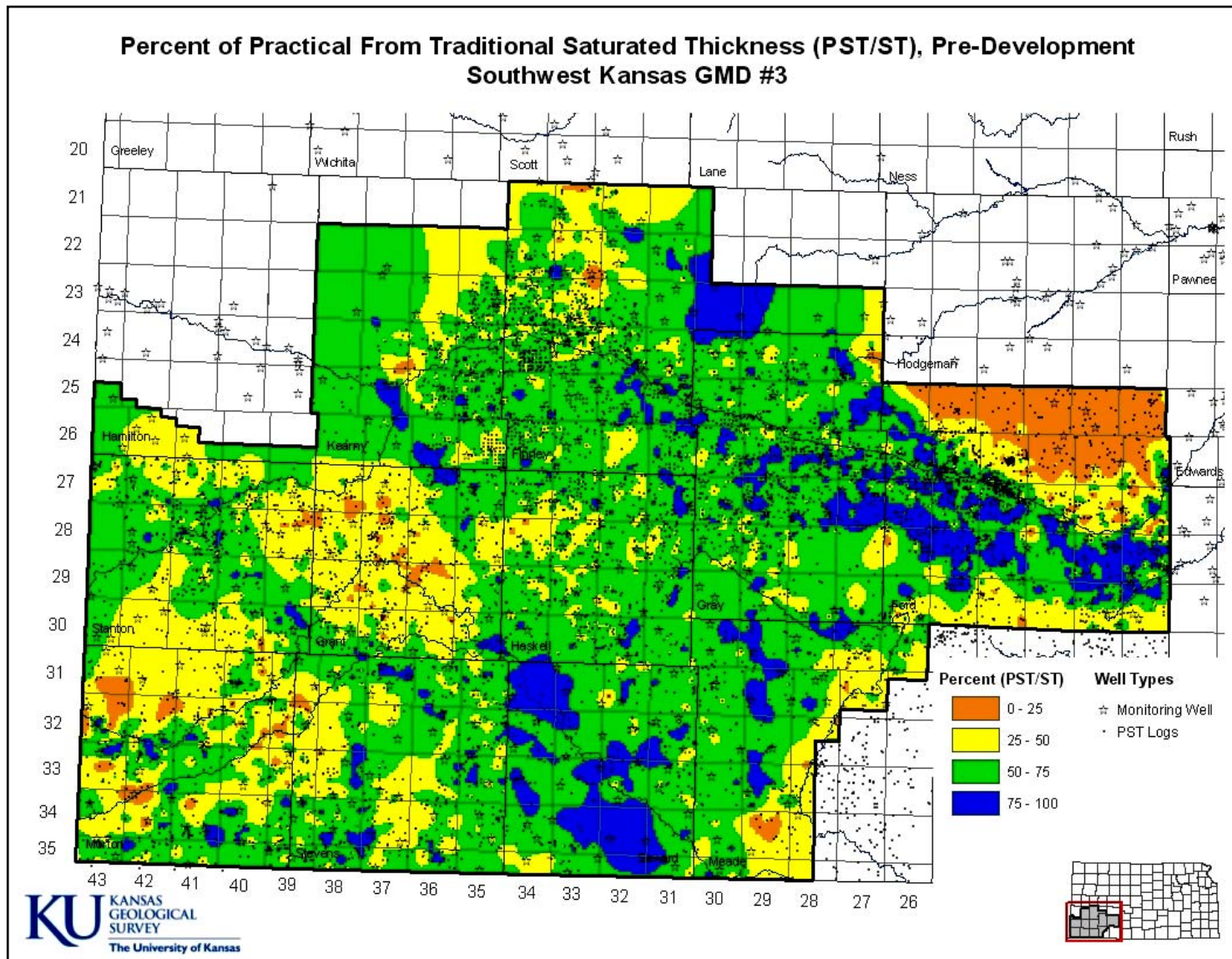


Figure 27. Predevelopment PST/ST fraction expressed as a percent.

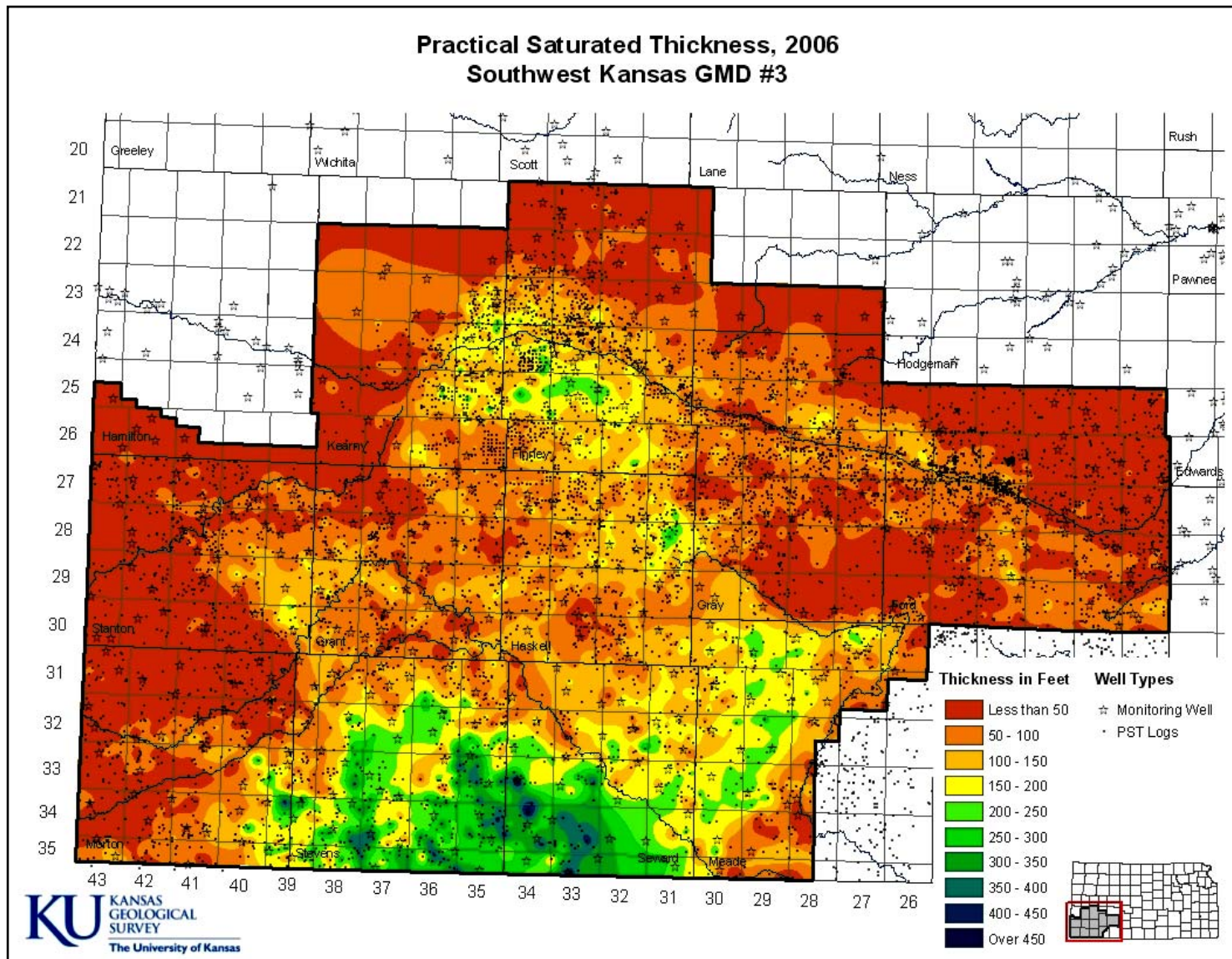


Figure 28. 2006 PST in GMD 3.

Discussion

The purpose of this research effort was to produce maps of the practical saturated thickness (PST) of the Ogallala portion of the High Plains aquifer in GMD 3 for the pre-development period and for the year of the most recent set of annual measurements. PST is the net thickness of saturated, permeable sand and sand and gravel and differs from the saturated thickness (ST), which includes the thickness of all water-saturated sediments between the water table and the bedrock surface. As the project developed, it became clear that to better understand the mapped distribution and increase the usefulness of the project results, subsurface mapping was needed in 2-D and 3-D for both the saturated and unsaturated portions of the Cenozoic sequence in order to look more closely at relationships between permeable and less permeable zones. By expanding the project scope, past and future changes in PST over time can be examined with reference to the 3-D framework of these zones and incorporated into tailored management plans as needed. The project results will also be more useful for later ground-water modeling projects currently in the planning process.

The complex distribution of permeable and low permeability sediments in the Cenozoic sequence results from a wide variety of geologic processes that acted throughout the Neogene (Miocene-Pliocene) and Quaternary within GMD 3 and regions to the west. The ancestral Arkansas and Cimarron rivers likely transported in and deposited most of the Cenozoic sediments of southwest Kansas (Smith, 1940; Frye and Leonard, 1952; Izett and Honey, 1995). As a result the fluvially dominated sedimentary architecture consists of micro- to mega-scale, hierarchically arranged, discrete packets of sediment bounded by erosional surfaces resulting from short- to long-term cycles of erosion and deposition induced by changes in stream regimen (Figure 30; Diffendal, 1982; Miall, 1996). Long-period changes in stream regimen are attributable to episodes of uplift and erosion of the central Rocky Mountains and the piedmont adjacent to the mountain front, climate change, and local subsidence due to evaporite dissolution (Leonard, 2002; Molnar, 2004; and Wizniewski and Pazzaglia, 2002; Macfarlane and Wilson, 2006). The later reworking, remobilization, and deposition of these deposits by wind and water, including the formation of caliche layers and cemented zones, adds further complexity to the structure of these deposits (Frye and Leonard, 1952; Gustavson and Holliday, 1999).

Alternating sequences of coarse- and fine-grained sediments that contain evidence of buried soils at the northeast Haskell County index monitoring well borehole indicate of cycles of erosion, deposition, and culminating in periods of stability (Osterkamp et al., 1987). The thin basal sand and gravel consisting of locally eroded and transported in sediment may represent the upper part of a channel fill sequence within the NW-SE trending incised paleovalley that extends from southern Finney to Meade County. The thick clayey silt above may have been deposited in a flood-plain environment. The thick sand and gravel sequence above the clayey silt interval is coarser grained than the basal sand and gravel. Sediment composition is dominantly arkosic consisting of quartz and orthoclase and microcline feldspars. Subtle cyclical changes in gamma-ray intensity along the interval of the borehole that penetrates this sequence do not appear to be related to upward changes of grain size from coarse to fine but may reflect changes in sediment mineralogic and petrologic composition. Gravel clasts recovered with the cuttings range in size up to approximately 5 cm (approximately 2 inches) in diameter. The driller reported that based on the behavior of the rig, it is likely that clasts much larger in size than those recovered in the

cuttings are present in this part of the sequence. The entire sequence appears to be a cut-and-fill channel sequence within a braided or coarse-grained meandering river channel belt (Figure 31). The interbedded clayey silt, silt, and fine- to coarse-sand sequence in the upper part of the borehole is much finer grained than the underlying sand and gravel and may represent deposition



Figure 30. Erosional surfaces delineating sand and gravel, cut-and-fill sequences in the Cenozoic succession exposed in a gravel pit near the Cimarron River in NW NE Section 35, T. 33 S., R. 32 W.

by streams with waning competency. Thus, it appears that sediments representing two major cycles of erosion, deposition, and erosion are present at the monitoring site.

To a first approximation, the subsurface mapping of permeable fraction does not require a stratigraphic framework. The raw data in the drillers' logs and the input to RockWorks 2004® are tied to intervals defined arbitrarily or on the basis of observed lithology changes by the driller and not on the basis of stratigraphy or geologic time. RockWorks 2004® is not designed to produce predictive, geologic-process models, but rather models and visualizations of the subsurface based purely on the data and its distribution. The primary disadvantage in this approach is that interpretation is limited to what is portrayed in the visualizations.

A recurrent theme in the published literature on the geology of southwest Kansas is the difficulty of trying to develop a regional stratigraphic framework that ties the outcropping and subsurface



Figure 31. Cut-and-fill channel sequence exposed in a gravel pit in the Ogallala Formation in NE NE Section 33, T. 33 S., R. 28 W.

sections of the Cenozoic sequence together (see, for example, Feder et al., 1964). Previous work on the outcropping Cenozoic emphasizes the difficulties of correlation between nearby exposures and boreholes (Frye et al., 1956; Gutentag, 1963; and Feder et al., 1964). Our inability to develop such a regional framework results from the lack of laterally extensive markers in the sequence that can be used for dating and correlation purposes. Ongoing research at the Kansas Geological Survey attempts to use chemostratigraphic methods to the Cenozoic sequence to show that a stratigraphic framework can be assembled based on ash bed dating, paleontologic, and carbon isotope systematics and carbon content.

Such a framework could serve as a basis for enhancing our understanding of the environments and geologic processes that actively operated during the Cenozoic and would be useful for better delineation of aquifer and confining units within the Ogallala. However, to develop a model of the sedimentary architecture that could be used in a predictive sense would require orders of magnitude more information than is currently or is ever likely to be available.

A degree of caution is required in the interpretation of the permeable-fraction fence diagrams developed from the smoothed models. The visualizations are meant to portray relationships between the larger-scale, higher and lower fraction, permeable zones within the sequence and as a result may not adequately represent smaller scale details that would be recorded in the log from

a single well site. Much of the subsurface is in shades of green, which indicates that the Cenozoic sequence ranges from 45% to 70% permeable sediment. Examination of these zones in the unsmoothed models with high fidelity indicates that the green zones consist of a complex of interlayered, thinner higher and lower fraction, permeable zones (Figure 32).

This work confirms that with careful selection, drillers' logs can be a useful source of information on the dominant features of the subsurface geology and the permeable fraction distribution. Spot-checks of the drillers' logs from some areas reveals a consistency between drillers with respect to the description of subsurface geology. In the northeast Haskell County area, logs of 5 nearby boreholes drilled by Henkle Drilling & Supply Company, Inc., and Dunham Drilling, Inc., compared favorably with that described in the Clarke Well and Equipment driller's log and the KGS sample log of the northeast Haskell County index monitoring well borehole. All but one of the boreholes was less than a mile away from the Haskell site. Additionally, this comparability between logs from different boreholes suggests that some lithologically similar units are locally traceable in the subsurface. This is also confirmed in the two panels of the fence diagram for the northeast Haskell County area (Figures 24-25).

The maps in figures 7 and 8 indicate that where the Cenozoic sequence is thickest in the central part of the GMD, a higher percentage of it is capable yielding water than in eastern and most of the western parts. In the fence diagrams thick, subregionally extensive intervals of permeable sediment are present at various levels within the Cenozoic section and generally coincide with the mid-section of the GMD where the total thickness is greater. The existence of these thick, persistent zones of high permeable fraction is a clear indication that recognizable, preferred pathways for lateral and vertical water transmission exist within the aquifer at least at the subregional scale in many areas at more than one level (Figures 14,15). Likewise, tabular and sinuous zones of low permeable sediment can be traced laterally over appreciable distances in the subsurface. These low permeable units could be considered subregional confining layers. Lastly, the fence diagrams indicate that the valleys incised into bedrock are as likely to be filled with higher percentage permeable sediment as they are to be filled with moderate to lower percentages of permeable sediments. Because of this, it may be more difficult to locate productive zones for public water supply beyond the usable lifetime of the Ogallala for irrigation.

In many areas of GMD 3 a significant fraction of the Ogallala aquifer under pre-development did not and does not currently contribute to well yield except as leakage from layers of less permeable sediment. The usable lifetime of the aquifer for irrigation projection is computed based on ST, the annual rate of decline of the water table, and an assumed minimum ST required for a well to produce enough water to make center pivot irrigation possible. The annual rate of decline of the water table is apparently sensitive to aquifer heterogeneity at least in the short term (Figure 25). However, projections based on ST are likely to be overoptimistic because they do not take aquifer heterogeneity into account. For example, in those areas of the District where the PST/ST ratio is less than half (Figure 29), a revised estimate of the usable lifetime would also be less than half the 2006 estimate (Wilson, 2007) if PST were substituted for ST in the calculation. In these low PST/ST ratio areas the majority of the saturated aquifer consists of less permeable

sediment that not only does not contribute to well yield but also may act locally as one or more leaky confining layers. Leaky confining layers reduce hydraulic connectedness of more permeable zones within the aquifer as a whole (Gutentag et al., 1972) and increase well drawdown during pumping and potentially well yield during a pumping cycle (Gutentag et al., 1974). These areas should be given careful consideration in formulating tailored subunit management plans.

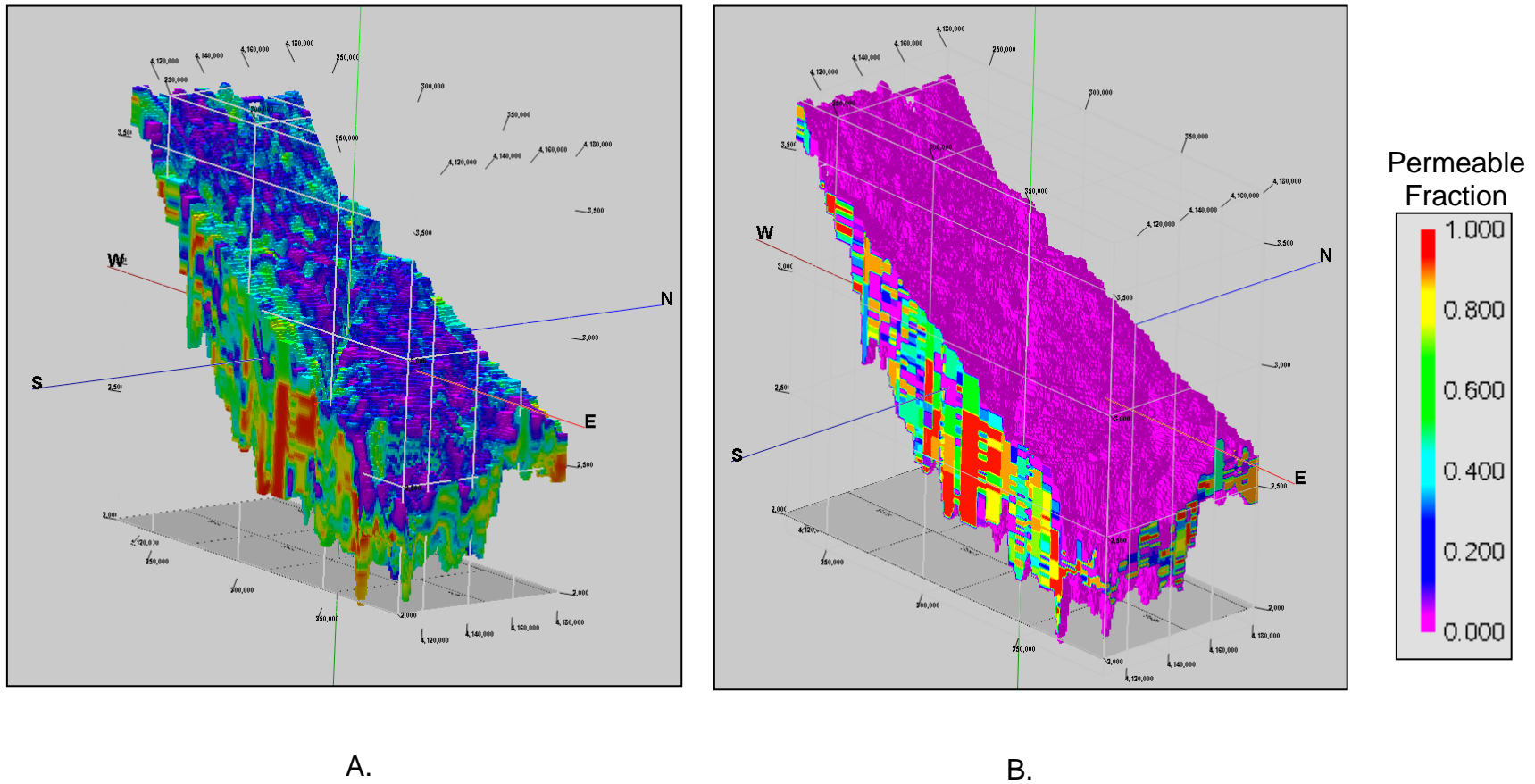


Figure 32. Comparison of the strip subregion models generated using the closest point algorithm with smoothing (A) and without smoothing with the high-fidelity option to better honor the input data (B).

REFERENCES CITED

- Berg, R.C., McKay, E.D., Keefer, D.A., Bauer, R.A., Johnstone, P.D., Stiff, B.J., Pugin, A., Weibel, C.P., Stumpf, A.J., Larson, T.H., Su, W., J., and Homrighous, G.T., 2002, Three-dimensional geologic mapping for transportation planning in central northern Illinois: data selection, map construction, and model development: *in* Geological Models for Groundwater flow modeling.
<http://www.isgs.uiuc.edu/research/3Dworkshop/2002/workshops.shtml>
- Bredehoeft, J.D., and Farvolden, R.N., 1964, Disposition of aquifers in intermontane basins of northern Nevada: International Association of Hydrologic Sciences, Publ. Num. 64, p. 197-212.
- Diffendal, R.F., Jr., 1982, Regional implications of the geology of the Ogallala Group (upper Tertiary) of southwestern Morrill County, Nebraska, and adjacent areas: Geological society of America Bulletin v. 93, p. 964-976.
- Doveton, J.H., 1986, Log analysis of subsurface geology concepts and computer methods: New York, Wiley Interscience, 273 p.
- Fader, S.W., Gutentag, E.D., Lobmeyer, D.H., and Meyer, W.R., Geohydrology of Grant and Stanton counties, Kansas: Kansas Geological Survey Bulletin 168, 147 p.
- Folk, R.L., 1968, Petrology of sedimentary rocks: Austin, Texas, Hemphill's, 170 p.
- Frye, J.C., 1942, Geology and ground-water resources of Meade County, Kansas: Kansas Geological Survey Bulletin 45, 152 p.
- Frye, J.C., and Leonard, A.B., 1952, The Pleistocene geology of Kansas: Kansas Geological Survey Bulletin 99, 230 p.
- Gustavson, T.C., and Holliday, V.T., 1999, Eolian sedimentation and soil development on a semiarid to subhumid grassland, Tertiary Ogallala and Quaternary Blackwater Draw formations, Texas and New Mexico High Plains: Journal of Sedimentary Research v. 69, p. 622-634.
- Gutentag, E.D., Lobmeyer, D.H., McGovern, H.E., and Long, W.A., Ground water in Finney County, southwestern Kansas: US Geological Survey Hydrologic Atlas HA-442, 2 sheets.
- Gutentag, E.D., and Stullken, L.E., 1974, Ground water in Haskell county, southwestern Kansas: US Geological Survey Hydrologic Atlas HA-515, 2 sheets.
- Gutentag, E.D., Lobmeyer, D.H., and Slagle, S.E., 1981, Geohydrology of southwestern Kansas: Kansas Geological Survey Irrigation Series 7, 73 p.

- Hibbard, C.W., 1953, The insectivores of the Rexroad fauna, upper Pliocene of Kansas: *Journal of Paleontology*, v. 27, no.1, p. 21-32.
- Hibbard, C.W., 1958, New stratigraphic names for early Pleistocene deposits in southwestern Kansas: *American Journal of Science*, v. 256, no. 1, pp. 54-59.
- Hibbard C.W., and Taylor, D.W., 1960, Two late Pleistocene faunas from southwestern Kansas: *Michigan University Museum of Paleontology Contribution*, v. 16, no. 1, 223 p.
- Huang, W.T., 1962, *Petrology*: New York, McGraw-Hill Book Co., 480 p.
- Izett, G.A., and Honey, J.G., 1995, Geologic map of the Irish Flats NE quadrangle, Meade County, Kansas: US Geological Survey Miscellaneous Investigation Series Map I-2498, 1:24,000, 1 sheet.
- Leonard, E.M., 2002, Geomorphic and tectonic forcing of late Cenozoic warping of the Colorado piedmont: *Geology*, vol. 30, no. 7, p. 595-598.
- Macfarlane, P.A., Combes, J., Turbek, S., and Kirshen, D., 1993, Shallow subsurface bedrock geology and hydrostratigraphy of southwestern Kansas: Kansas Geological Survey Open-File Report 93-1a, 13 p. and 18 maps, 1:500,000 scale.
- Macfarlane, P.A., Schloss, J., and Bissinger, L., 1998, An updated map of the extent of the confined and unconfined Dakota aquifer in Southwest Kansas Groundwater Management District 3: Kansas Geological Survey Open-file Report 98-37, 4 p.
- Macfarlane, P.A., Wilson, B.B., and Bohling, Geoffrey, 2005, Practical saturated thickness of the Ogallala in two small areas of Southwest Kansas Groundwater Management District 3: Kansas Geological Survey Open File Report 2005-29, 33 p.
- Macfarlane, P.A., and Wilson, B.B., 2006, Enhancement of the bedrock-surface-elevation map beneath the Ogallala portion of the High Plains aquifer, western Kansas: Kansas Geological Survey Technical Series 20, 28 p. and 2 map plates.
- McMahon, P.B., Dennehy, K.F., Michel, R.L., Sophocleous, M.A., Ellett, K.M., and Hurlbut, D.B., 2003, Water movement through thick unsaturated zones overlying the central High Plains aquifer, southwestern Kansas, 2000-2001: US Geological Survey Water Resources Investigations Report 03-4171, 32 p.
- Miall, A.D., 1996, *The geology of fluvial deposits*: Berlin, Springer-Verlag, 582 p.
- Molnar, P., 2004, Late Cenozoic increase in the accumulation rates of terrestrial sediment: how might climate change have affected erosion rates? *Annual Reviews Earth Planet Sci.*, v. 32, p. 67-89.

- Osterkamp, W.R., Fenton, M.M., Gustavson, T.C., Hadley, R.F., Holliday, V., Morrison, R.B., and Toy, T.J., 1987, Great Plains: *in* Graf, W.L., ed, Geomorphic Systems of North America, Geological Society of America, Centennial Special Volume 2, 163–210.
- RockWare, 2004, RockWorks v. 2004: Golden, RockWare 364 p.
- Russell, H.A.J., Brennand, T.A., Logan, C., and Sharpe, D.R., 1998, Standardization and assessment of geological descriptions from water well records, Greater Toronto and Oak Ridges Moraine areas, southern Ontario: *in* Current Research 1998-E, Geological Survey of Canada, p. 89-102.
- Schoewe, W.H., 1949, The geography of Kansas, pt 2, physical geography: Transactions of the Kansas Academy of Science, 52(3), p. 261–333.
- Schwartz, F.W., and Zhang, H., 2003, Fundamentals of ground water: New York, John Wiley and Sons, Inc., 583 p.
- Seni, S.J., 1980, Sand-body geometry and depositional systems, Ogallala formation, Texas: Texas Bureau of Economic Geology Report of Investigations 105, 36 p.
- Shepard, F.P., 1954, Nomenclature based on sand-silt-clay ratios: Journal of Sedimentary Petrology, v. 24, p. 151-158.
- Smith, H.T.U., 1940, Geologic studies in southwestern Kansas: Kansas Geological Survey Bulletin 34, 212 p.
- Stullken, L. E., Watts, K.R., and Lindgren, R.J., 1985, Geohydrology of the High Plains aquifer, western Kansas: U.S. Geological Survey Open-File Report 85-4198, 86 p.
- Wilson, B.B., 2007, Ground-water levels in Kansas – a briefing to the Kansas Legislature House Agriculture and Natural Resources Committee: Kansas Geological Survey Open-file Report 2007-1, 15 p.
- Wisniewski, P.A., and Pazzaglia, F.J., 2002, Epeirogenic controls on Canadian River incision and landscape evolution, Great Plains of northeastern New Mexico: Journal of Geology, v. 110, p. 437-456.

APPENDIX A:
2-D MODEL ERROR DISTRIBUTIONS

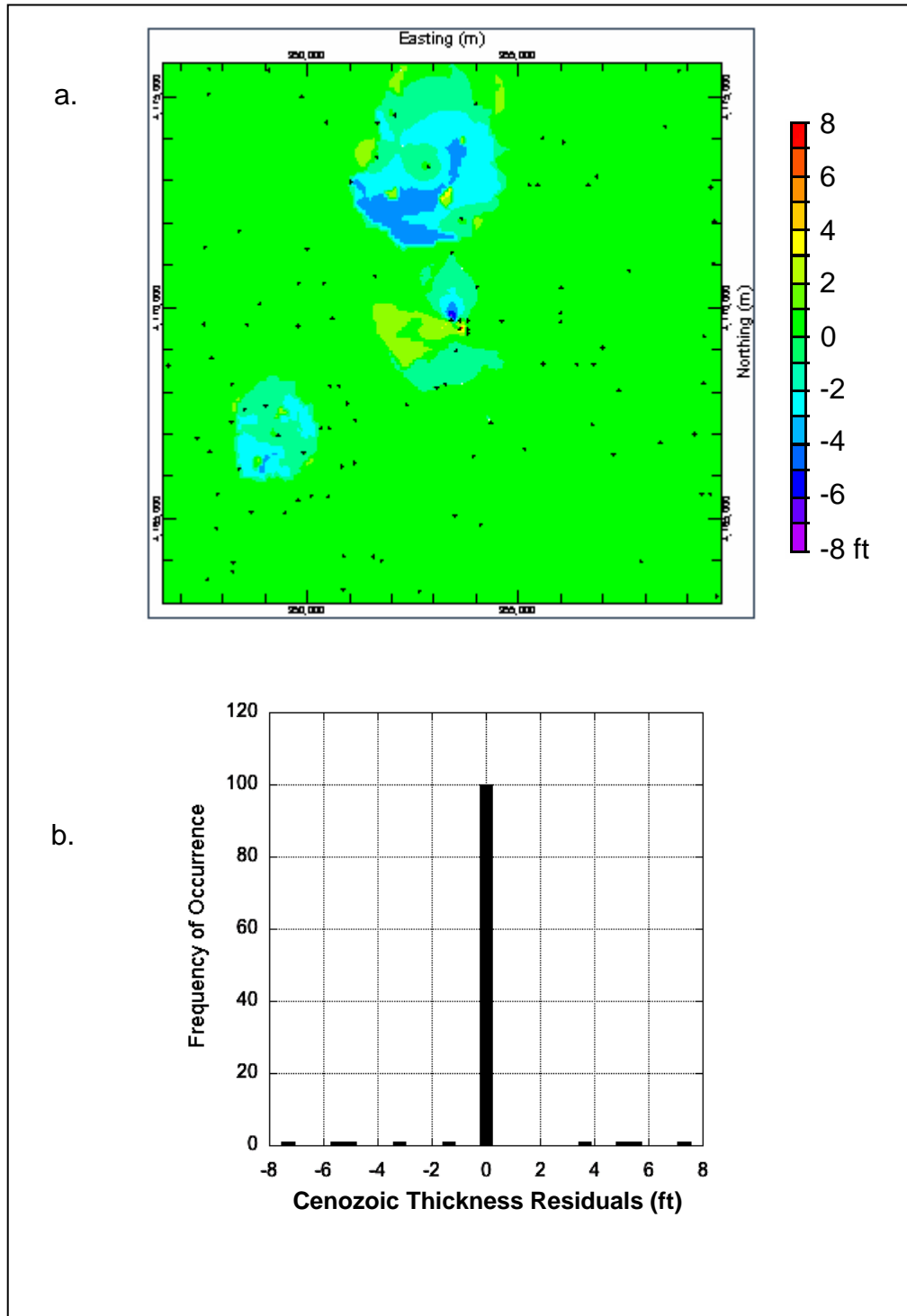


Figure A1. Distribution of residuals plotted from modeling of the Cenozoic deposit thickness in the northeast Haskell area in map (a) and histogram (b) forms and derived using the default kriging algorithm to compute model grid values in RockWorks® 2004.

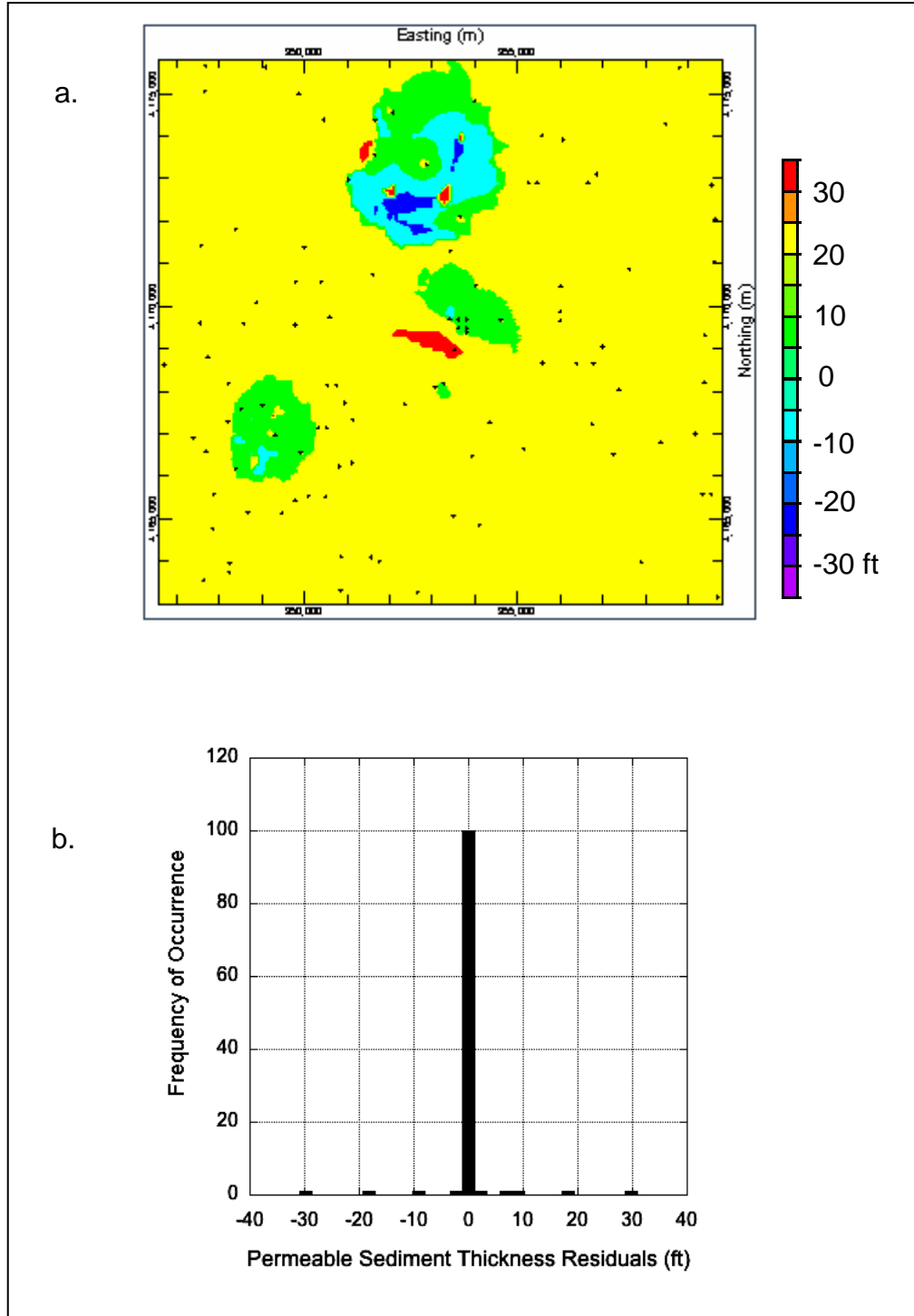


Figure A2. Distribution of residuals plotted from modeling of aggregate water-yielding sediment thickness in the northeast Haskell area in map (a) and histogram (b) forms and derived using the default kriging algorithm to compute model grid values in RockWorks® 2004.

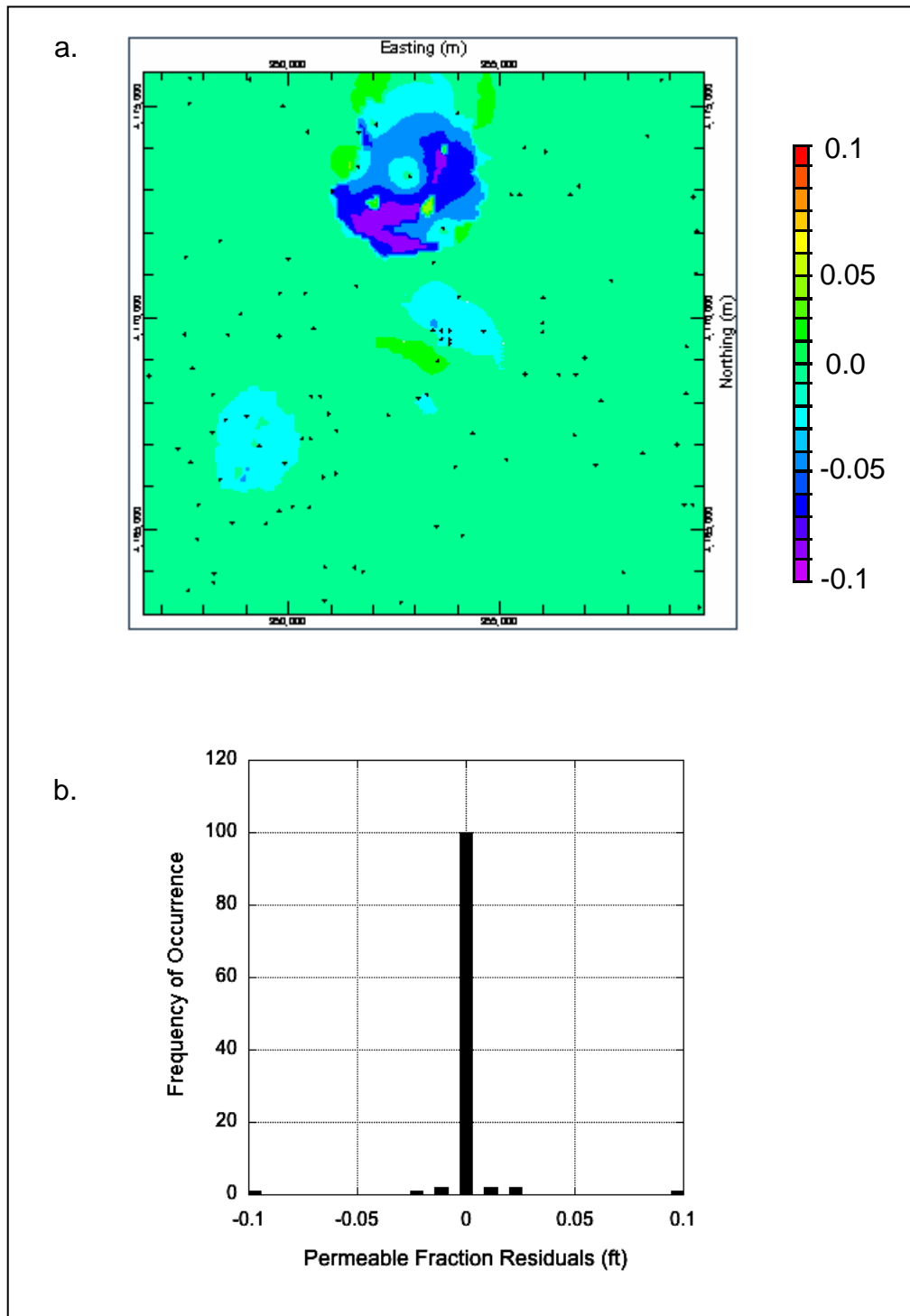


Figure A3. Distribution of residuals plotted from modeling of the water-yielding fraction in the northeast Haskell area in map (a) and histogram (b) forms derived using the default kriging algorithm to compute model grid values in RockWorks® 2004.

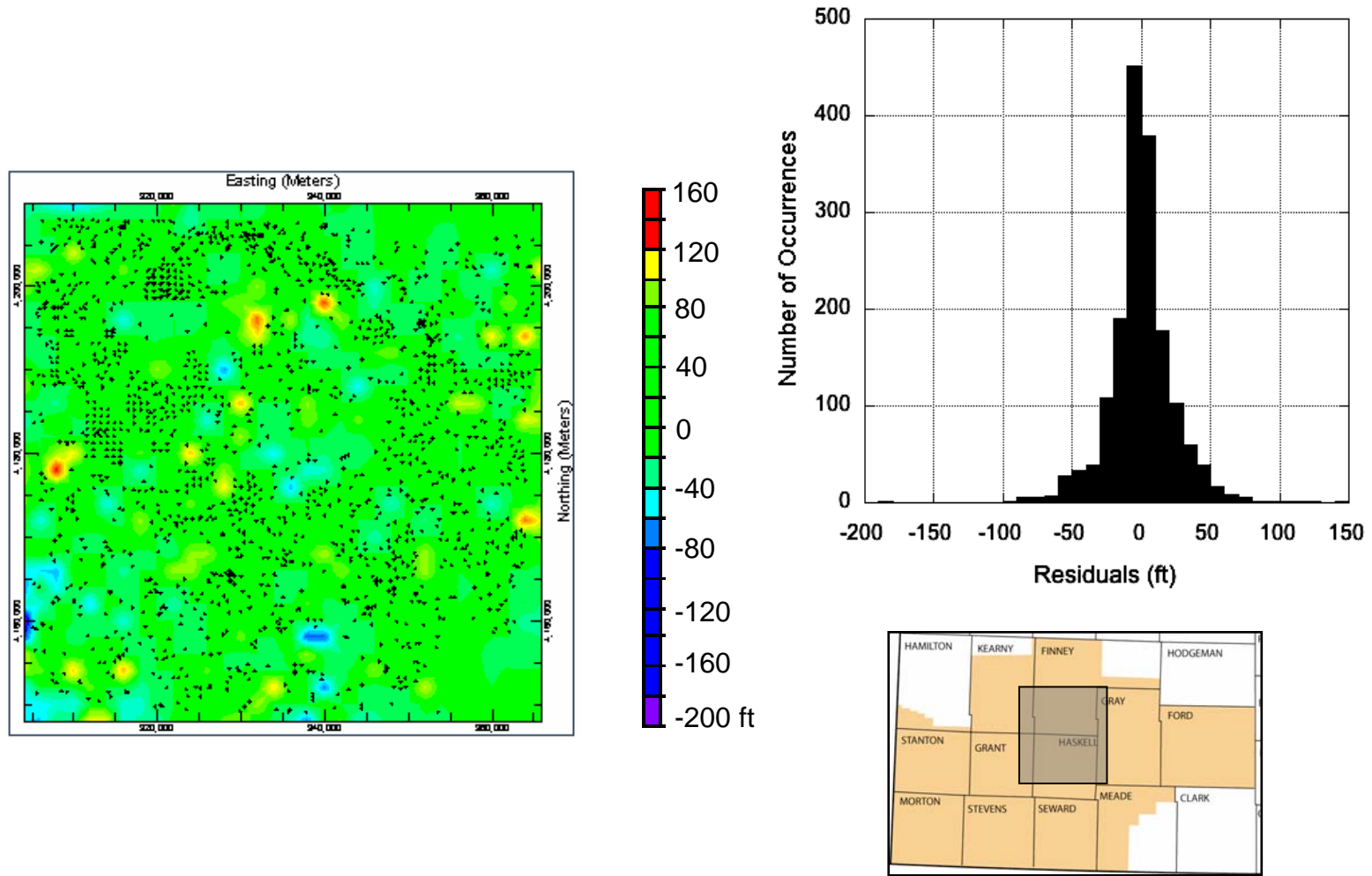


Figure A4. Distribution of residuals from mapping the Cenozoic thickness in the central GMD 3 subregion using the closest point algorithm. The residuals were computed as the difference at each data point between the input thickness and modeled values and the residuals distribution is shown as a histogram in the graph on the right. The closest point model grid algorithm was used to produce the map shown in the figure on the left.

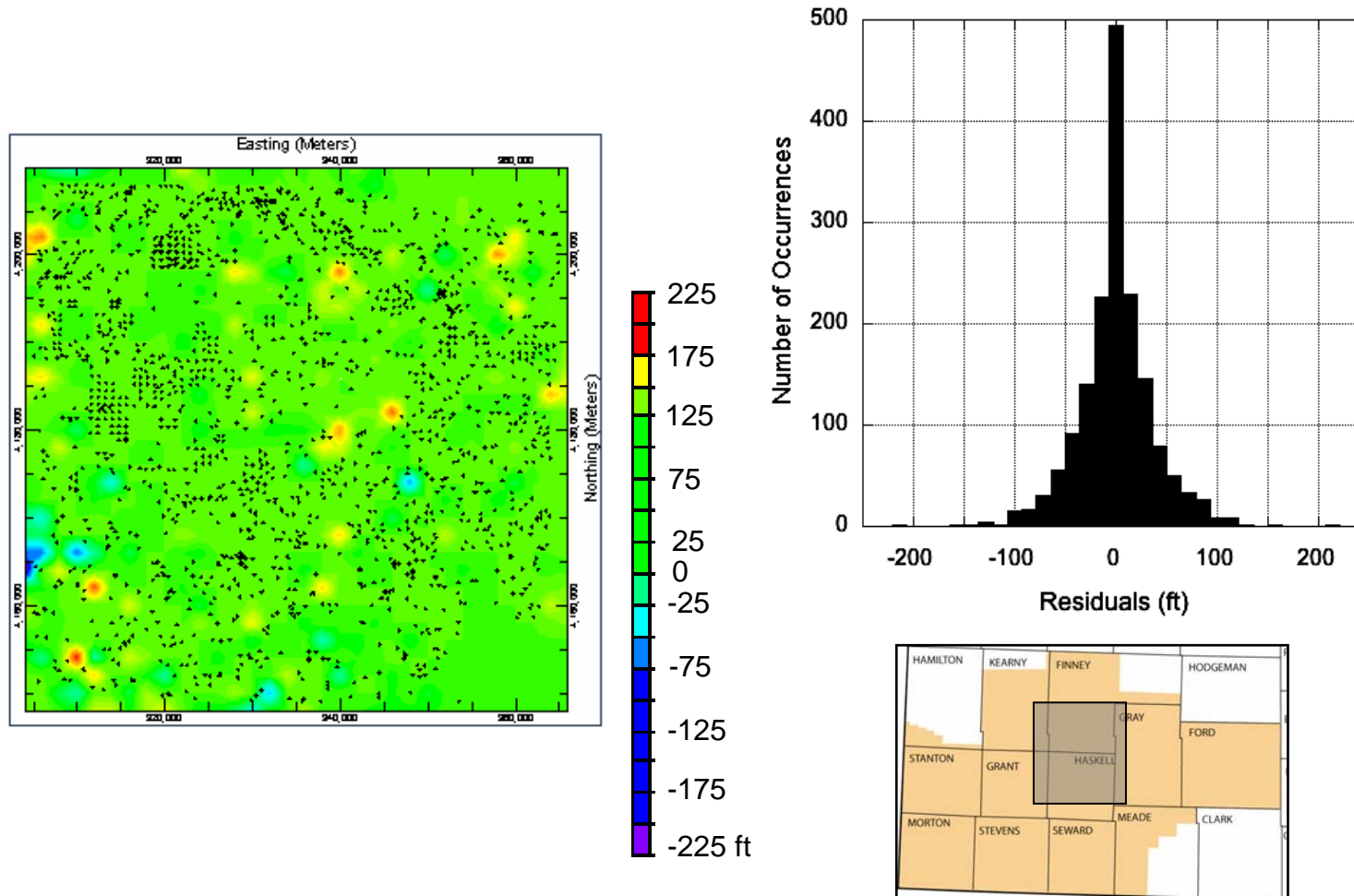


Figure A5. Distribution of residuals from mapping the aggregate thickness of water-yielding deposits in the Cenozoic in the central GMD 3 subregion using the closest point algorithm. The residuals were computed as the difference at each data point between the input thickness and modeled values. The residuals distribution is shown as a histogram in the graph on the right. The closest point model grid algorithm was used to produce the residuals map shown in the figure on the left.

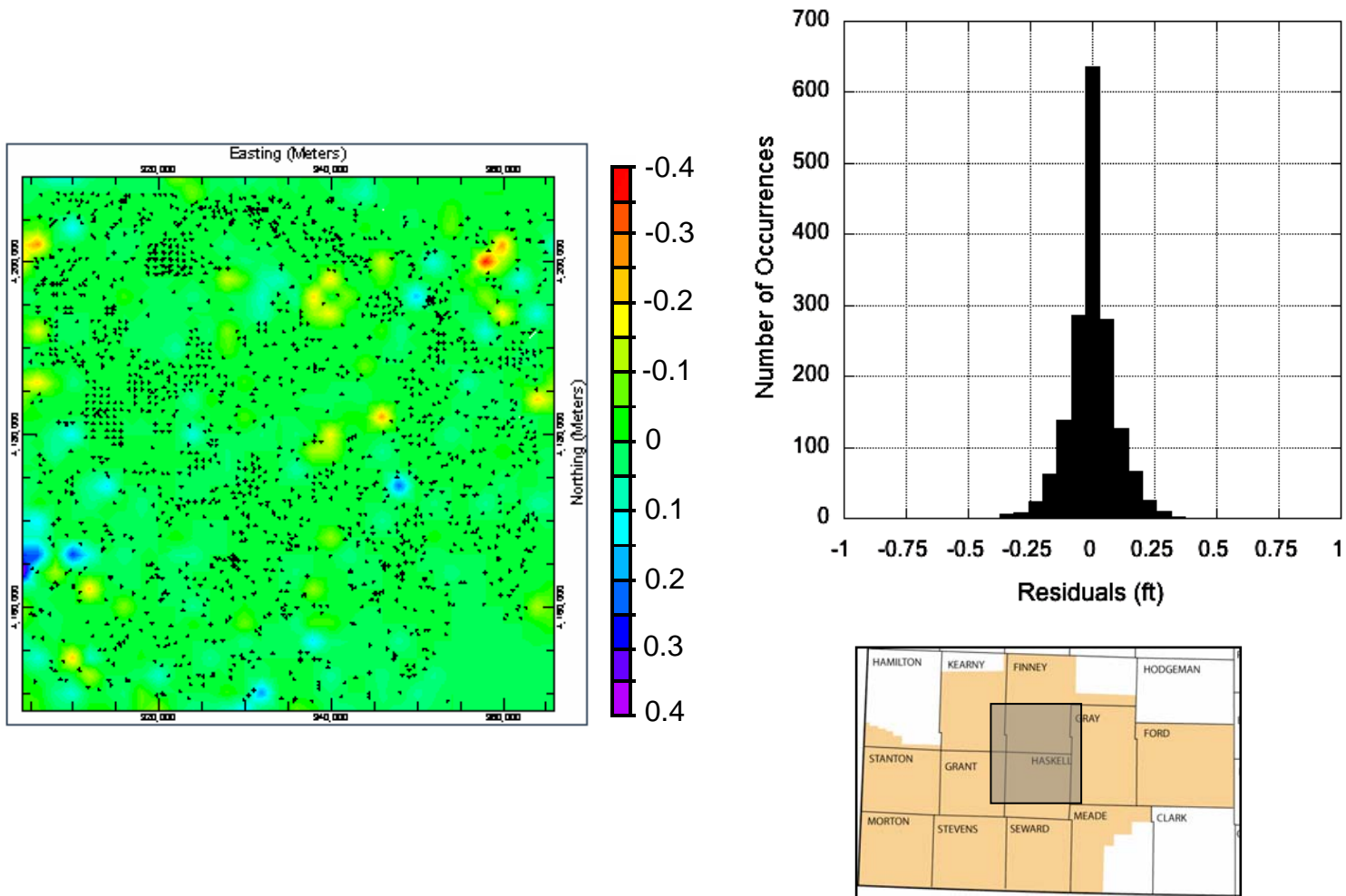


Figure A6. Distribution of residuals from mapping the fraction of water-yielding deposits in the Cenozoic in the central GMD 3 subregion using the closest point algorithm. The residuals were computed as the difference at each data point between the input fraction and modeled values. The residuals distribution is shown as a histogram in the graph on the right.

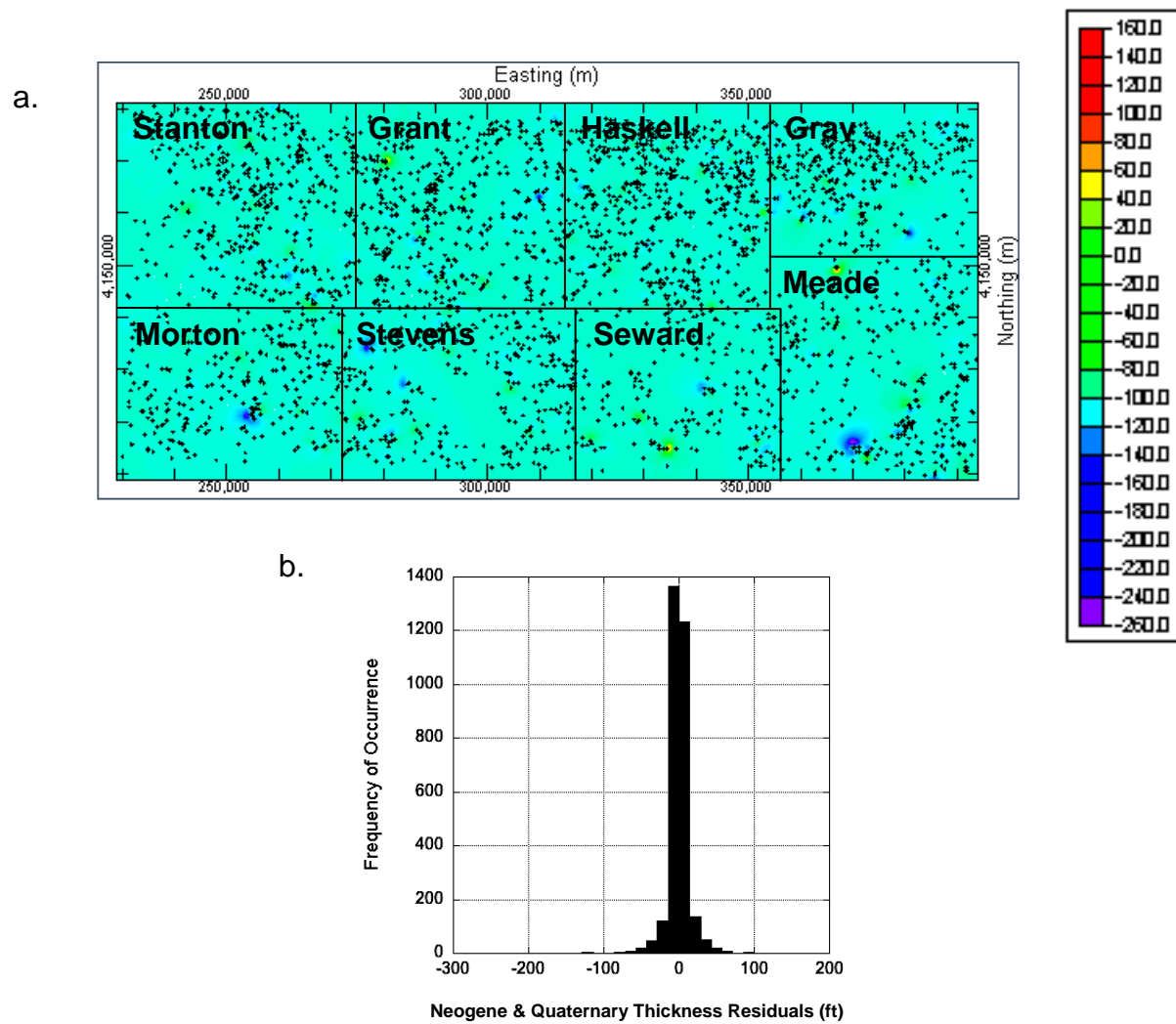


Figure A7. Map (a) and histogram (b) of the residuals from modeling the thickness of Cenozoic deposits in the strip subregion.

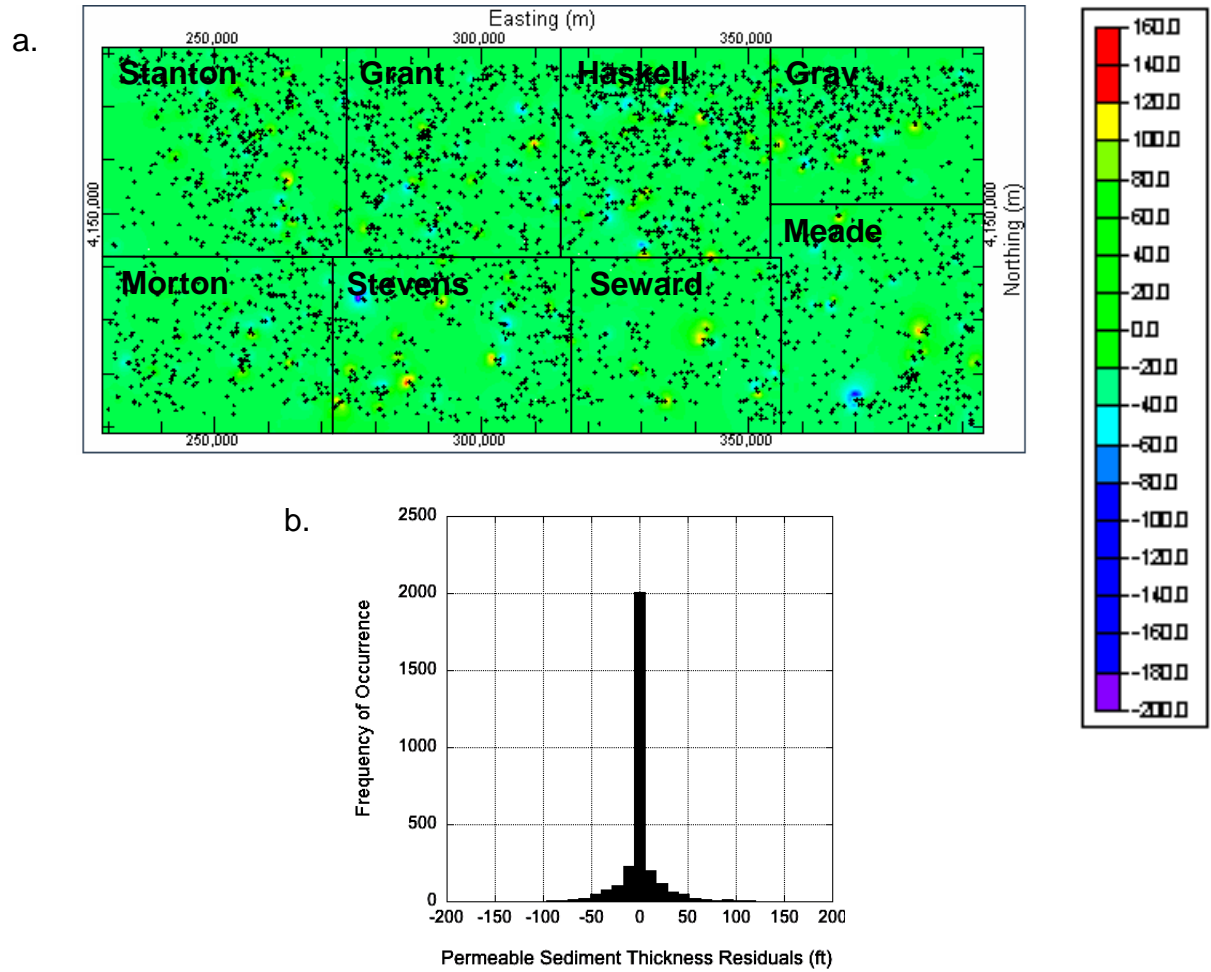


Figure A8. Map (a) and histogram (b) of the residuals from modeling the aggregate thickness of water-yielding sediment in Cenozoic deposits mapped across the strip subregion.

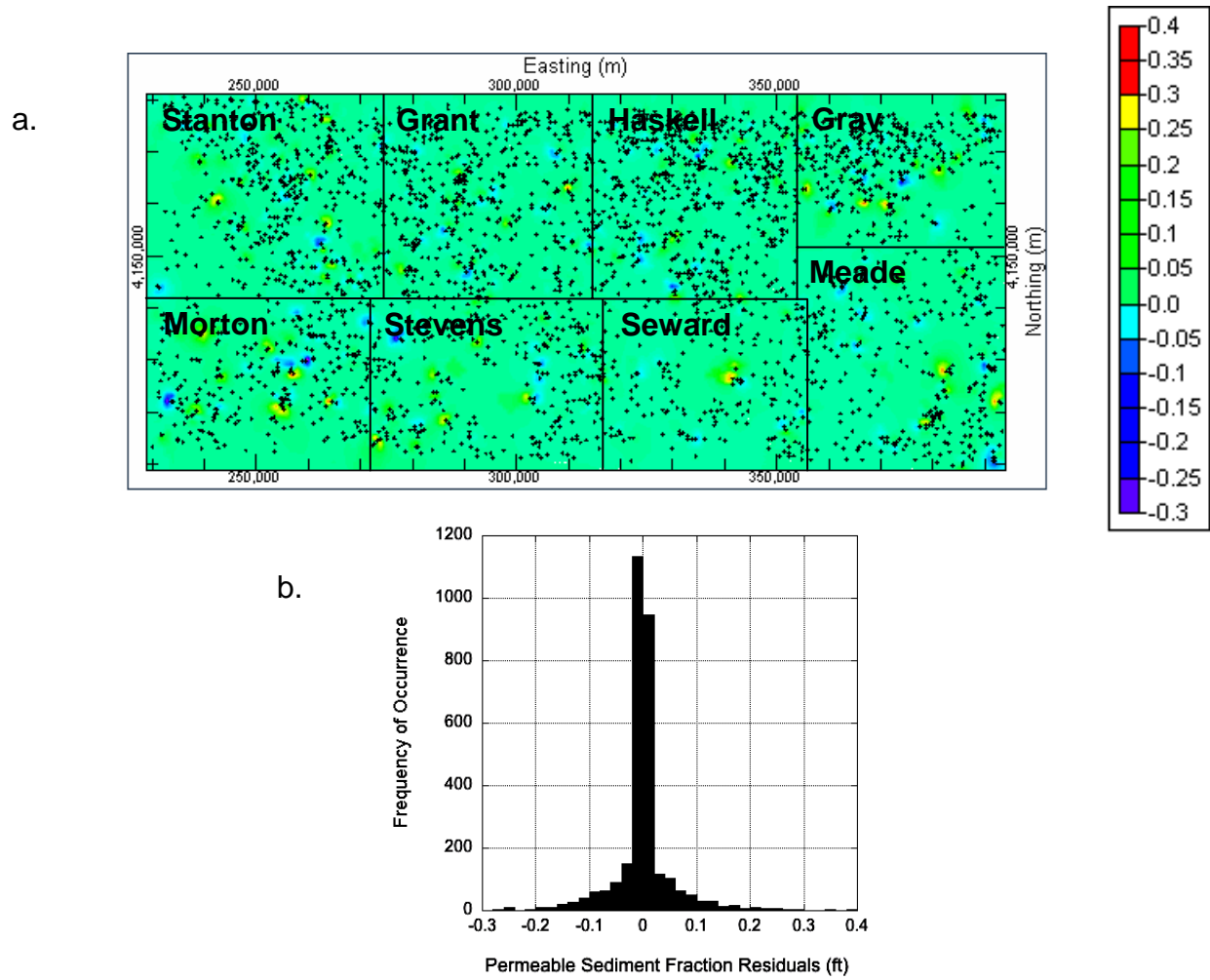


Figure A9. Map (a) and histogram (b) of the residuals from modeling the aggregate fraction of water-yielding sediment in Cenozoic deposits mapped across the strip subregion.